THE UNIVERSITY OF ADELAIDE

The Application of Next Generation Phenotyping Tools to a Wheat Breeding Programme

James Douglas WALTER

A thesis submitted in fulfillment of the requirements for the degree of Doctor of Philosophy

School of Agriculture, Food and Wine
Plant Genetics, Genomics and Breeding

THE UNIVERSITY of ADELAIDE

February 2020

Contents

Publications

This thesis contains three original research articles published in peer reviewed journals. Statements of authorship are included at the beginning of each chapter containing an original research article.

WALTER, J., EDWARDS, J., CAI, J., MCDONALD, G., MIKLAVCIC, S. J., & KUCHEL, H. (2019). High-throughput field imaging and basic image analysis in a wheat breeding programme. *Frontiers in Plant Science* **10**, 449.

WALTER, J., EDWARDS, J., MCDONALD, G., & KUCHEL, H. (2018). Photogrammetry for the estimation of wheat biomass and harvest index. *Field Crops Research* **216**, 165-174.

WALTER, J. D. C., EDWARDS, J., MCDONALD, G., & KUCHEL, H. (2019). Estimating biomass and canopy height with LiDAR for field crop breeding. *Frontiers in Plant Science* **10**, 1145.

Abstract

With the advent of high-throughput genotyping modern plant breeding has reached a new frontier of high-volume, high-density, yet low-cost, genomic data. Previously the acquisition of this data has been a logistical bottleneck within breeding programmes, yet with genomic data now abundantly available to breeding programmes, it has been speculated that the collection of phenotype data will become the next operational bottleneck. That being the inability to phenotype all material for all desired traits within a programme . The journey to improve the collection of phenotypic data is well underway, with focus being placed upon next generation phenotyping (NGP) technologies, such as high-throughput field phenotyping systems, to aid in the pairing of genotype to phenotype. Numerous sensors and methods of deployment have been investigated for application within small-plot field trials and suggested as tools for wheat and other field-crop breeding programmes, though few have explored how these can be deployed at scale or the suitability of collected data for use by breeders. This thesis investigates the deployment of commercially available digital cameras and LiDAR sensors within large-scale wheat breeding field trials, assessing the suitability of collected data for its application within the analytical pipelines of breeding programmes.

Digital cameras were deployed opportunistically within large-scale wheat breeding trials, and through basic open-source image analysis methods, were capable of objectively assessing colour-based traits traditionally scored with visual assessment, producing levels of heritability similar to or greater than traditional methods. As part of this process a tractor-based high-throughput phenotyping platform was developed for the deployment of digital cameras, leveraging upon infrastructure present within the breeding programme and enabling images to be captured at a speed of 7,400 plots per hour. Given the success of

digital cameras to measure colour-based traits, digital cameras were also deployed manually at a small scale to measure above ground biomass, plant height and harvest index, using photogrammetric techniques. Though data capture and processing methods were low-throughput, correlations between digital and manually collected measurements were strong (up to r = 0.94), highlighting the potential of the three-dimensional point cloud data type. To further this investigation LiDAR sensors were deployed on the high-throughput phenotyping platform to collect point cloud data of wheat plots from multiple field sites and collection dates. Processed point cloud data correlated strongly to traditional measurements of above ground biomass and canopy height and was shown to be highly repeatable and suitable for integration in routine breeding analyses.

The findings of this work demonstrate that commercially available digital cameras and LiDAR sensors can be deployed within large-scale wheat breeding trials, in a high-throughput, non-destructive and non-disruptive manner, for the accurate and repeatable measurement of traits which are traditionally subjective, laborious and/or destructive. Investigation of these measurements showed their suitability for inclusion within routine breeding analyses, giving breeders confidence in the data collected by next generation phenotyping technologies. The findings of this work are not only relevant to wheat breeders, but also to breeders of other field-crops and scientists conducting field research at a large scale.

Declaration of Authorship

I certify that this work contains no material which has been accepted for the award of any other degree or diploma in my name, in any university or other tertiary institution and, to the best of my knowledge and belief, contains no material previously published or written by another person, except where due reference has been made in the text. In addition, I certify that no part of this work will, in the future, be used in a submission in my name, for any other degree or diploma in any university or other tertiary institution without the prior approval of the University of Adelaide and where applicable, any partner institution responsible for the joint-award of this degree.

I acknowledge that copyright of published works contained within this thesis resides with the copyright holder(s) of those works.

I also give permission for the digital version of my thesis to be made available on the web, via the Universitys digital research repository, the Library Search and also through web search engines, unless permission has been granted by the University to restrict access for a period of time.

I acknowledge the support I have received for my research through the provision of an Australian Government Research Training Program Scholarship.

Signed:

Date: 14/02/2020

Acknowledgements

There have been many people who have contributed to my studies in some way, shape or form over the past five years; from conversations over coffee through to dedicating years of time supervising me. To everyone who has played some part in this, thank you.

First and foremost I should acknowledge my supervisors, Haydn Kuchel, James Edwards and Glenn McDonald, for their support and guidance over the past four years. Haydn, thank you for seeing my potential fit for this project and for taking a chance on me, in hindsight I can't imagine a project that I would have been better suited to, or enjoyed more. Your guidance and encouragement for me to push and apply myself have been vastly beneficial to my professional and personal development, I look forward to working with you in the years to come. James, thank you for your guidance, near universal availability and patience in dealing with my no doubt seemingly endless questions. You've taught me a great deal over the course of this project, from the core principles of plant breeding to the finer points of craft beer, and I am sure this will continue in future. Glenn, thank you for the immense amount of time and effort you have contributed to my education, not only during the course of this project, but also throughout my honours and undergraduate degrees. Your advice, guidance and dry wit have always been appreciated, I hope it is a relief knowing there will be no more drafts of my work to read!

Thank you to the AGT Roseworthy team (past and present) for providing such a great place to work and for accepting me as part of the team. Special thanks are due to Simeon Hemer, Rowan Prior and Darcy Moore for their invaluable work managing and maintaining the trial sites I used and for providing tractor chauffeuring services as required, without your contributions this project wouldn't have been possible. Furthermore, I would be remiss not to acknowledge the essential contributions of Nathan Lloyd, who sacrificed much of his time designing, building and wiring the 'phenomobile'. Nathan without your

help much of this project would still be a concept and not a reality. To the AGT breeding team (past and present) thank you you for your support and encouragement over the years, I look forward to working together in future.

To Adam Norman, I don't know how you did it, but thank you for aligning me with this project and enabling my journey into the world of plant breeding. Your support and friendship over the past eight (nine?) years has been greatly appreciated and I look forward to working with you in future.

Thanks also go to my colleagues, both past and present, at Limagrain (Piet Reyns, Eva Ampe and Jan Sentjens) and UniSA (Stan Miklavcic and Jinhai Cai), particularly for their assistance in dealing with sensors and software. While it is always a challenge working with technology, it has been a pleasure working with you.

To my parents, your support and encouragement over the years has provided me the opportunity to pursue both my interests and higher education, ultimately allowing me to work in an area I truly enjoy. For this I will be forever grateful. To the remainder of my family and my friends, thank you for your encouragement and support, you can now stop asking 'are you done yet?'

To Alanah, thank you for sticking with me throughout this long and sometimes arduous journey, having you by my side has made it all that much easier. This part of the journey is finally over, let's ensure we make the most of the next.

Contextual Statement

This thesis has been prepared in publication format and is comprised of original research articles, published in peer reviewed journals, as the main body of work. These articles are preceded by a Literature Review and followed by a General Discussion of the contribution this work makes to the field of plant breeding.

The review of literature in Chapter 1 covers articles published prior to the compilation of the review in January 2016 and establishes the base of knowledge for the conception of experiments, and resulting publications contained within the remainder of the thesis. As a result, more recent publications are not included within the Literature Review but are included and discussed within the subsequent publications and the General Discussion of the thesis. The review covers the basics of breeding programme structure and the fit of traditional phenotyping methods within these programmes. Furthermore, proposed applications of new phenotyping technologies, including the sensors and platforms, of which these technologies consist of, are outlined and discussed.

From the Literature Review it was identified that while many sensors show potential for application within breeding programmes, they can often be prohibitively expensive, or require highly specialised skills to process the collected data. Given their ready availability, low cost and ease of use, commercially available digital cameras were identified as a sensor of great potential for deployment within breeding programmes. Recording light from the red, green and blue spectra, digital cameras effectively capture the colour spectra observable to the human eye and allow for the assessment of colour-based traits, such as canopy cover and senescence, traditionally assessed through visual scoring. While digital cameras have previously been investigated for the assessment of these and other visually assessed traits within the literature, the suitability of these assessments for breeding programmes, as well as truly high-throughput methods of data collection, had yet

to be explored. Chapter 2 contains the original research article 'High-Throughput Field Imaging and Basic Image Analysis in a Wheat Breeding Programme', published in Frontiers in Plant Science, April 2019, under the specialty section Technical Advances in Plant Science, as part of the research topic High-Throughput Field Phenotyping to Advance Precision Agriculture and Enhance Genetic Gain. The rationale behind this research was to fill a knowledge gap, in which there had been no evaluation of phenotyping sensors, the suitability of the data they produce for use by breeders, or their deployment through high-throughput field phenotyping platforms, within a large commercial breeding programme. Furthermore, the comparison of these technologies to measurements breeders routinely record, such as visual scores, have been lacking, particularly in regard to digital cameras. To address this, the article establishes easily reproduceable open-source methods for the assessment of colour-based visual traits of interest using digital cameras, demonstrating their use within a breeding programme in conjunction with a tractor-mounted high-throughput image boom. Digital measures are rigorously investigated in comparison to visual scores, with statistics of key importance to breeding programmes, such as trait heritability and genetic and residual correlations, being discussed.

Following the successful demonstration of digital cameras and basic image analysis to assess colour-based traits within wheat field plots, the versatility of digital cameras as a next generation phenotyping tool was further investigated for traits traditionally assessed through physical measurement, rather than visual assessment. This continued investigation of digital imaging forms the basis for Chapter 3, which contains the original research article 'Photogrammetry for the estimation of wheat biomass and harvest index' which was published in Field Crops Research, February 2018. The aim of this article was to investigate the use of commercially-available digital cameras to generate high-fidelity three-dimensional point cloud data, for the non-destructive estimation of wheat above ground biomass, harvest index and canopy height. At the time of publication few studies in the literature had investigated the use of point cloud data for measuring above ground biomass, or associated traits, in wheat, with the potential of this data relatively unknown. This article successfully demonstrates the use of relatively cheap commercial digital cameras and software to capture and process ground-based images of wheat field plots into point

clouds for the estimation of above ground biomass, harvest index and canopy height. Furthermore, it discusses the suitability of these methods and generated data to wheat breeding programmes, as well as opportunities to explore high throughput methods.

Chapter 4 builds upon the results of Chapters 2 and 3, continuing to focus on above ground biomass and investigating how it can be effectively measured with high-throughput in large-scale field trials, as well as how this information could be utilised by breeders. From Chapter 3, point cloud data was established to be capable of estimating above ground biomass and canopy height, however the set of methods utilised did not allow a sufficiently high-throughput, in their current form, for direct application within breeding programmes. An alternative sensor for the collection of point cloud data, identified in Chapter 1, is LiDAR. To this end, the high-throughput imaging boom described in Chapter 2, was fitted with LiDAR sensors for deployment within the large-scale field trials of a wheat breeding programme. The subsequent research, lead to the publication of the original research article 'Estimating Biomass and Canopy Height with LiDAR for Field Crop Breeding' in Frontiers in Plant Science, August 2019, under the specialty section Technical Advances in Plant Science, as part of the research topic High-Throughput Field Phenotyping to Advance Precision Agriculture and Enhance Genetic Gain, which is presented in Chapter 4. The aim of this research was to deploy a high-throughput LiDAR system within field trials in different environments and determine the suitability of LiDAR to non-destructively measure above ground biomass and canopy height, within the context of a wheat breeding programme. This research addresses specific gaps in the literature, where previously LiDAR estimations of above ground biomass and canopy height have been investigated only at single sites, as well as a lack of applied LiDAR use within large-scale field trials, where repeatability and suitability of data integration to breeding programmes have yet to be discussed.

Chapter 5 contains the General Discussion of the thesis, summarising the key findings of the research articles within and their significance to the field of plant breeding. The current, and continually improving, state of technology is discussed, along with the present and future paths for research in this field. Finally, it explores how next generation phenotyping and other new technologies can be effectively adopted and deployed within breeding programmes.

Chapter 1

Literature Review

1.1 Introduction

Plant breeding is a rapidly evolving discipline that is willing to adopt new technologies to improve the efficiency of selection and maximise genetic gain from available resources. A testament to this is the quick uptake and integration of molecular technologies, such as molecular markers and next generation sequencing, which are now common place among many breeding programmes worldwide. Until recently acquiring genotypic information has been viewed as a major operational bottleneck within plant breeding programmes, however with the surge of new genotyping technologies and the decreasing costs associated with them, it has been proposed that this bottleneck has now shifted to acquiring phenotypic data (Cobb et al., 2013). Given that genetic data is now so freely available, collecting phenotype data, for any trait of interest, could be considered a limiting step within breeding programmes. To overcome this, new phenotyping technologies and strategies will need to be developed, evaluated and deployed, requiring a multidisciplinary approach between computer scientists, engineers and plant scientists. Within this review these technologies are referred to in terms of Next Generation Phenotyping (NGP) technologies, that is technologies beyond those which are currently deployed within breeding programmes. The term NGP is favoured rather than High-throughput Phenotyping (HTP), as HTP implies measurements are being collected more quickly than traditional measurements (such as visual scoring), though it is possible for NGP technologies to be low throughput but have substantial gains in accuracy and/or efficiency. This review

looks at the role of phenotyping within a wheat breeding programme and investigates current and emerging phenotyping technologies, as well as their applications and limitations in meeting the needs of breeding programmes.

1.2 Phenotyping in Wheat Breeding

The term phenotype was originally proposed and described by (Johannsen, 1911) as the ability to determine the 'type' of all organisms based on measurements or description. Phenotype is now commonly used throughout plant breeding and plant science to describe the expression of genes to physical traits. Historically phenotypic selection has been the sole selection tool for plant breeders and, even before the advent of modern plant breeding, phenotypic selection was used to achieve improvement in early domesticated crops (Allard, 1964; Halloran, 1979).

In early Australian wheat (*Triticum aestivum* L.) breeding programmes, easily observable traits, such as disease resistance, height and maturity, were primary drivers of selection (Hollamby, 1983). These traits are often less genetically complex, with their selection leading to rapid genetic advancement (Halloran, 1979). As time and the understanding of genetics progressed, linkages between the expression of phenotypes and individual genes of desirable traits were discovered, providing phenotypic markers to aid selection. Prime examples of these markers can be seen in the linkage of the physiologic condition pseudo-black chaff with the major stem rust resistance gene *Sr2* (Sheen et al., 1968; Juliana et al., 2015) and leaf tip necrosis with the major leaf rust resistance gene *Lr34* (Singh, 1992; Juliana et al., 2015), with both of these phenotypic markers aiding breeders in the selection of rust resistant material.

While phenotypic selection has allowed a great deal of progress to be made in wheat breeding, it is not without limitations. A wide range of traits, such as those which are quantitative, environmentally influenced, visually hard to detect or quality related, do not lend themselves to quick and efficient phenotyping (Halloran, 1979; Hollamby, 1983; Kuchel et al., 2005), making them troublesome breeding objectives within plant breeding programmes and ultimately reducing the progress of genetic gain.

This bottleneck was somewhat alleviated with the introduction of molecular markers and marker assisted selection (MAS) to breeding programmes, enabling breeders to select for a specific trait, or traits, and screen early generation material with greater confidence. The merit of molecular markers compared to phenotyping as a selection tool for quantitative traits was investigated in maize (*Zea mays* L.) by Yousef & Juvik (2001). They concluded that MAS could offer simultaneous gains in multiple traits, as well as operate as a useful selection tool in the case of difficult or expensive-to-phenotype traits. Implementing MAS to a wheat breeding programme has been described by Kuchel et al. (2005) and Kuchel et al. (2007), with multiple MAS strategies being investigated and the most viable of these applied in a functioning breeding programme. In the practical application of MAS, Kuchel et al. (2007) noted the importance of this strategy when phenotypic selection is difficult. While MAS has proven to be a useful tool for the introgression and selection of qualitative traits into breeding material, it is still limited in its ability to aid in selection of complex quantitative traits, such as yield (Dekkers & Hospital, 2002). The use of molecular markers within breeding programmes was originally limited by the low speed and high cost of obtaining this genetic information, though this was soon overcome by the introduction of high-throughput genotyping and next generation sequencing technologies (Cobb et al., 2013; Araus & Cairns, 2014).

The next advance to wheat breeding will likely arise from the uptake and application of genomic selection (GS), the process of using genome wide dense molecular marker maps to predict potential breeding values and select based on predicted performance (Meuwissen et al., 2001). While GS may yet revolutionise wheat breeding, as it has dairy cattle breeding (Bouquet & Juga, 2013), the need for phenotyping is still present, and potentially greater, with GS training populations requiring detailed phenotypic data to create accurate prediction models (Cobb et al., 2013; Lei et al., 2014).

As new technologies, such as MAS and GS, have been introduced to breeding programmes the opportunity to increase population sizes, screening larger number of lines and increasing the rate of genetic gain, has arisen (Araus & Cairns, 2014; Cooper et al., 2014); at this point, however, the operational bottleneck of phenotyping returns. Even with the use of MAS and GS, breeders are limited by the number of early generation lines which can be phenotyped, even for simple traits such as maturity and height. To manage this, the size

of populations must be capped at a manageable number. Improving the ability to phenotype populations would enable this cap to be increased and greater genetic gain could be achieved.

In recent years a push for high-throughput precision phenotyping has begun within plant breeding and research communities (Walter et al., 2015), the goal of which being to abolish current phenotyping bottlenecks.

1.3 Wheat Breeding Scenario

To understand how these phenotyping technologies may be integrated into a wheat breeding programme, it is necessary to examine the structure of a breeding programme to identify where limitations occur and how they could be overcome. There are many variations in breeding programme design, both broad concepts, such as mass selection, pedigree and bulk selection, as well as variations and combinations thereof (Allard, 1964; Halloran, 1979; Hollamby, 1983). The individual structure of each programme will determine the specifics of how new technologies may be applied, however, general themes can be identified across many programmes.

For the purpose of this review an example of a selected bulk breeding programme (Allard, 1964; Halloran, 1979), with artificial early generation selection, will be used to illustrate the potential of new technologies within a wheat breeding programme. Each stage of the programme is outlined in Figure 1.1, with indications as to where different methods of selection may be used.

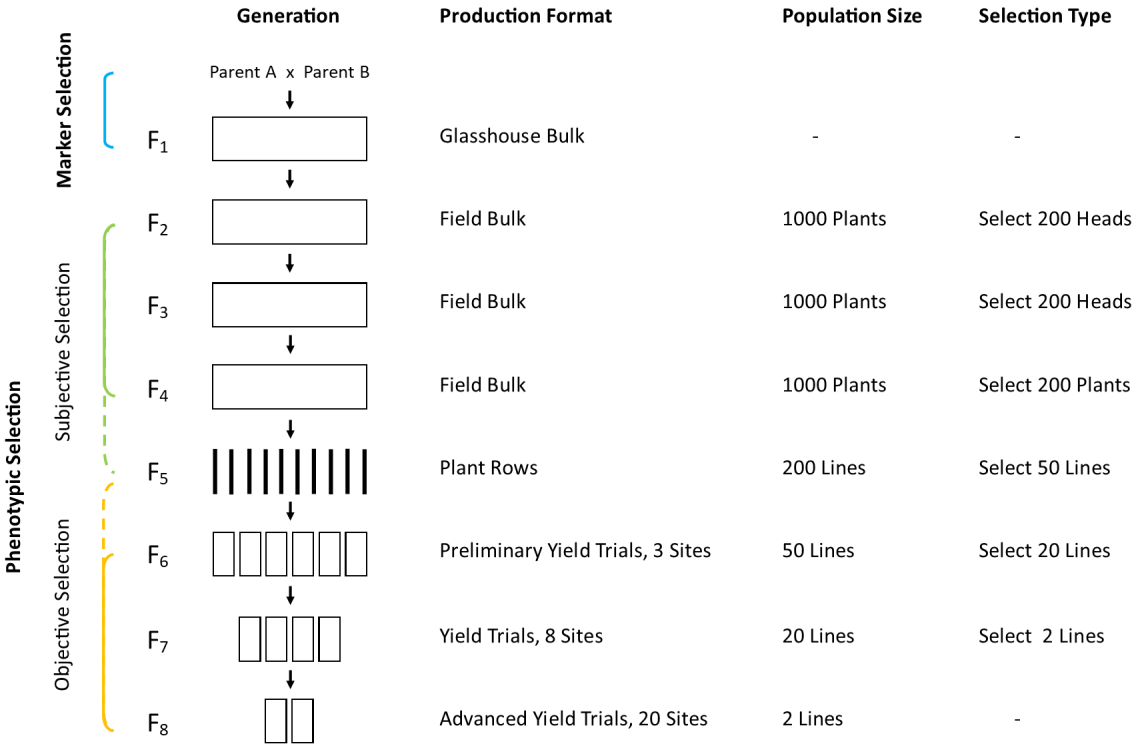

FIGURE 1.1: An example wheat breeding programme with production format, amount of material and type of selection in each generation. Dashed lines indicate potential selection methods to be used.

In breeding programmes larger numbers of populations and larger population sizes allow for higher levels of genetic diversity and greater potential for genetic gain to be made (Cooper et al., 2014). This can be achieved through greater selection intensity in early - mid generations (Figure 1.1; F_1 - F_5, selecting only the most desired lines and dramatically reducing the population size as it progresses to variety release. The scenario depicted in Figure 1.1 represents a single cross, out of potentially hundreds, within the breeding programme. For the purpose of this review a scenario with 100 crosses, resulting in 100 populations, will be used. The number of plants or plots requiring assessment in a single cycle of the programme, assuming two replicate yield trials, is outlined in Table 1.1.

Even in this scenario with 100 crosses, a significant amount of genetic material is produced. With current practices initial selection in early generations may be achieved with MAS, however once this is completed, subsequent selection will be achieved by phenotyping and yield trials, requiring a great deal of time and labour.

TABLE 1.1: Number and type of units to be assessed from a 100 cross breeding scenario depicted in Figure 1.1

Generation	Units to be assessed	Units
F_1	100,000	Individual plants
F_2	100,000	Individual plants
F_3	100,000	Individual plants
F_4	100,000	Individual plants
F_5	20,000	Plant rows
F_6	30,000	Yield plots
F_7	32,000	Yield plots
F_8	8,000	Yield plots

1.4 Potential of New Technologies

The introduction of new phenotyping technologies has the potential to increase the sensitivity, precision and accuracy of current measurements while maintaining or increasing the speed of current practices. Currently, to screen large numbers of lines accurately it is common for breeders to allocate a 1-9 scale or a percentage score to the trait of interest (Cobb et al., 2013). While this method allows for rapid scoring of breeding lines and offers a simple way to compare promising and poor lines, it is not inherently accurate and can be subjective depending on the scorer (Bock et al., 2010).

This visual phenotyping commonly occurs early in the breeding programme (Figure 1.1) for simple traits such as maturity, height and disease resistance. This allows for quick and easy selection, but due to the sheer number of lines may still be a rate limiting step in the breeding programme. Implementing next generation phenotyping technologies and subsequently high-throughput phenotyping at this stage of the programme could potentially eliminate this bottleneck, allowing breeders to increase population sizes, score greater numbers of lines and therefore increase genetic gain. At this early stage of the programme material is often grown as short rows, spaced individual plants or hill plots, due to low availability of seed and to accommodate large numbers of lines. This creates a challenge when considering new phenotyping technologies, which have primarily been used to monitor canopies of field plots and paddocks.

As breeding lines progress through early selection and more in-depth phenotypic data is required; fast, simple and flexible methods are still favoured. If objective and more accurate phenotyping methods are used they are often slow or physically demanding (Deery et al., 2014), making them a less efficient use of resources. The potential of new technologies for phenotyping lies in the ability to quickly capture objective phenotypic data for large numbers of breeding lines in the field, through non-destructive and physically undemanding measures, which can be repeated over the season at multiple sites.

Once wheat breeding lines reach the advanced stages of a programme, grain yield usually becomes the predominant selection criterion and the value proposition of NGP decreases, moving from a selection tool to an exploratory tool. At this point lines have gone through multiple stages of visual phenotypic selection and any remaining lines are typically deemed agronomically suitable for release, with the final selection decisions being made primarily on yield and to some extent, end-use quality. While further phenotyping may not provide data for direct selections, it can provide additional data points to incorporate into statistical analyses, which may improve the heritability of grain yield and ultimately aid selection. Multi-variate analyses have been shown to be an effective method for analysing this type of data, increasing heritability of a desired trait and aiding selection (Rameeh, 2014).

One of the most widely proposed uses for these new technologies is phenotyping training populations for GS (Cabrera-Bosquet et al., 2012; Cobb et al., 2013; Lei et al., 2014). This would provide quick and accurate phenotypic data for modelling purposes and would be especially useful when large training sets of many thousands of lines are used. However, at present GS is in its infancy and has not been demonstrated in large-scale breeding programmes. Nevertheless, as described above, there are other applications of NGP within traditional breeding programmes.

There have been numerous studies of NGP in controlled environments, with specialised facilities being established for this purpose (for example the Australian Plant Phenomics Facility (2015) and the European Plant Phenotyping Network (2015)). A number of commercially available products have been produced (such as those available from LemnaTec (2015) and WPS (2015), which have proven to be useful tools for plant physiologists, but

are not easily, or obviously integrated into plant breeding programmes. As the technologies used in these controlled environment systems evolve, the challenge has been, and is, to adapt them for use in field trials for large-scale field research programmes such as plant breeding.

1.5 Sensors, Platforms and Applications

Next generation phenotyping technologies can be classified broadly into two categories; sensors and platforms. Sensors being the data or image capturing equipment, and platforms being the equipment used to deploy the sensor (Deery et al., 2014).

1.5.1 Sensors

In this emerging field of next generation phenotyping, a number of different sensors are required to attain the different types of data desired. This includes sensors used to characterise plants and their traits of interest, and geospatial sensors, to link data captured to a geological location for repeated measurements and later referencing. For the purpose of this review, sensors will be explored in the two categories of phenotyping and geospatial, describing the functions and applications relevant to each.

1.5.2 Phenotyping Sensors

Sensors used for phenotyping fall into two broad categories, point sensors and imaging sensors, the distinction between these categories and examples of these sensors are outlined in (Table 1.2). The predominant sensors used for phenotyping, along with common applications and advantages and disadvantages, are listed in Table 1.3 and described in greater detail in the subsequent sections.

Red, Green and Blue (RGB) Sensors

Red, green and blue (RGB) imagers capture light from the visible spectrum and are found most commonly in conventional digital cameras (Deery et al., 2014). RGB imagers are well suited to capturing data on crop canopies and have been shown to be an effective means of calculating field canopy cover (Adamsen et al., 1999; Lukina et al., 1999; Casadesús et al., 2007; Li et al., 2010), and determining leaf area index (LAI) (Liu & Pattey, 2010). This is achieved through an image segmentation process, where the crop canopy is separated from the background image.

RGB images have been shown to correlate strongly with the normalised difference vegetation index (NDVI) (Adamsen et al., 1999; Lukina et al., 1999; Casadesús et al., 2007), a commonly calculated index for measuring plant health, and through this have been used to calculate senescence within a wheat crop (Adamsen et al., 1999).

While canopy cover and NDVI are rarely high priority selection criteria themselves (Table 1.5), they could be used to evaluate material for early vigour or senescence/stay green. While this data might not be used for direct selection, it may further strengthen statistical analyses of grain yield in advanced material.

TABLE 1.2: The different categories of sensors and the way in which they capture data, with examples.

Sensor	Type	Data Capture	Example Sensors
Point	-	Logs data from a single geospatial point at a single time point	Infrared Thermometer, Spectroradiometer
	Line Scanning	Captures individual data points along a planar field at a single time point and can produce 3D point clouds with platform movement	LiDAR
Image	*Frame*	Captures a spatial matrix of 2D pixels from a single time point	RGB Camera, Thermal Camera, Multispectral Camera
	Line Scanning	Captures a single line of pixels or points at a single time point and uses the movement of the platform to produce an image	Push-broom Hyperspectral Camera

TABLE 1.3: Common sensors used for phenotyping, their applications and advantages and disadvantages.

Sensor	Data	Applications	Main Advantages	Main Disadvantages
RGB	2D spatial matrix	Canopy Cover, Senescence, Object Detection, 3D Modelling	Low entry cost	Captures only visible light
Spectral	2D spatial matrix or 3D hypercube	Vegetation Indices, Disease Detection	Captures light not visible to the human eye with many derivable outputs	Many sensors have limited spectral bands (multispectral) and/or are expensive (hyperspectral)
Thermal	2D spatial matrix	Canopy Temperature, Drought Resistance, Yield Potential	Captures light not visible to the human eye and a 'snapshot' of canopy temperature	Sensitive to environmental conditions
LiDAR	3D point cloud	3D Modelling, Plant Height, Above ground Biomass	Reduces the need for physically demanding phenotyping methods	Requires specialist skills to install and configure
Fluorescence	2D spatial matrix	Photosynthesis, Disease Detection	The most capable imaging sensor for detecting and measuring chlorophyll	Sensitive to light conditions

Perhaps a more exciting use of RGB images is that of object detection and texture analysis. To achieve this, algorithms are designed and written with the purpose of allowing computers to 'see' the image and detect specific traits (Dee & French, 2015). This is a growing field of research, with few published studies, however such techniques have been used to count the number of pepper fruits (Song et al., 2014) and wheat spikes (Li et al., 2014), as well as estimate panicle detection in oats (Boyle et al., 2015), under controlled environments. These techniques could prove especially useful to wheat breeding, for the purposes of detecting plant numbers, tiller numbers and spike numbers and perhaps even detecting anther extrusion, providing reliable and accurate information on important agronomic traits. However, adaption of these techniques to field data has yet to be demonstrated.

Another application of RGB imaging gaining popularity, due to the accessibility of cheap unmanned aerial vehicles (UAVs), is that of three-dimensional (3D) modelling, where large numbers of overlapping two-dimensional (2D) images are stitched together to create a 3D point cloud and model. This technique has been demonstrated by Murakami et al. (2012) for measuring height and lodging of buckwheat, with measurements being accurate within a few centimetres. Three-dimensional modelling from aerial images has the potential to be a useful tool during the early stages of a breeding programme (Figure 1.1; F_1 - F_5) for determining variation in plant height, or in later generation material for the determination of plant height, lodging and above ground biomass.

Spectral Sensors

Spectral sensors are receptive to wavelengths inside and outside of the visible spectrum and are available in a number of different forms, commonly hyperspectral cameras, multispectral cameras and near-infrared cameras and sensors.

Hyperspectral cameras capture light from visible to near-infrared spectrums (400 – 1000 nm) in narrow bands, typically 1 – 10 nm wide (Haboudane et al., 2004; Mulla, 2013; Devadas et al., 2015; Mahesh et al., 2015) and at low resolutions. Hyperspectral cameras can be of either push-broom (line-scanning) or snapshot (frame imaging) design. Multispectral cameras, unlike hyperspectral, respond only to a few narrow wavelength bands (Mulla,

2013), commonly in the red, green, blue and near-infrared spectrums, however they still capture at low resolutions.

Possibly the most common spectral sensors used in agriculture today are near-infrared/red sensors, popularised by the Greenseeker (Trimble, 2015) and similar products, which are used to calculate the normalised difference vegetation index (NDVI):

$$NDVI = \frac{NIR - VIS}{NIR + VIS} \tag{1.1}$$

where NIR is near-infrared and VIS is visible light. NDVI provides a ratio of near-infrared light (reflected by chlorophyll) and red light (absorbed by chlorophyll), measured through an active laser, and is commonly used to determine vegetation health.

This index has become popular within agricultural research and production, however there are a myriad of confounding factors that can influence readings in field conditions (Mulla, 2013), such as saturation of the index once canopy closure has occurred in healthy plots (Mulla, 2013). For this reason, NDVI appears to lend itself more to research or commercial production, rather than plant breeding, where genetic and environmental factors are at play. A plethora of other indices exist (extensive lists compiled by Sankaran et al. (2010) and Devadas et al. (2015)), though many of these indices become very specific, and may be better suited to plant physiology research rather than breeding programmes.

While many of these indices may not be suitable for direct application within breeding programmes, the creation of new indices or the use of individual wavelengths may be a feasible approach for the detection and quantification of plant diseases within breeding programmes. This would be highly beneficial within wheat breeding programme, where resistance to disease is an important selection criterion, especially during early generations. Currently, accurate foliar disease detection has been demonstrated in wheat, for both stripe rust (Moshou et al., 2006) and leaf rust (Devadas et al., 2015), with both of these being detected independently from nitrogen deficiency. Further research into this area, spanning a broad range of wheat foliar and soil borne diseases, may prove multi and/or hyperspectral sensors an important tool for use within wheat breeding programmes.

Thermal Sensors

Thermal cameras capture infrared wavelengths in the range of 3000 - 14000 nm, commonly 3000 - 5000 nm, providing a visual representation of temperature (Lei et al., 2014). This has proven to be a useful research tool for physiologists, with data captured from crop canopies showing high correlation to a number of traits such as transpiration rate, stomatal conductance, plant water status, water use and grain yield (Jones, 2004; Pask & Reynolds, 2012). It has also been suggested as a potential selection tool for breeders (Pask & Reynolds, 2012), to aid in selecting greater yields and drought tolerance.

Despite its suggestion as a selection tool, thermal sensing is not without limitations, with a wide range of variables that can alter temperature readings, including ambient temperature, light intensity, wind speed and sensor angle (Jones, 2004; Leinonen & Jones, 2004; Deery et al., 2014; Walter et al., 2015). Aerial thermal imaging may alleviate some of these limitations, with a single image capturing many, or all, plots within a trial at a single time point, minimising or eliminating any temporal changes, thus making this an obvious choice for breeding programmes should they wish to collect thermal data.

LiDAR Sensors

LiDAR sensors create 3D point clouds, calculated from the time of flight between emission and reflectance of an active scanning laser (Rosell Polo et al., 2009). This happens hundreds to thousands of times a second, with laser emissions typically occurring in a wide arc to give spatial data and therefore the ability to create a 3D model from the point cloud. Point cloud data can also be transformed into a 2D image comprised of pixels (raster image), more suited to standard image analysis procedures (Deery et al., 2014).

The novelty of LiDAR sensors to recreate crop canopies in 3D has resulted in numerous studies investigating this sensor's potential application in agricultural research. Calculating above ground biomass has been a particularly popular application and has been successfully demonstrated in wheat (Ehlert et al., 2009; Eitel et al., 2014), maize (Li et al., 2015) and arctic shrubs (Greaves et al., 2015). While more work is still required, especially in making this a tool easily adopted by researchers, each of these studies conclude that

LiDAR-estimated values are a suitable substitute for current destructive measurements. This is of particular importance to breeding programmes where destructive measurements cannot be conducted on early generation material (due to limited seed availability). LiDAR systems offer the opportunity to take repeated measurements throughout the season, tracking the accumulation of above ground biomass or other desired traits.

Other applications for LiDAR systems that have shown promise are measuring canopy height (Ehlert et al., 2009; Andujar et al., 2013; Deery et al., 2014; Li et al., 2015) and crop density (Hosoi & Omasa, 2009; Saeys et al., 2009). Deery et al. (2014) have also suggested the possibility of using LiDAR to identify individual plant organs and were able to separate wheat heads from the rest of the canopy, which was demonstrated by Saeys et al. (2009).

Fluorescence Sensors

Fluorescence imaging uses rapid illumination from the ultra violet spectrum to cause fluorescence, primarily in chlorophyll, which is then captured using a digital camera with a CCD sensor (Sankaran et al., 2010; Deery et al., 2014; Lei et al., 2014). Fluorescence imaging requires close proximity to the target (>1m) and an even distribution of illumination for accurate fluorescence levels to be captured (Deery et al., 2014).

As fluorescence primarily measures response of chlorophyll it is a useful tool for measuring photosynthesis and plant health (Lichtenthaler & Babani, 2000). Examples of fluorescence imaging use can be seen for water stress (Lichtenthaler & Babani, 2000), citrus canker infection and mechanical stress (Belasque et al., 2008). Despite its capabilities, fluorescence imaging is unlikely to be adopted for large-scale field research, due to the equipment required and difficulties of sensor proximity and lighting (Deery et al., 2014).

1.5.3 Geospatial Sensors

Geospatial sensors are an important part of next generation phenotyping systems, allowing data collected in the field to be georeferenced. These sensors are commonly found in the form of Global Positioning System (GPS) receivers. GPS systems are already common

throughout Australian agriculture, and are typically installed in tractors and harvesters to guide movement and allow the implementation of precision agricultural practices; this is common in both commercial scale field operations, as well as research trial work.

GPS receivers obtain a signal from four or more GPS satellites and triangulate a geographic position based from this information (Keskin et al., 2009). Real time kinematic (RTK) GPS is the most accurate of these systems providing a GPS location within 2 cm accuracy (James, 2009). This is achieved by using a base station, in addition to the GPS satellites, which applies signal correction and increases accuracy (James, 2009). This high resolution is a necessity for next generation phenotyping technologies, both for tracking data collection and for mapping purposes (White et al., 2012), and has been repeatedly demonstrated for georeferencing images and data (Comar et al., 2012; Busemeyer et al., 2013; Andrade-Sanchez et al., 2014; Deery et al., 2014).

1.5.4 Platforms

Platforms themselves can be divided into aerial or ground-based (Table 1.4), with these categories described in greater detail below.

TABLE 1.4: Common platforms used for phenotyping and their advantages and disadvantages.

Platform		**Advantages**	**Disadvantages**
Aerial	*Blimp*	Cheap Easy to deploy	Uses a limited resource (helium) Unstable in wind Cumbersome to store
	Unmanned Aerial Vehicle	Easily transportable and deployable Automatic flight and data capture	Medium spatial resolution Requires good weather Small payload Short flight time
	Manned Aircraft	Traverse large areas High payload Multi-sensor capture	Low spatial resolution Requires good weather Expensive
Mobile Ground	*Hand-held*	Easy to implement	Labour intensive Time consuming
	Mobile	Automatic data capture High spatial resolution	Expensive Specialist skills required to build and configure the system Typically slow moving

Aerial Platforms

Aerial imaging has traditionally been conducted with manned aircraft, requiring skilled licenced pilots and equipment operators, and is usually associated with a high cost. Manned aircraft can traverse large areas quickly, carry heavy payloads and record from multiple sensors simultaneously, however they are limited by weather conditions and have relatively low spatial resolutions for field trial work due to their relatively high flight altitude.

Unmanned Aerial Vehicles (UAVs) offer a number of advantages over manned aircraft as a sensory platform and can be classified as either fixed wing or multi-rotor systems. Both fixed wing and multi-rotor systems can carry comparable payloads and have similar flight times, however fixed wing systems can generally cover a greater distance from increased altitude and speed. UAV systems can be controlled autonomously through software, allowing missions to be planned and executed with little human intervention (Araus & Cairns, 2014). General advantages UAVs offer over manned aircraft are typically a greater spatial resolution due to relatively low altitude flights, flexible flight times and lower cost (Zhang & Kovacs, 2012). Even sensors which were once prohibitively large and heavy, such as hyperspectral cameras and LiDAR, are being developed for UAVs and are available commercially (PrecisionHawk, 2015; RIEGL, 2015), albeit at a high cost.

UAVs offer an attractive imaging solution to plant breeding programmes, as they can quickly and efficiently collect data over large areas and can be deployed on an ad-hoc basis. Despite this UAVs are yet to be proven as solid research tools; they are limited by flight time and harsh environmental conditions, and sensors suitable for UAVs may not currently have the spatial resolution to determine individual plants, rows or small plots within wheat breeding trials. Furthermore, regulations surrounding UAV use vary from country-to-country and are possibly the main impediment of UAV uptake and application (Zhang & Kovacs, 2012). This is an especially pertinent issue in Australia, where all non-recreational use of UAVs must be conducted by trained and licensed operators, as part of a licenced company or organisation (Civil Aviation Safety Authority, 2015).

An alternative option to manned and unmanned aircraft, are blimps, which are priced cheaply in comparison, and can carry multiple sensors at once (Murakami et al., 2012;

Araus & Cairns, 2014; Lei et al., 2014). However, once inflated they are difficult to move and unstable in even light wind, limiting their use to small trials, as well as taking up large amounts of room when stored (Araus & Cairns, 2014; Lei et al., 2014).

Mobile Ground Platforms

Precision ground phenotyping has traditionally been conducted on foot with hand-held equipment, such as digital infrared thermometers for measuring canopy temperature or sensors for measuring NDVI. However, these methods are slow, which can result in large temporal variation in measurements, and can be labour intensive (Deery et al., 2014).

Mobile ground platforms maintain the precision and accuracy captured with hand-held measurements, carrying high quality sensors such as used for hand-held phenotyping. Payload weight is unrestricted, allowing for multiple sensors to be mounted and is limited only by mounting space on the platform. Mobile ground platforms come in many forms, such as purpose-built push frames (White & Conley, 2013), self-propelled frames and buggies (Andrade-Sanchez et al., 2014; Deery et al., 2014), or modified vehicles such as tractors (Rosell Polo et al., 2009; Comar et al., 2012).

The main advantage of these platforms is that only a single traversal of a field is required per time point, capturing the data from multiple sensors simultaneously, while maintaining a high spatial resolution. However, current mobile ground platforms are generally not fast, with speeds being controlled by the walking pace of the operator for manual platforms and typically around 1 – 4 km/h for automated platforms (Deery et al., 2014; Pittman et al., 2015), leading to similar types of temporal variation as observed with hand measurements.

1.6 Targets and Technologies for Wheat Breeding

With all of these technologies now available, the question of their purpose and fit within a wheat breeding programme arises; when considering this, the structure (e.g. Figure 1.1) and objectives of the breeding programme must be kept in mind.

As seen in Figure 1.1 the majority of phenotypic selection occurs early in the programme, however, current technologies (described above) may not lend themselves to capturing data from individual plants or short rows and may require large rows, or plots for accurate data capture. With this in mind Table 1.5 was produced, listing potential traits of interest within a wheat breeding programme and speculating on the feasibility of different sensors to capture the phenotype of that trait. Traits were given an overall priority based on their potential use to the breeding programme (Kuchel and Edwards, *Pers. Comm.* 2015). The suitability of individual sensors to capture phenotype data of specific traits was assessed on the capabilities of each sensor, as described in the current literature. The overall feasibility of successfully phenotyping and integrating data for each trait within a breeding programme exists semi-independently from the suitability of individual sensors. In this case algorithm and software development required to measure the trait, and the practicality of using the required sensors within the programme, were also considered. Table 1.5 is an example produced for one breeding programme, with priorities (and the feasibility) likely to differ from programme to programme.

In this scenario, relatively simple agronomic traits were given a high priority, partially as they should be achievable within a reasonable timeframe, but also as they are time or labour-intensive traits to measure. These traits provide a fairly complete picture of crop growth, especially if captured frequently over time, and may lend themselves well to phenotypic modelling and validation.

As these technologies develop and move from early adoption to common use, the feasibility of traits will change, allowing more difficult traits such as flowing time and individual disease detection to be accurately measured and integrated into the programme.

TABLE 1.5: An example of trait priority for a wheat breeding programme, with the feasibility[1] of measuring each trait and the suitability[2] of different sensors to be used for that measurement. Feasibility, priority and suitability are scored on a 1-9 scale, with 1 being low priority/highly unlikely and 9 being high priority/highly likely.

Trait	**Priority**	**Feasibility**	*RGB (Singular)*	*RGB (Stereo)*	*NIR*	*Hyperspectral*	*Multispectral*	*Fluorescence*	*Thermal (IR)*	*LiDAR*
Plant No.	**9**	**9**	9	9	4	2	2	1	2	6
Spike No.	**9**	**8**	9	9	1	1	1	1	1	7
Above ground Biomass	**8**	**9**	2	6	1	1	4	1	1	9
Plant Height	**8**	**9**	1	6	1	1	1	1	1	9
N content	**8**	**7**	1	1	7	7	7	1	1	3
Green Leaf Area	**4**	**9**	9	9	9	5	7	1	1	8
Flag Leaf Chlorophyll	**3**	**4**	2	2	8	8	8	7	1	1
Head Colour	**2**	**5**	7	7	1	1	1	1	1	1
Glaucousness	**2**	**2**	2	2	1	3	3	1	1	1
Senescence (Rate of	**5**	**7**	8	8	5	5	5	1	1	1
Yellows	**6**	**6**	7	7	2	3	3	1	1	1
Leaf Tip Necrosis	**5**	**4**	5	5	2	3	3	1	1	1
Disease	**6**	**3**	6	6	2	8	8	7	4	1
Foliar	**4**	**3**	6	6	2	8	8	7	4	1
Crown Rot	**8**	**6**	7	7	2	6	6	4	6	1
Flowering Time	**9**	**3**	6	6	1	2	2	1	1	1
Head Shattering	**3**	**2**	5	5	1	2	2	1	1	1
Sprouting	**3**	**1**	5	5	3	3	3	1	1	1
(Flag) Leaf Width	**3**	**3**	8	8	1	1	1	1	1	5
Canopy Temperature	**3**	**8**	1	1	1	1	1	1	9	1
Growth Habit	**2**	**2**	2	2	1	1	1	1	1	3
Lodging	**7**	**8**	2	8	1	1	1	1	1	8
Plot Damage	**9**	**7**	5	5	3	5	5	1	2	6

[1]Feasibility is the likelihood of implementing sensors to a large-scale breeding programme (including the production of algorithms and software for image processing) and successfully measuring the desired trait within a 3 year timeframe

[2]Sensor suitability is scored as the likelihood of that sensor measuring the trait of interest

With the current state of sensor technology, mobile ground platforms appear to be the more appropriate option, as opposed to aerial platforms, for wheat breeding programmes looking to implement these technologies. This is primarily due to increased spatial resolution by the proximity of sensors to the crop canopy; an advantage that will however, eventually be lost as sensor technology improves and the spatial resolution achievable from aerial platforms increases. Though the current speed achievable from mobile ground platforms does not allow for truly high-throughput phenotyping, without the high spatial resolution they achieve it is not possible to measure more detailed traits (such as plant and spike number).

1.7 Current Limitations

It is clear that there are a wide range of technologies that will play a role in next generation phenotyping systems, but with these technologies, there are a range of issues that are yet to be addressed to facilitate their uptake for plant breeding programmes. These issues are discussed in the sections below.

1.7.1 System Development

The task of building a field phenotyping system is a challenge in itself, especially in the case of mobile ground systems, and in most circumstances will require the assistance of mechanical and software engineers. These engineers are required for the design, production and/or modification of the platform as well as the integration of imaging, geospatial and data storage systems. Even in the case of simple ground based platforms, such as described by White & Conley (2013), skills are required for frame construction and integration of sensors and associated systems. In general, phenotyping platforms will require the sensors, mounting systems, power, connections to data loggers and where necessary software for operation and control (White et al., 2012).

The exception to this may be small scale custom built or pre-built consumer ready UAVs which can be built or set up with relative ease. In many ways UAVs are a much simpler

solution than mobile ground platforms; consumer ready systems need only minimal levels of assembly (attachment of wings/rotors/cameras etc.) and often come supplied with software for flight control. Custom built UAVs will require some skill and understanding of the components to assemble, with open-source and licensed software packages available for flight control. There are currently no consumer ready mobile ground platforms or sensor integration software packages available for purchase, or available through open-source, with both platforms and software typically being developed in-house.

1.7.2 Data Processing and Analysis

Data processing and analysis poses a significant challenge for the implementation of NGP systems. The majority of data processing and analysis requires specialist skills, which in most cases, are unique to each sensor. In the case of multiple sensors, simultaneously logged data must first be integrated to form a complete data set, a potentially extensive process, typically achieved with proprietary protocols developed in-house (White et al., 2012). Aside from processing data to a state at which analyses can be conducted, it is often necessary to adjust or calibrate measurements to account for changes in light intensity, environmental and/or biological factors, to reduce variability in the data (Cobb et al., 2013; Araus & Cairns, 2014).

There are currently no standards for the processing or analysis of data, with methods being discerned on a case-by-case basis. A number of freely available software options for image analysis are available (Lobet et al., 2013), however, the majority of this software focuses analysis on specific traits which are not applicable for field-based phenotyping.

Despite the lack of standard procedures for processing and analysis there has been much speculation as to how these broad procedures may be approached and improved in the future (White et al., 2012; Cobb et al., 2013; Araus & Cairns, 2014). Automation and ease of use are key themes within these speculations, reducing human input and therefore saving resources, though this comes at a cost of reduced adaptability and the requirement of more specialised software design (Cobb et al., 2013; Araus & Cairns, 2014). Even in the case of fully automated systems, outputs must be checked and validated regularly to detect unforeseen errors and prevent nonsensical analyses (Cobb et al., 2013). It is highly likely

that advanced statistical tools, beyond the current standards, will be required to analyse this data (White et al., 2012).

More complex analyses can be time consuming and require a great deal of computing power, with this only escalating as the amount of data increases (White et al., 2012). Time frames of data processing and analysis are not commonly reported, with implications of these time 'sinks' in plant breeding programmes being difficult to fully comprehend. Simple threshold analyses can be conducted for thousands of plots in under 15 minutes, with little to no processing required, yet merely processing mosaic images of field trials for later analysis may take more than a day of high-performance computer processing. In the case of the breeding scenario in Figure 1.1, if advanced yield plots were to be assessed across 20 field sites using UAVs, merely processing the data from a single sensor would require 20 or more days of computing power.

1.7.3 Data Management and Storage

The management and storage of data acquired by these phenotyping systems is proving to be yet another challenge to their integration within plant breeding programmes, with this being a substantially more difficult task than acquiring the data itself (Cobb et al., 2013). White et al. (2012) calculated that in the scenario of a breeding programme with 20,000 plots to be phenotyped, a single pass of these plots with a phenotyping system acquiring four 10 mega-pixel images per plot (3 RGB and 1 thermal IR) would create 80 gigabytes of data after being stored with a 1:10 compression. This considers only raw data, with the amount of data increasing dramatically as processed data is stored, not to mention the addition of multiple sampling times or sensors such as LiDAR and hyperspectral cameras, or data that does not lend itself to efficient compression. Once accounting for these factors, the proposition of managing and storing all this data becomes a significant challenge.

There are currently no standardised systems available for handling phenotype data, with expertise required to establish in-house solutions (Cobb et al., 2013). It is entirely possible that in the years ahead, storage of phenotype data will follow the same trend occurring with genotype data; where the cost of data acquisition is cheaper than the cost of storing

the data itself (Stein, 2010). In the case of genotype data, Stein (2010) has proposed that cloud computing and storage could be an economic solution.

As phenotyping systems become integrated into breeding programmes, it is highly likely that phenotypic data will be combined with genotypic data. This creates the unique challenge of altering already established databases, capable of holding genotype information, to hold phenotype information, or to create new databases which are capable of both. There are currently a number of public databases attempting this feat, such as PHENOPSIS DB (Fabre et al., 2011), the Rice Mutant Database (Zhang et al., 2006) and The Triticeae Toolbox (Triticeae Coordinated Agricultural Project, 2015). These currently available database tools may be more suited to researchers rather than plant breeders, however, they demonstrate the capabilities of the technology.

1.7.4 Data Integration and Application

Throughout this review a variety of uses and applications for new phenotyping technologies have been identified, yet despite this, there has yet to be practical implementation of these technologies in plant breeding, or more specifically wheat breeding programmes. To achieve this, each programme will need to individually determine which traits and data are important (e.g. Table 1.5) and implement technologies capable of recording this data (i.e. appropriate sensors and platforms).

1.8 Summary

Phenotyping has been a long-standing selection method for wheat breeding programmes, and is again receiving attention now that genotypic information can be attained so quickly and cheaply. Wheat breeding programmes have now reached a point where population sizes are prohibitively large to phenotype and finding a solution to overcome this is a priority.

Numerous sensors and platforms have been investigated for next generation phenotyping in general research, and these tools may be useful for passing the phenotyping limitation

within plant breeding programmes. Sensors and platforms used by breeding programmes will need to be tailored to each individual programme and their breeding objectives.

As yet these technologies have not been successfully demonstrated within a breeding programme and there are currently many limitations preventing their uptake. Phenotyping platforms can be difficult to build and operate, data processing can be complex and the implications of managing and storing the amount of data which could be produced within a breeding programme is yet to be realised. To overcome this, these technologies need to be implemented into large-scale, functioning, breeding programmes, where their advantages and disadvantages can be assessed. This will allow selection of the most effective technologies, and the opportunity to alter breeding strategies where necessary, to increase rates of genetic gain within the programme.

Bibliography

ADAMSEN, F. G., PINTER, P. J., BARNES, E. M., LAMORTE, R. L., WALL, G. W., LEAVITT, S. W., & KIMBALL, B. A. (1999). Measuring wheat senescence with a digital camera. *Crop Science* **39**, 719–724.

ALLARD, R. W. (1964). *Principles of Plant Breeding*. John Wiley & Sons, Inc., United States of America, second edition.

ANDRADE-SANCHEZ, P., GORE, M. A., HEUN, J. T., THORP, K. R., CARMO-SILVA, A. E., FRENCH, A. N., SALVUCCI, M. E., & WHITE, J. W. (2014). Development and evaluation of a field-based high-throughput phenotyping platform. *Functional Plant Biology* **41**, 68–79.

ANDUJAR, D., RUEDA-AYALA, V., MORENO, H., ROSELL-POLO, J. R., ESCOLA, A., VALERO, C., GERHARDS, R., FERNANDEZ-QUINTANILLA, C., DORADO, J., & GRIEPENTROG, H. W. (2013). Discriminating crop, weeds and soil surface with a terrestrial lidar sensor. *Sensors* **13**, 14662–14675.

ARAUS, J. L. & CAIRNS, J. E. (2014). Field high-throughput phenotyping: the new crop breeding frontier. *Trends in Plant Science* **19**, 52–61.

AUSTRALIAN PLANT PHENOMICS FACILITY (2015). The plant accelerator (high-throughput phenotyping) [online]. Available at: http://www.plantphenomics.org.au/services/accelerator/ [Accessed 13th September 2015].

BELASQUE, J., GASPAROTO, M. C. G., & MARCASSA, L. G. (2008). Detection of mechanical and disease stresses in citrus plants by fluorescence spectroscopy. *Applied Optics* **47**, 1922–1926.

BOCK, C. H., POOLE, G. H., PARKER, P. E., & GOTTWALD, T. R. (2010). Plant disease severity estimated visually, by digital photography and image analysis, and by hyperspectral imaging. *Critical Reviews in Plant Sciences* **29**, 59–107.

BOUQUET, A. & JUGA, J. (2013). Integrating genomic selection into dairy cattle breeding programmes: a review. *Animal* **7**, 705–713.

BOYLE, R., CORKE, F., & HOWARTH, C. (2015). Image-based estimation of oat panicle development using local texture patterns. *Functional Plant Biology* **42**, 433–443.

BUSEMEYER, L., MENTRUP, D., MOLLER, K., WUNDER, E., ALHEIT, K., HAHN, V., MAURER, H. P., REIF, J. C., WURSCHUM, T., MULLER, J., RAHE, F., & RUCKELSHAUSEN, A. (2013). Breedvision - a multi-sensor platform for non-destructive field-based phenotyping in plant breeding. *Sensors* **13**, 2830–2847.

CABRERA-BOSQUET, L., CROSSA, J., VON ZITZEWITZ, J., SERRET, M. D., & ARAUS, J. L. (2012). High-throughput phenotyping and genomic selection: The frontiers of crop breeding converge. *Journal of Integrative Plant Biology* **54**, 312–320.

CASADESÚS, J., KAYA, Y., BORT, J., NACHIT, M. M., ARAUS, J. L., AMOR, S., FERRAZZANO, G., MAALOUF, F., MACCAFERRI, M., MARTOS, V., OUABBOU, H., & VILLEGAS, D. (2007). Using vegetation indices derived from conventional digital cameras as selection criteria for wheat breeding in water-limited environments. *Annals of Applied Biology* **150**, 227–236.

CIVIL AVIATION SAFETY AUTHORITY (2015). Civil aviation safety authority [online]. Available at: https://www.casa.gov.au/ [Accessed 10th September 2015].

COBB, J. N., DECLERCK, G., GREENBERG, A., CLARK, R., & MCCOUCH, S. (2013). Next-generation phenotyping: requirements and strategies for enhancing our understanding of genotype-phenotype relationships and its relevance to crop improvement. *Theoretical and Applied Genetics* **126**, 867–887.

COMAR, A., BURGER, P., DE SOLAN, B., BARET, F., DAUMARD, F., & HANOCQ, J. F. (2012). A semi-automatic system for high throughput phenotyping wheat cultivars in-field conditions: description and first results. *Functional Plant Biology* **39**, 914–924.

COOPER, M., MESSINA, C. D., PODLICH, D., TOTIR, L. R., BAUMGARTEN, A., HAUSMANN, N. J., WRIGHT, D., & GRAHAM, G. (2014). Predicting the future of plant breeding: complementing empirical evaluation with genetic prediction. *Crop & Pasture Science* **65**, 311–336.

DEE, H. & FRENCH, A. (2015). From image processing to computer vision: plant imaging grows up foreword. *Functional Plant Biology* **42**, III–V.

DEERY, D., JIMENEZ-BERNI, J., JONES, H., SIRAULT, X., & FURBANK, R. (2014). Proximal remote sensing buggies and potential applications for field-based phenotyping. *Agronomy* **4**, 349.

DEKKERS, J. C. M. & HOSPITAL, F. (2002). The use of molecular genetics in the improvement of agricultural populations. *Nature Reviews Genetics* **3**, 22–32.

DEVADAS, R., LAMB, D. W., BACKHOUSE, D., & SIMPFENDORFER, S. (2015). Sequential application of hyperspectral indices for delineation of stripe rust infection and nitrogen deficiency in wheat. *Precision Agriculture* **16**, 477–491.

EHLERT, D., ADAMEK, R., & HORN, H.-J. (2009). Laser rangefinder-based measuring of crop biomass under field conditions. *Precision Agriculture* **10**, 395–408.

EITEL, J. U. H., MAGNEY, T. S., VIERLING, L. A., BROWN, T. T., & HUGGINS, D. R. (2014). Lidar based biomass and crop nitrogen estimates for rapid, non-destructive assessment of wheat nitrogen status. *Field Crops Research* **159**, 21–32.

EUROPEAN PLANT PHENOTYPING NETWORK (2015). European plant phenotyping network [online]. Available at: http://www.plant-phenotyping-network.eu/eppn/home [Accessed 13th September 2015].

FABRE, J., DAUZAT, M., NEGRE, V., WUYTS, N., TIREAU, A., GENNARI, E., NEVEU, P., TISNE, S., MASSONNET, C., HUMMEL, I., & GRANIER, C. (2011). Phenopsis db: an information system for arabidopsis thaliana phenotypic data in an environmental context. *Bmc Plant Biology* **11**, 7.

GREAVES, H. E., VIERLING, L. A., EITEL, J. U. H., BOELMAN, N. T., MAGNEY, T. S., PRAGER, C. M., & GRIFFIN, K. L. (2015). Estimating aboveground biomass and leaf

area of low-stature arctic shrubs with terrestrial lidar. *Remote Sensing of Environment* **164**, 26–35.

HABOUDANE, D., MILLER, J. R., PATTEY, E., ZARCO-TEJADA, P. J., & STRACHAN, I. B. (2004). Hyperspectral vegetation indices and novel algorithms for predicting green lai of crop canopies: Modeling and validation in the context of precision agriculture. *Remote Sensing of Environment* **90**, 337–352.

HALLORAN, G. M.; KNIGHT, R. M. K. S. S. D. H. B. (1979). *A Course Manual in Plant Breeding*. Australian Vice Chancellors' Committee, Canberra, Australia.

HOLLAMBY, G. M. (1983). *The Staff of Life, The History of Plant Breeding at Roseworthy Agricultural College*. Griffin Press, Roseworthy, Australia.

HOSOI, F. & OMASA, K. (2009). Estimating vertical plant area density profile and growth parameters of a wheat canopy at different growth stages using three-dimensional portable lidar imaging. *ISPRS Journal of Photogrammetry and Remote Sensing* **64**, 151–158.

JAMES, M. (2009). Differential gps guidance systems for field work in agriculture. *R&D Conference "Precision in arable farming: current practice and future potential", Grantham, Lincolnshire, UK, 28th-29th October 2009* pages 77–88.

JOHANNSEN, W. (1911). The genotype conception of heredity. *American Naturalist* **45**, 129–159.

JONES, H. G. (2004). Application of thermal imaging and infrared sensing in plant physiology and ecophysiology. In Callow, J. A., editor, *Advances in Botanical Research Incorporating Advances in Plant Pathology, Vol 41*, volume 41 of *Advances in Botanical Research*, pages 107–163. Academic Press Ltd-Elsevier Science Ltd, London.

JULIANA, P., RUTKOSKI, J. E., POLAND, J. A., SINGH, R. P., MURUGASAMY, S., NATESAN, S., BARBIER, H., & SORRELLS, M. E. (2015). Genome-wide association mapping for leaf tip necrosis and pseudo-black chaff in relation to durable rust resistance in wheat. *Plant Genome* **8**, 12.

KESKIN, M., SAY, S. M., & KESKIN, S. G. (2009). Evaluation of a low-cost gps receiver for precision agriculture use in adana province of turkey. *Turkish Journal of Agriculture and Forestry* **33**, 79–88.

KUCHEL, H., FOX, R., REINHEIMER, J., MOSIONEK, L., WILLEY, N., BARIANA, H., & JEFFERIES, S. (2007). The successful application of a marker-assisted wheat breeding strategy. *Molecular Breeding* **20**, 295–308.

KUCHEL, H., YE, G. Y., FOX, R., & JEFFERIES, S. (2005). Genetic and economic analysis of a targeted marker-assisted wheat breeding strategy. *Molecular Breeding* **16**, 67–78.

LEI, L., QIN, Z., & DANFENG, H. (2014). A review of imaging techniques for plant phenotyping. *Sensors* **14**, 20078–20111.

LEINONEN, I. & JONES, H. G. (2004). Combining thermal and visible imagery for estimating canopy temperature and identifying plant stress. *Journal of Experimental Botany* **55**, 1423–1431.

LEMNATEC (2015). Products [online]. Available at: http://www.lemnatec.com/products/ [Accessed 13th September 2015].

LI, Q., JINHAI, C., BERGER, B., & MIKLAVCIC, S. (2014). Study on spike detection of cereal plants. *2014 13th International Conference on Control Automation Robotics & Vision (ICARCV). Proceedings* pages 228–233.

LI, W., NIU, Z., HUANG, N., WANG, C., GAO, S., & WU, C. Y. (2015). Airborne lidar technique for estimating biomass components of maize: A case study in zhangye city, northwest china. *Ecological Indicators* **57**, 486–496.

LI, Y., CHEN, D., WALKER, C. N., & ANGUS, J. F. (2010). Estimating the nitrogen status of crops using a digital camera. *Field Crops Research* **118**, 221–227.

LICHTENTHALER, H. K. & BABANI, F. (2000). Detection of photosynthetic activity and water stress by imaging the red chlorophyll fluorescence. *Plant Physiology and Biochemistry* **38**, 889–895.

LIU, J. & PATTEY, E. (2010). Retrieval of leaf area index from top-of-canopy digital photography over agricultural crops. *Agricultural and Forest Meteorology* **150**, 1485–1490.

LOBET, G., DRAYE, X., & PERILLEUX, C. (2013). An online database for plant image analysis software tools. *Plant Methods* **9**, 7.

LUKINA, E. V., STONE, M. L., & RANN, W. R. (1999). Estimating vegetation coverage in wheat using digital images. *Journal of Plant Nutrition* **22**, 341–350.

MAHESH, S., JAYAS, D. S., PALIWAL, J., & WHITE, N. D. G. (2015). Hyperspectral imaging to classify and monitor quality of agricultural materials. *Journal of Stored Products Research* **61**, 17–26.

MEUWISSEN, T. H. E., HAYES, B. J., & GODDARD, M. E. (2001). Prediction of total genetic value using genome-wide dense marker maps. *Genetics* **157**, 1819–1829.

MOSHOU, D., BRAVO, C., WAHLEN, S., WEST, J., MCCARTNEY, A., DE BAERDEMAEKER, J., & RAMON, H. (2006). Simultaneous identification of plant stresses and diseases in arable crops using proximal optical sensing and self-organising maps. *Precision Agriculture* **7**, 149–164.

MULLA, D. J. (2013). Twenty five years of remote sensing in precision agriculture: Key advances and remaining knowledge gaps. *Biosystems Engineering* **114**, 358–371.

MURAKAMI, T., YUI, M., & AMAHA, K. (2012). Canopy height measurement by photogrammetric analysis of aerial images: Application to buckwheat (fagopyrum esculentum moench) lodging evaluation. *Computers and Electronics in Agriculture* **89**, 70–75.

PASK, AJD., P. J. M. D. & REYNOLDS, M. E. (2012). *Physiological Breeding II: A Field Guide to Wheat Phenotyping*. CIMMYT, Mexico, D.F.

PITTMAN, J. J., ARNALL, D. B., INTERRANTE, S. M., MOFFET, C. A., & BUTLER, T. J. (2015). Estimation of biomass and canopy height in bermudagrass, alfalfa, and wheat using ultrasonic, laser, and spectral sensors. *Sensors* **15**, 2920–2943.

PRECISIONHAWK (2015). Sensors]. Available at: http://www.precisionhawk.com/ [Accessed 17th September 2015].

RAMEEH, V. (2014). Multivariate regression analyses of yield associated traits in rapeseed (brassica napus l.) genotypes. *Advances in Agriculture* **2014**, 5.

RIEGL (2015). Unmanned laser scanning [online]. Available at: http://www.riegl.com/products/unmanned-scanning/ [Accessed 17th September 2015].

ROSELL POLO, J. R., SANZ, R., LLORENS, J., ARNO, J., ESCOLA, A., RIBES-DASI, P., MASIP, J., CAMP, F., GRACIA, F., SOLANELLES, F., PALLEJA, T., PAL, L., PLANAS, S., GIL, E., & PALACIN, J. (2009). A tractor-mounted scanning lidar for the non-destructive measurement of vegetative volume and surface area of tree-row plantations: A comparison with conventional destructive measurements. *Biosystems Engineering* **102**, 128–134.

SAEYS, W., LENAERTS, B., CRAESSAERTS, G., & DE BAERDEMAEKER, J. (2009). Estimation of the crop density of small grains using lidar sensors. *Biosystems Engineering* **102**, 22–30.

SANKARAN, S., MISHRA, A., EHSANI, R., & DAVIS, C. (2010). A review of advanced techniques for detecting plant diseases. *Computers and Electronics in Agriculture* **72**, 1–13.

SHEEN, S. J., EBELTOFT, D. C., & SMITH, G. S. (1968). Association and inheritance of black chaff and stem rust reactions in conley wheat crosses. *Crop Science* **8**, 477–480.

SINGH, R. P. (1992). Association between gene lr34 for leaf rust resistance and leaf tip necrosis in wheat. *Crop Science* **32**, 874–878.

SONG, Y., GLASBEY, C. A., HORGAN, G. W., POLDER, G., DIELEMAN, J. A., & VAN DER HEIJDEN, G. (2014). Automatic fruit recognition and counting from multiple images. *Biosystems Engineering* **118**, 203–215.

STEIN, L. D. (2010). The case for cloud computing in genome informatics. *Genome Biology* **11**, 7.

TRIMBLE (2015). Greenseeker crop sensing system [online]. Available at: http://www.trimble.com/Agriculture/greenseeker.aspx [Accessed 4th November 2015].

TRITICEAE COORDINATED AGRICULTURAL PROJECT (2015). The triticeae toolbox [online]. Available at: https://triticeaetoolbox.org/ [Accessed 19th November 2015].

WALTER, A., LIEBISCH, F., & HUND, A. (2015). Plant phenotyping: from bean weighing to image analysis. *Plant Methods* **11**, 11.

WHITE, J. W., ANDRADE-SANCHEZ, P., GORE, M. A., BRONSON, K. F., COFFELT, T. A., CONLEY, M. M., FELDMANN, K. A., FRENCH, A. N., HEUN, J. T., HUNSAKER, D. J., JENKS, M. A., KIMBALL, B. A., ROTH, R. L., STRAND, R. J., THORP, K. R., WALL,

G. W., & WANG, G. Y. (2012). Field-based phenomics for plant genetics research. *Field Crops Research* **133**, 101–112.

WHITE, J. W. & CONLEY, M. M. (2013). A flexible, low-cost cart for proximal sensing. *Crop Science* **53**, 1646–1649.

WPS (2015). Overview products plant phenotyping [online]. Available at: http://www.wps.eu/en/plant-phenotyping/overview-products-plant-phenotyping [Accessed 13th September 2015].

YOUSEF, G. G. & JUVIK, J. A. (2001). Comparison of phenotypic and marker-assisted selection for quantitative traits in sweet corn. *Crop Science* **41**, 645–655.

ZHANG, C. H. & KOVACS, J. M. (2012). The application of small unmanned aerial systems for precision agriculture: a review. *Precision Agriculture* **13**, 693–712.

ZHANG, J. W., LI, C. S., WU, C. Y., XIONG, L. Z., CHEN, G. X., ZHANG, Q. F., & WANG, S. P. (2006). Rmd: a rice mutant database for functional analysis of the rice genome. *Nucleic Acids Research* **34**, D745–D748.

Chapter 2

High-Throughput Field Imaging and Basic Image Analysis in a Wheat Breeding Programme

Statement of Authorship

Title of Paper	High-throughput field imaging and basic image analysis in a wheat breeding programme
Publication Status	☑ Published ☐ Accepted for Publication ☐ Submitted for Publication ☐ Unpublished and Unsubmitted work written in manuscript style
Publication Details	Walter J, Edwards J, Cai J, McDonald G, Miklavcic SJ and Kuchel H (2019) High-Throughput Field Imaging and Basic Image Analysis in a Wheat Breeding Programme. Front. Plant Sci. 10:449. doi: 10.3389/fpls.2019.00449

Principal Author

Name of Principal Author (Candidate)	James Walter		
Contribution to the Paper	Designed infrastructure and contributed to development of software used in the publication, developed methods, collected/analysed/interpreted data, wrote manuscript and acted as corresponding author.		
Overall percentage (%)	75%		
Certification:	This paper reports on original research I conducted during the period of my Higher Degree by Research candidature and is not subject to any obligations or contractual agreements with a third party that would constrain its inclusion in this thesis. I am the primary author of this paper.		
Signature		Date	24/5/2019

Co-Author Contributions

By signing the Statement of Authorship, each author certifies that:

i. the candidate's stated contribution to the publication is accurate (as detailed above);

ii. permission is granted for the candidate in include the publication in the thesis; and

iii. the sum of all co-author contributions is equal to 100% less the candidate's stated contribution.

Name of Co-Author	James Edwards		
Contribution to the Paper	Supervised development of work, designed infrastructure and contributed to development of software used in the publication, helped to interpret data, evaluate and edit the manuscript.		
Signature		Date	29/5/2019

Name of Co-Author	Jinhai Cai		
Contribution to the Paper	Designed infrastructure and developed software used within the publication, helped to evaluate and edit the manuscript.		
Signature		Date	30/05/2019

Name of Co-Author	Glenn McDonald
Contribution to the Paper	Supervised development of work, helped to interpret data, evaluate and edit the manuscript.
Signature	Date 31/5/19

Name of Co-Author	Stanley J. Miklavcic
Contribution to the Paper	Designed infrastructure and contributed to the development software used within the publication, helped to evaluate and edit the manuscript.
Signature	Date 24/5/19

Name of Co-Author	Haydn Kuchel
Contribution to the Paper	Supervised development of work, designed infrastructure and contributed to development of software used in the publication, helped to interpret data, evaluate and edit the manuscript.
Signature	Date 29/5/19

frontiers in Plant Science

ORIGINAL RESEARCH
published: 24 April 2019
doi: 10.3389/fpls.2019.00449

High-Throughput Field Imaging and Basic Image Analysis in a Wheat Breeding Programme

James Walter[1,2], James Edwards[1,2], Jinhai Cai[3], Glenn McDonald[1], Stanley J. Miklavcic[3] and Haydn Kuchel[1,2]*

[1] School of Agriculture, Food and Wine, The University of Adelaide, Glen Osmond, SA, Australia, [2] Australian Grain Technologies Pty Ltd., Roseworthy, SA, Australia, [3] Phenomics and Bioinformatics Research Centre, School of Information Technology and Mathematical Sciences, University of South Australia, Mawson Lakes, SA, Australia

Visual assessment of colour-based traits plays a key role within field-crop breeding programmes, though the process is subjective and time-consuming. Digital image analysis has previously been investigated as an objective alternative to visual assessment for a limited number of traits, showing suitability and slight improvement to throughput over visual assessment. However, easily adoptable, field-based high-throughput methods are still lacking. The aim of the current study was to produce a high-throughput digital imaging and analysis pipeline for the assessment of colour-based traits within a wheat breeding programme. This was achieved through the steps of (i) a proof-of-concept study demonstrating basic image analysis methods in a greenhouse, (ii) application of these methods to field trials using hand-held imaging, and (iii) developing a field-based high-throughput imaging infrastructure for data collection. The proof of concept study showed a strong correlation (r = 0.95) between visual and digital assessments of wheat physiological yellowing (PY) in a greenhouse environment, with both scores having similar heritability (H^2 = 0.85 and 0.76, respectively). Digital assessment of hand-held field images showed strong correlations to visual scores for PY (r = 0.61 and 0.78), senescence (r = 0.74 and 0.75) and Septoria tritici blotch (STB; r = 0.76), with greater heritability of digital scores, excluding STB. Development of the high-throughput imaging infrastructure allowed for images of field plots to be collected at a rate of 7,400 plots per hour. Images of an advanced breeding trial collected with this system were analysed for canopy cover at two time-points, with digital scores correlating strongly to visual scores (r = 0.88 and 0.86) and having similar or greater heritability. This study details how high-throughput digital phenotyping can be applied to colour-based traits within field trials of a wheat breeding programme. It discusses the logistics of implementing such systems with minimal disruption to the programme, provides a detailed methodology for the basic image analysis methods utilized, and has potential for application to other field-crop breeding or research programmes.

Keywords: phenotyping, physiological yellows, senescence, septoria tritici blotch, canopy cover

OPEN ACCESS

Edited by:
Andreas Hund,
ETH Zürich, Switzerland

Reviewed by:
Harsh Raman,
New South Wales Department of Primary Industries, Australia
Jorge E. Mayer,
Ag RD&IP Consult P/L, Australia

****Correspondence:***
James Walter
james.walter@agtbreeding.com.au

Specialty section:
This article was submitted to Technical Advances in Plant Science, a section of the journal Frontiers in Plant Science

Received: *30 January 2019*
Accepted: *25 March 2019*
Published: *24 April 2019*

Citation:
Walter J, Edwards J, Cai J, McDonald G, Miklavcic SJ and Kuchel H (2019) High-Throughput Field Imaging and Basic Image Analysis in a Wheat Breeding Programme. Front. Plant Sci. 10:449. doi: 10.3389/fpls.2019.00449

INTRODUCTION

Visual assessment of traits within field trials is subjective and laborious. However, it is an essential process for plant breeders who wish to observe the phenotype of material within their programme and determine genotype-by-environment effects. In recent years numerous high-throughput digital phenotyping methods have been proposed (Busemeyer et al., 2013; White and Conley, 2013; Andrade-Sanchez et al., 2014; Deery et al., 2014; Bai et al., 2016; Underwood et al., 2017; Jimenez-Berni et al., 2018), all of which offer to alleviate the current visual phenotyping bottleneck which exists within modern plant breeding programmes (Cobb et al., 2013; Araus and Cairns, 2014). Despite this, truly high-throughput systems which are easily integrated within large-scale breeding programmes are yet to be developed and used.

Typically, these phenotyping platforms are equipped with an array of sensors, with popular choices including red, green and blue (RGB) cameras, multi-spectral cameras, normalised difference vegetation index (NDVI) sensors and LiDAR. RGB cameras, in particular, have a long history with field phenotyping and in a number of studies have been effective in estimating canopy cover of field crops (Lukina et al., 1999; Casadesús et al., 2007; Liu and Pattey, 2010; Mullan and Reynolds, 2010). The popularity of these methods, from both a research and farmer perspective, has culminated in the development of a simple mobile application, which enables users to conduct simple *in-situ* estimates of canopy cover from their mobile devices (Oklahoma State University, 2015). The use of RGB cameras as a phenotyping tool has focused on digital images to estimate canopy cover or as an alternative to NDVI (Casadesús et al., 2007; Morgounov et al., 2014). However, they have also been used to a lesser extent to assess senescence (Adamsen et al., 1999; Hafsi et al., 2000), crop nitrogen content (Li et al., 2010), early vigour (Kipp et al., 2014) and soil water evaporation (Mullan and Reynolds, 2010). Image analysis techniques used to asses this range of traits also have the potential to be applied to other colour-based traits, such as disease assessment, which may provide wheat breeders with an objective system of assessment for specific traits within their breeding programme.

In the current study, we collected data on four traits [physiological yellowing (PY), senescence, Septoria tritici blotch (STB), and canopy cover] from within a Southern Australian bread wheat breeding programme, using high-throughput image collection and basic, open-source, image analysis.

Physiological yellowing of bread wheat (*Triticum aestivum* L) and durum wheat (*T. durum*) can have a number of possible causes, however, there is little literature surrounding the trait, with only a single study and two industry fact sheets exploring the effect (Australian Grain Technologies, 2013, 2016; Schwenke et al., 2015). Further to the reported yield impacts, farmer perception often marks material expressing PY as undesirable, due to its "disease-like" symptoms.

Senescence is yellowing of green leaves and the eventual browning and drying of leaf material as a crop matures. Senescence occurs naturally with time and can be used as indicator of maturity or the impact of abiotic stress (Distelfeld et al., 2014).

Septoria tritici blotch is a foliar disease of wheat due to infection by the fungus *Zymoseptoria tritici*. Resistance for STB is actively sought within breeding programmes (Brown et al., 2015). Expression of STB is observed as yellow/brown lesions on leaves, containing small black fruiting bodies (pycnidia). Assessment of STB in breeding programmes typically occurs in inoculated disease nurseries to ensure there is adequate incidence of the disease.

Canopy cover is the proportion of soil covered by the crop canopy, and is primarily used for the assessment of early vigour. It is associated with the reduction of soil water evaporation (Rebetzke et al., 2004; Mullan and Reynolds, 2010) and weed competitiveness (Lemerle et al., 1996; Coleman et al., 2001). In a more crude form it is also used to identify plant establishment issues in field trials.

While each of the traits investigated in the current study is physiologically different, they are linked through the colour-based nature of their visual assessment. Visual assessment for each of these traits is typically achieved through either a percentage score, or through a 1–9 scale of severity. This type of assessment lends itself to the application of image analysis, where percentage area within images can be calculated.

The aim of the current study was to develop a high-throughput digital imaging system capable of assessing colour-based traits observed within a wheat breeding programme. This was achieved in three stages:

(i) A proof of concept study in a greenhouse to develop a method and examine how effectively freely available image analysis software and consumer digital cameras can estimate colour-based traits.
(ii) Applying these concepts of hand-held digital imaging and basic image analysis to field trials to demonstrate their application in breeding programmes.
(iii) Using the results of i and ii to develop a field-based high-throughput imaging infrastructure, with a basic image analysis pipeline.

The first two years of the current study involved the development and testing of data capture and processing systems, and the third year tested these systems within a wheat breeding field trial.

MATERIALS AND METHODS

The three stages of the current study were conducted during the seasons of 2015, 2016, and 2017 using a combination of hand-held and high-throughput RGB imaging in greenhouse and field trials (**Table 1**). Images were collected opportunistically within a large-scale wheat breeding programme, across seven experiments, for PY, senescence, STB and canopy cover. While multiple traits were observed in the field, it is proposed that the image analysis methods can be applied to any colour-based trait of interest.

Greenhouse Imaging

Imaging of a potted experiment investigating the expression of PY was conducted to establish the feasibility of assessing

TABLE 1 | Summary of trials assessed in the current study.

Trial	Environment	Location	Position	Trait Measured	Observations (*n*)	Replicates
Greenhouse	*Controlled*	Roseworthy	34°31'58.40"S, 138°41'20.60"E	Physiological Yellows	72 (plants)	3
A	*Field*	Roseworthy	34°30'33.51"S, 138°40'26.03"E	Physiological Yellows	432	2
B	*Field*	Roseworthy	34°30'33.51"S, 138°40'26.03"E	Physiological Yellows	432	2
C	*Field*	Roseworthy	34°30'33.51"S, 138°40'26.03"E	Senescence	240	Partial (25%)
D	*Field*	Roseworthy	34°30'33.51"S, 138°40'26.03"E	Senescence	648	Partial (25%)
E	*Field*	Turretfield	34°32'13.81"S, 138°50'36.55"E	Septoria Tritici Blotch	202	2
F	*Field*	Winulta	34°15'12.41"S, 137°53'3.21"E	Canopy Cover	288	3

a colour-based trait with basic open-source image analysis methods. The experiment consisted of individually potted plants arranged in a randomised block design of three replicates, with treatments of genotype and presence/absence of chlorine (Cl^-) as described by Schwenke et al. (2015). Plants were grown in a greenhouse on the University of Adelaide, Roseworthy Campus. Further details of this experiment are described by Australian Grain Technologies (2016).

The severity of symptoms was assessed shortly after anthesis [Zadoks Growth Scale 69 (Z69) (Zadoks et al., 1974)], as the percentage of leaf area affected by PY, i.e., a visual estimate of the percentage of leaf material that was yellow. To obtain image analysis scores, RGB images were captured for every plant using a commercial digital camera (Canon 100D) at a resolution of 3456 × 5184 pixels (18 MP), with auto exposure. Plants were placed in front of a white background, to allow for simplified image processing and analysis. Images were captured from the side of pots, allowing for large amount of leaf area to be visible, with minimal occlusion.

Field Imaging

Following the testing of imaging in the potted greenhouse experiment, imaging methods were adapted and deployed within six wheat breeding field trials which examined a number of different traits (**Table 1**). Field plot trials consisted of small plots 1.32 m × 3.2 m (trials A–D, F) or 0.45 m × 1 m (trial E) in size, with each trial containing a single treatment of genotype, with varying levels of replication (**Table 1**), arranged in a completely randomised design. Field plots were managed by Australian Grain Technologies (AGT) within their wheat breeding programme, with plots in trial E grown within an inoculated STB nursery.

Visual and digital scores were recorded as percentage of yellow leaf area, with visual scores collected in the field following imaging. Exceptions to this were trial E, where visual STB severity was assessed using a 1:9 scale at the time of imaging and trial F, where visual scores were recorded as percentage canopy cover obtained by a visual estimate of canopy cover in individual images, and digital scores were calculated as the percentage of image area that was green.

Images of plots in trials A–E were captured at a nadir angle by using a hand-held camera (Canon 100D) over each plot, approximately 1.5 m above ground level. Images were captured at a resolution of 3456 × 5184 pixels (18 MP), with exposure settings adjusted *ad-hoc*. Nadir images were chosen because lateral images reveal only the first few plants in each row, with the rest of the plot being occluded. Images of plots in trial F were collected at a nadir angle using the High-throughput Imaging Boom (HIB; described in detail below). Plots were imaged early in the season (approximately Z25) and following anthesis (approximately Z69) to observe plot establishment and canopy cover. Images were captured automatically using the HIB at both time-points, with cameras set to 1/1000 and 1/2000 of a second shutter speed at the first and second time-points, respectively, *f*8.0 aperture and auto ISO to allow for exposure compensation.

Image Analysis

All images were processed in the FiJI distribution (Schindelin et al., 2012) of the open-source software ImageJ (Schneider et al., 2012), using the Threshold Colour plugin (**Supplementary Data 1**). Central regions of interest were applied to greenhouse images and field images, where plant material did not fill the frame.

A two-stage thresholding process was then used to separate firstly, all plant material from background material (i.e., white corflute in greenhouse and soil in field), and secondly yellow plant material from green. Examples of this process are shown for PY in **Figure 1**. Yellow thresholding was not required for the estimation of canopy cover. Thresholding was conducted using Hue, Saturation and Brightness (HSB) values, with these being visually determined for each experiment to obtain the most suitable thresholds. Once threshold images had been created, the number of plant material pixels and yellow pixels were counted, allowing the percent yellow leaf area score (or percent image area green) to be calculated. Detailed methods for thresholding and batch processing of images are available in **Supplementary Data 1**. Examples of processed images for senescence, STB and canopy cover are available in **Supplementary Data 2**.

Images obtained from field trials were resized to 25% of their longest edge (∼1 MP), to increase processing speed and avoid RAM limitations, when batch processing large numbers of images.

High-Throughput Imaging Boom Development

The High-throughput Imaging Boom shown in **Figure 2** was designed for the express purpose of integration into a large-scale wheat breeding programme. It features four commercially available digital cameras (Canon 70D) mounted inside weather

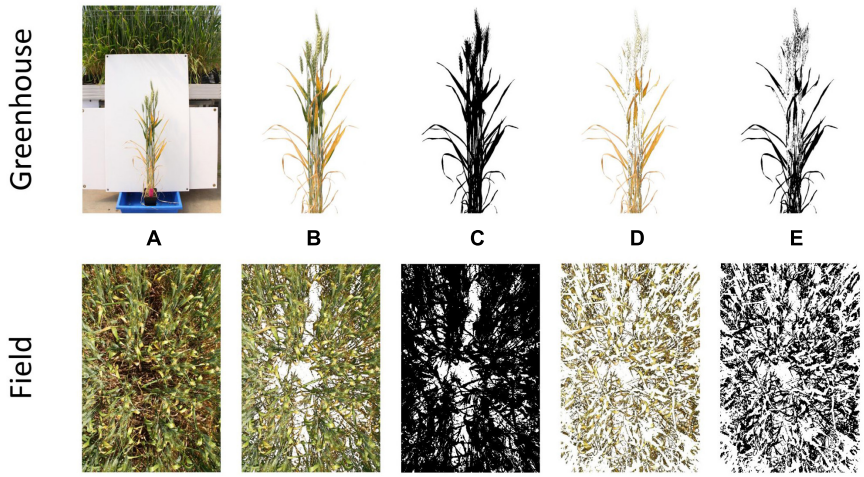

FIGURE 1 | Stages of the thresholding process for single plants grown in the greenhouse (top) and whole plots grown in the field (bottom). Depicted are the original image **(A)**, segmented plant material **(B)**, binary plant material threshold **(C)**, segmented yellow material **(D)**, and binary yellow material threshold **(E)**.

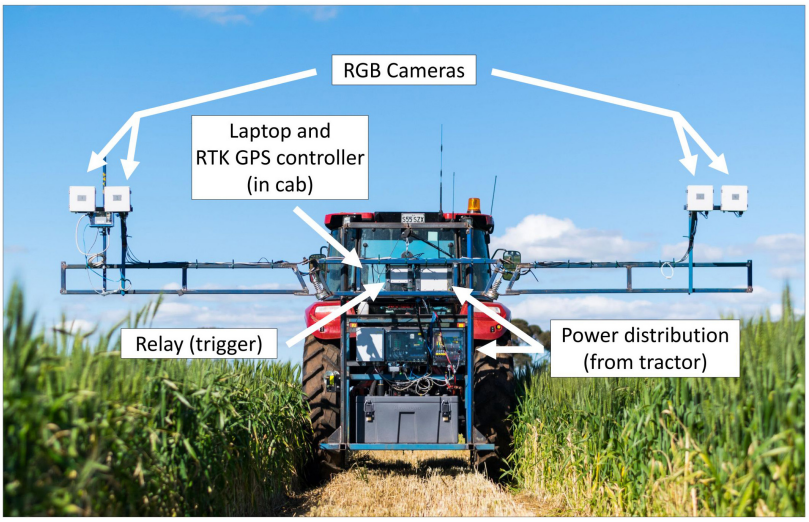

FIGURE 2 | The High-throughput Imaging Boom (HIB) developed and deployed as part of the current study, parked in a maintenance pathway of a wheat field trial. Annotations outline major components of the system.

sealed boxes on the boom arms. This setup allows two images per plot to be captured simultaneously, and the potential for future work to investigate applications of stereo imaging.

Image capture is triggered by a single relay, which is controlled by a laptop computer in the tractor cab. The laptop uses proprietary software to monitor GPS output from a Trimble FM1000 RTK GPS unit and trigger the relay from a set of predefined GPS coordinates, camera trigger delay and the distance between GPS receiver and the cameras. GPS coordinates are computed based on three corner coordinates of the trial site and the number of plot rows and columns present at the site. The HIB is driven to each of these three corners and the cameras positioned over the end plot. Once in position the GPS coordinates are saved within the software. After collecting the three GPS coordinates, individual triggering coordinates for each plot are interpolated from the three corner positions. A text file containing all trigger coordinates is saved and can be loaded into the software for every imaging event, meaning this setup process need only be completed once per field site.

The boom on which the cameras are mounted features arms of adjustable height, which fold in for transport, mimicking a standard spray boom used for plot maintenance within the wheat breeding programme. To further strengthen the concept of integrating the HIB within a field-crop breeding programme, the tractor to which it is attached can use the GPS autosteer function of the RTK GPS unit, adhering to the predefined maintenance pathways within the trial. These pathways are typically used for standard management practises such as fertiliser, herbicide and

fungicide application. This reduces operator error while driving the tractor, and allows repeated image capture throughout the season with a spatial accuracy of 2 cm. To operate the HIB the tractor is driven down maintenance pathways within each field trial, with boom arms placing the cameras centrally over one plot each side of the tractor.

As the tractor drives, image capture occurs automatically, with images stored on SD cards within individual cameras. The software running on the laptop computer monitors GPS message output from the RTK GPS unit, with this information being used to determine triggering of the relay in conjunction with the pregenerated trigger coordinate text file. This process accounts for tractor speed (calculated from GPS coordinates), signal travel time between laptop and camera shutter trigger (predefined within the software) and the distance between the GPS receiver and cameras. The tractor continues to travel along maintenance pathways in a serpentine manner, until all plots have been imaged.

The HIB was driven at 5 km/h during image capture. Cameras had manually set exposures, with a shutter speed of 1/1000 or 1/2000 of a second (for images at Z25 and Z69, respectively), an aperture of f8.0 and auto ISO to allow for exposure compensation. Images were captured in JPEG format for ease of post processing, and because of limitations in image write speed and buffer capacity of the cameras for RAW images.

Statistical Analysis

All statistical analysis was conducted in the R software package (R-Core Team, 2017). Mixed linear models were used to analyse all data sets through univariate and bivariate analyses of visual and digital measurements using ASReml (Butler et al., 2009). Pearson's correlations between raw data were calculated within univariate analyses, while genetic and residual correlations were calculated from bivariate analyses. Broad-sense trait heritability (Eq. 1), which can be described as the proportion of observed trait variation attributable to genetics (Visscher et al., 2008), was also calculated within univariate analyses.

$$H^2 = \frac{\sigma_G^2}{\sigma_G^2 + \sigma_E^2} \quad (1)$$

where H^2 is broad-sense heritability, σ_G^2 is the variance attributable to genetic effects and σ_E^2 the environmental variance.

Linear regressions between visual and digital measurements are presented from raw data, with regression equations calculated using Model II Linear Regression (Ludbrook, 1997, 2012).

RESULTS

Proof of Concept

The image analysis methods proposed in **Supplementary Data 1** were able to efficiently and consistently segment both plant material from the background image, and yellow plant material from total plant material (**Figure 1** top). Digital scores correlated strongly (r = 0.95) with visual scores assessed from individual plants (**Figure 3**), with genetic and residual correlations being similarly, strong (**Table 2**). Heritability for both measurements showed similarly, high values, with visual scores being slightly higher (**Table 2**).

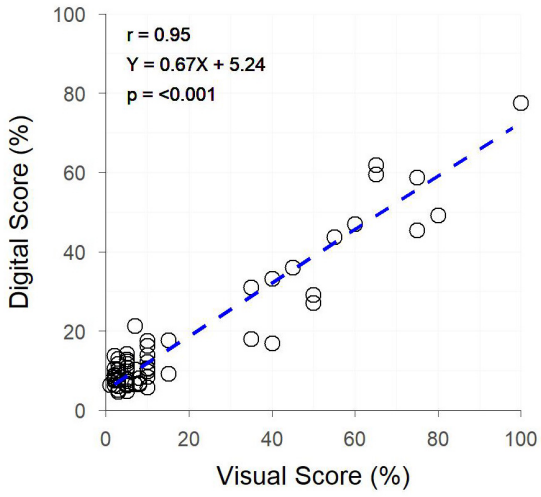

FIGURE 3 | The relationship between Digital Yellow Leaf Area and Visual Physiological Yellowing (PY) scores, for individually potted plants within a Greenhouse. Dashed line represents the linear regression between measurements.

RGB Imaging in Field Conditions

Following the success of applying the proposed image analysis methods to individual plants in a greenhouse environment, hand-held images of field plots were collected to further test the application of the methods and investigate their robustness under field conditions. As with greenhouse images, the image analysis methods proposed in the current study were capable of segmenting plant and background pixels, in this case from soil rather than a plain background, as well as separating yellow plant material from total plant material.

Significant correlations ($p < 0.001$) were observed between digital and visual scores across all field trials (**Figure 4**). A slightly weaker correlation between visual and digital scores was observed in trial A (r = 0.61), with trials B, C, D, and E having slightly stronger correlations (r = 0.74 – 0.78). For each trial, genetic correlations were stronger than raw correlations between visual and digital measurements, with residual correlations being smaller than raw correlations. For all but trial E, the heritability of the digital score was higher than that of the visual score (**Table 2**). This was particularly the case for trials A and B where the digital scores had heritability 0.28 and 0.27 units higher than the respective visual scores.

Images were collected by hand at a rate of approximately one image every four seconds across all field trials, or approximately 900 plots per hour. Image analysis took approximately 10 min per trial, with the bulk of this time spent finessing threshold values. Computer processing time was approximately 0.02 sec per image (0.12 sec per image when including the process of importing images to FiJI). Visual scores (Trials A–E) took over double that

TABLE 2 | The correlation coefficients (r) for raw data, genetic and residual correlations between visual and digital scores, and the heritability (H^2) of individual data sets collected for the traits physiological yellowing (PY), senescence, Septoria tritici blotch (STB) and canopy cover.

Trait	Trial	Raw Correlation	Genetic Correlation	Residual Correlation	H^2 – Visual	H^2 – Digital
Physiological Yellows	*Greenhouse*	0.95	0.98	0.92	0.85	0.76
	A	0.61	0.86	0.32	0.46	0.74
	B	0.78	0.86	0.66	0.46	0.73
Senescence	*C*	0.74	0.83	0.43	0.76	0.81
	D	0.75	0.92	0.44	0.67	0.74
Septoria tritici blotch	*E*	0.76	0.86	0.47	0.73	0.59
Canopy Cover	*F – Time 1 (Z25)*	0.88	0.82	0.82	0.11	0.08
	F – Time 2 (Z69)	0.86	0.92	0.75	0.59	0.72

time, with one score recorded approximately every nine seconds or 400 plots per hour.

Deploying Digital Phenotyping Methods on a High-Throughput Infrastructure

The final step in the current study was to deploy the digital phenotyping methods (**Supplementary Data 1**) on high-throughput infrastructure designed to work effectively within a field-crop breeding programme. Advanced yield plots were imaged using the HIB to assess canopy cover.

Both early and late assessments of canopy cover (approximately Z25 and Z69, respectively) showed strong correlations between digital and visual scores (r = 0.88 and 0.86, respectively) (**Figure 5**). Early assessment of canopy cover produced genetic and residual correlations of equal strength, both of which were slightly weaker than the raw correlation, though for assessment at Z69 genetic and residual correlations were, respectively, stronger and weaker than the raw correlation (**Figure 5**). Heritabilities were low for digital and visual scores at Z25, though slightly higher for visual scores, but greatly increased at Z69, with the digital score having a greater heritability than the visual score (**Table 2**).

The HIB achieved a throughput of approximately 7,400 plots per hour, with the 9,600 plot trial site containing trial F being imaged in 80 min; equating to approximately two unique images per second. Analysis of plot images took approximately 10 min. Accurate *in situ* visual assessment of canopy cover is challenging due to the oblique perspective of the scorer, however, a throughput of approximately 400 plots per hour would be expected, based on scoring rate of other traits in the current study.

DISCUSSION

Image analysis as a phenotyping tool is a common practise within greenhouse and controlled environment experiments, and a number of commercial platforms and facilities offer streamlined approaches for data collection and analysis (for example the LemnaTec Scanalyzer[1], and the Australian Plant Phenomics Facility[2]). These systems allow the collection of high temporal resolution data with ease, and are commonly used for the assessment of green leaf area, and subsequently for the assessment other traits such as of the rate of senescence (Atieno et al., 2017). However, these systems are expensive to establish and are limited to assessment of plants grown in controlled environments within pots.

The image analysis methods proposed in the current study offer a low-budget, open-source alternative to the controlled environment systems described above, and are suitable for the collection of digital scores comparable to visual scores of colour-based traits. The example presented in the current study shows the application of these methods to PY. However, as shown by the results of Objectives 2 and 3, these methods are robust across other colour-based traits. The strong correlation between digital and visual assessments of PY in the greenhouse experiment is unsurprising, as the imaging of individual plants in front of a uniform white background provides ideal conditions to implement this type of image analysis. There is little occlusion present, and plant material pixels can be easily segmented within the images due to the vastly different hue values of plant and background material pixels. Despite these ideal conditions, there are limitations to the use of the proposed methods for assessing colour-based traits which do not express uniformly across all plant organs, as the proposed methods are basic and not capable of isolating individual plant organs for analysis. In the case of the current study, stems and ears of plants often remained green while leaves expressed PY, resulting in images still containing a many green pixels. This ultimately reduced the percentage of the plant classed as yellow, leading to a slope <1 for the linear regression between visual and digital scores (**Figure 3**). Regardless of this limitation, the high heritability of PY for both digital and visual scores in the greenhouse experiment demonstrated the accuracy that is achievable under ideal conditions.

Despite the high-quality data obtainable under controlled conditions, field phenotyping is favoured within plant breeding programmes, to gain an understanding of genotype performance when subject to realistic and relevant environmental conditions and to examine genotype-by-environment interactions (Araus and Cairns, 2014). In contrast to controlled environment imaging, field imaging occurs under conditions that are far from ideal. The main contributing factors to this being the

[1]https://www.lemnatec.com/products/high-throughput-phenotyping-solutions/greenhouse-scanalyzer/

[2]https://www.plantphenomics.org.au/

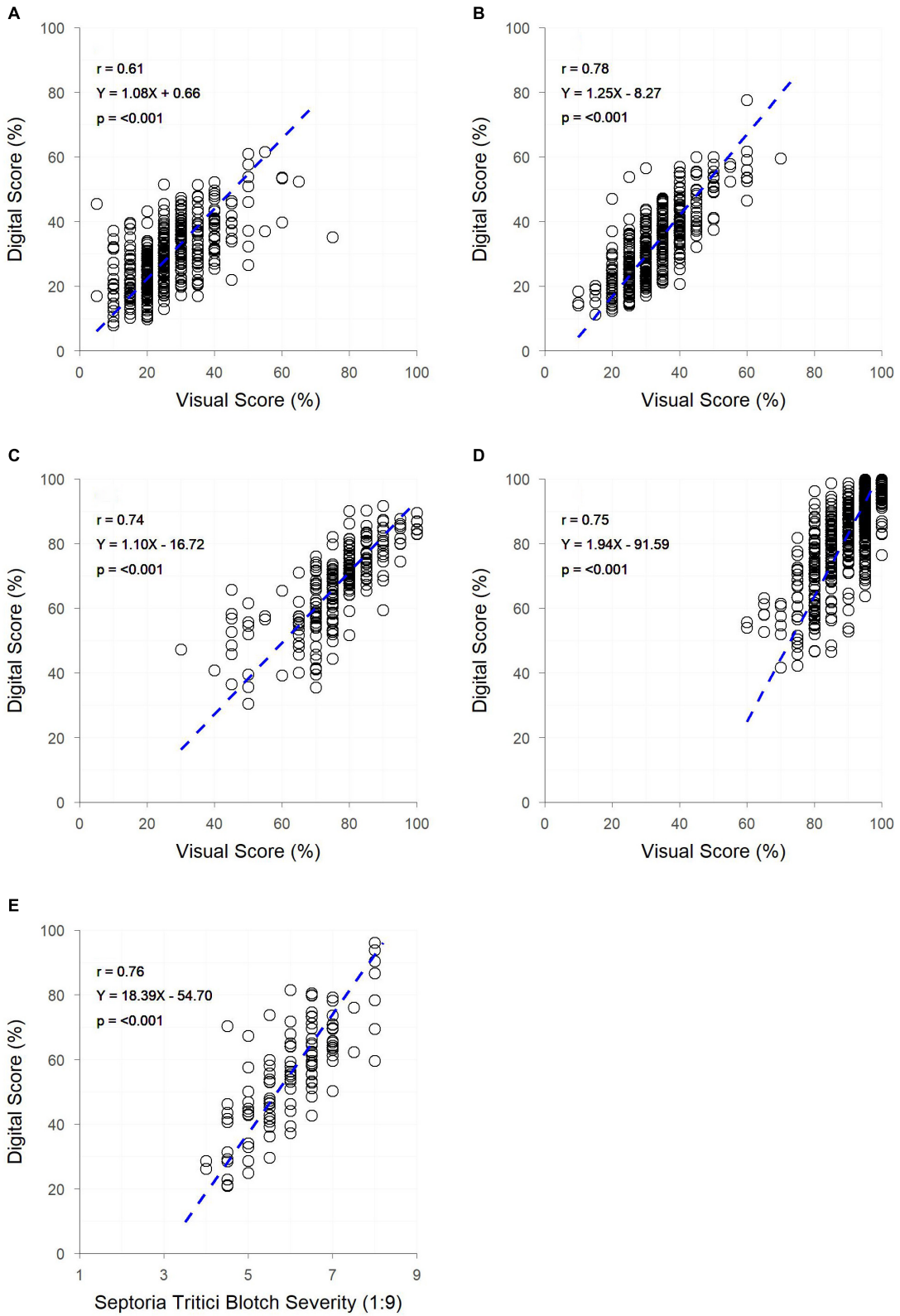

FIGURE 4 | The relationships between visual and digital scores for digital yellow leaf area and visual PY score in field trials **(A,B)** digital yellow leaf area and visual senescence score for field trials **(C,D)** and digital yellow leaf area and visual Septoria tritici blotch (STB) severity score for field trial **(E)**. Dashed lines represent the linear regression between measurements.

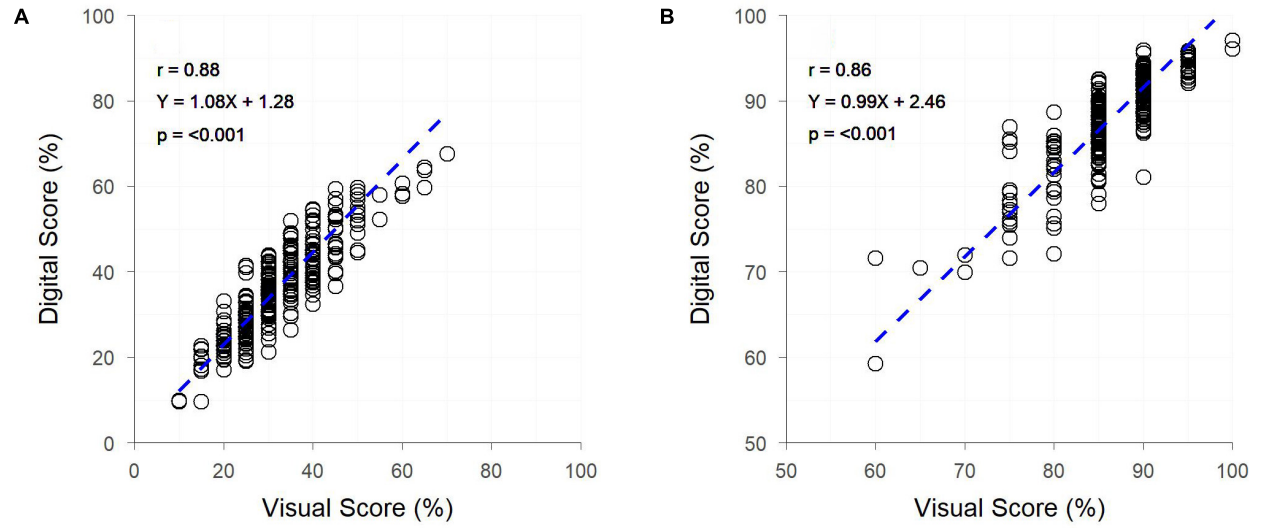

FIGURE 5 | The relationships between visual and digital scores for percent image area green and visual assessment of percentage canopy cover, for field trial F at two time-points – Zadoks Growth Scale 25 **(A)** and 69 **(B)**. Dashed lines represent the linear regression between measurements.

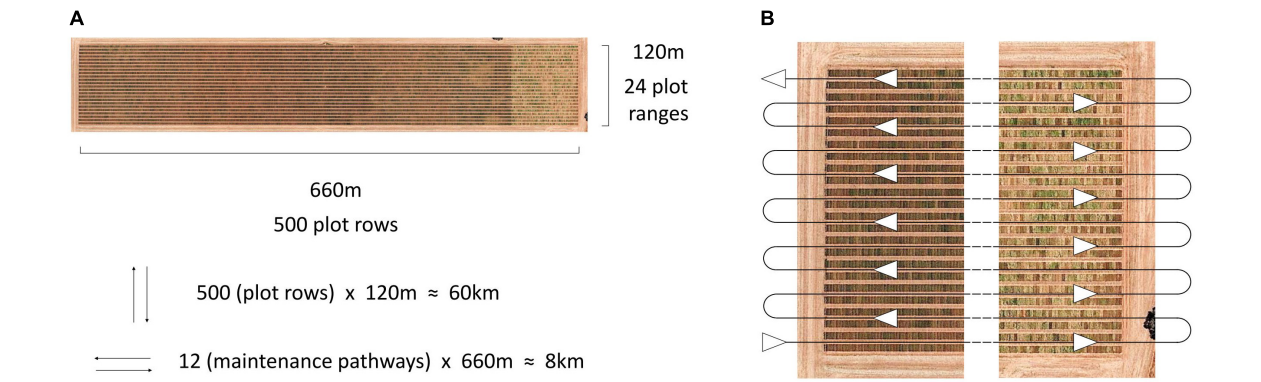

FIGURE 6 | Aerial image of an Australian large-scale wheat breeding site, annotated with dimensions of the site and the number of plot rows, plot ranges and travel distances based on direction **(A)**, and the serpentine path along site maintenance pathways, travelled by the HIB in the current study, allowing for two plots to be imaged simultaneously **(B)**. Image: Google, 2017, Digital Globe.

large amount of occlusion which occurs within the crop canopy, preventing plant material in the lower canopy from being fully visible (Casadesús et al., 2007), and the potential for plant pixels and soil pixels to have similar hue values, resulting in a more difficult segmentation process. Despite these limitations, there are still strong similarities between image analysis of greenhouse and field images, as can be seen in the results of Objectives 1 and 2 in the current study. In the case of PY, where images were obtained from both greenhouse and field trials (A and B), direct comparisons can be made around the quality of data collected. While the strongest correlation between digital and visual data was observed in the glasshouse experiment, the heritability of digital and visual scores was similar. Weaker correlations were observed between digital and visual scores within field trials, though the heritability of digital scores was generally greater than for visual scores, indicating that digital scores provide a more accurate assessment of the trait.

The ability to apply the image analysis methods of the current study to a range of traits across multiple field trials demonstrates the robustness of these simple methods. For each field trial (A–F) positive relationships were observed between digital and visual scores, irrespective of the trait, with digital scores generally resulting in a similar or improved heritability compared to visual scores (**Table 2**). The high heritability of all traits assessed digitally (excluding canopy cover at Z25) indicates the potential to achieve genetic gain through selection for or against the trait. Though heritability of canopy cover was low at Z25, this does not necessarily mean that genetic gain cannot be made for early canopy cover. The low heritability observed in the current study can likely be explained by the variable germination and establishment of plots within the trial, a result of variable soil

and poor environmental conditions. These conditions resulted in canopy cover scores being driven by equal levels of genetic and residual variation, leading to a low heritability (**Table 2**). The potential to achieve genetic gain through selection in these traits is further supported by the relationship observed between raw, genetic and residual correlations, where the raw correlation is not driven purely by the residual, for any of the traits observed. In each instance (excluding canopy cover at Z25) the genetic correlation is greater than the raw and residual correlation, with the residual correlation being weaker than the raw. In trials where residual correlations were high, residuals could be fitted as co-variates within breeding analyses to better model non-genetic effects within the trial. Whether investigating the genetics, or accounting for residual effects in trait performance, the results of the current study show that digital methods can be exchanged with visual methods, while producing greater or maintaining similar heritability. The lower heritability of digital scores, compared to visual scores, observed in trial E is likely a result of (i) the amount of STB occluded from the camera sensor – as the pathogen is spread from the bottom of the canopy up, through rain-splash (Steinberg, 2015), and (ii) patches of senesced grass weeds within the plots. The presence of weeds has likely contributed to the lower heritability in the digital scores of trial F at Z25, with small broadleaf weeds being present in images and contributing to the amount of green pixels present. In both trials E and F visual scores can easily account for occluded leaves or the presence of weeds, which will result in a higher estimate of heritability.

Few studies have compared digital image analysis scores with visual scores of the same trait, opting instead for comparisons to sensor produced visual indices or alternative traits (Adamsen et al., 1999; Lukina et al., 1999; Casadesús et al., 2007; Li et al., 2010; Liu and Pattey, 2010; Mullan and Reynolds, 2010; Kipp et al., 2014). However, direct comparisons between digital and visual scores have been made by Hafsi et al. (2000) and Stewart and McDonald (2014), where individual leaves were isolated on a plain background to obtain images and visual scores. In each of these studies digital scores were found to be effective at estimating the trait of interest (senescence and STB, respectively), corresponding to the results of the current study.

It should be noted that the studies mentioned above used a variety of image analysis methods, some similar to the current study, using thresholds and/or segmentation (Lukina et al., 1999; Li et al., 2010; Liu and Pattey, 2010; Mullan and Reynolds, 2010; Kipp et al., 2014; Stewart and McDonald, 2014). Others have used numerical approaches across the whole image, looking at pixel colour values and ratios (Adamsen et al., 1999; Hafsi et al., 2000; Casadesús et al., 2007).

Despite the variety in previously described methods, image analysis within field experiments is currently far from common practise, with relatively few examples within the literature. Perhaps the most extensive example of using image analysis within large field trials, as well as in the context of plant breeding, is presented by Mullan and Reynolds (2010) where four bread wheat populations were repeatedly imaged and analysed to provide canopy cover values over time. A further example presented by Kipp et al. (2014) showed image analysis to be a superior method of early vigour assessment, compared to spectral sensing. The subject of image collection and processing time was raised in each of these studies, with Mullan and Reynolds (2010) stating an imaging rate of approximately one image every five seconds and an image processing rate of approximately three images per second. Kipp et al. (2014), on the other hand, merely state that their image collection and processing methods are too time consuming for application to large-scale field trials. The processes of image collection and analysis in the current study were conducted in similar times to those reported by Mullan and Reynolds (2010). The combination of image capture and analysis showed a time advantage over visual scores from field trials A–E in the current study, in which images were collected using a hand-held camera, with image collection taking approximately half the time of visual scoring and image processing taking approximately 10 min per trial. This shows that even in the absence of high-throughput methods, digital imaging can save time when scoring breeding or research experiments.

To be adopted by plant breeding programmes, or by large-scale research in general, image analysis methods should be highly automated. This has previously been acknowledged by Casadesús et al. (2007) when investigating digital image analysis for the derivation of visual indices, and is often satisfied through batch processing of images. This was the approach taken in the methods of the current study, greatly reducing the user input required. Further reducing user input could be achieved through the scripting of certain processing steps, however, manual input is still required to correctly apply thresholds to a new set of images. To apply true automation to this process avenues of computer vision and machine learning would need to be explored, such as in the work of Guo et al. (2017), however, such work requires a highly specialised skill set to undertake.

Further to the requirements of automated data processing, high-throughput data collection methods are essential. Platforms for the high-throughput collection of field phenotypic data have been proposed in the literature (Busemeyer et al., 2013; White and Conley, 2013; Andrade-Sanchez et al., 2014; Deery et al., 2014; Bai et al., 2016; Underwood et al., 2017; Jimenez-Berni et al., 2018), though there are currently limited commercial options available. As it stands, a platform that is affordable, truly high-throughput, and easily integrated into large scale breeding and research operations, has yet to be produced.

The HIB used in the current study shows great potential for future deployment within large scale research and plant breeding programmes, meeting the requirements of affordability, high throughput and ease of integration into current trial operations. Traditionally high-throughput phenotyping platforms described in the literature have travelled directly over plots (Busemeyer et al., 2013; White and Conley, 2013; Andrade-Sanchez et al., 2014; Deery et al., 2014; Bai et al., 2016; Underwood et al., 2017; Jimenez-Berni et al., 2018), following the direction of seeding. This allows for thorough data collection over the entire plot, whether multiple images of the canopy or other sensor data, though it greatly increases driving distance and is difficult to implement within standard breeding trials. This is illustrated in **Figure 6**, where travel along

individual plot rows is nearly eight times the distance of travelling along field maintenance tracks, where two plots are imaged simultaneously (one either side of the pathway), when traversing a large-scale field trial in a wheat breeding programme.

Travelling along maintenance pathways within the field trial also offers the benefit of integrating with current field maintenance practises and can take advantage of tractor RTK GPS autosteer profiles that have previously been generated for the maintenance of trial sites. In the current study, GPS coordinates and output from the tractor's RTK GPS autosteer system were used to automatically trigger image capture. This allowed a "hands-off" data collection approach, as well as ensuring that repeated imaging occurred in the same position for each plot, with a 2 cm tolerance for error. Further to this, the use of autosteer reduces the chance of operator error, assisting in the prevention of accidental damage to field trials.

The small tolerance for error within the image capture system will allow for the extension of this system to earlier stages of the breeding programme, which is often grown in small plots or individual plant rows (Halloran et al., 1979). As demonstrated by the STB images in the current study, the image analysis methods proposed are suitable for application to small plots and are likely transferrable to single rows and potentially single plants. This will be of great interest to plant breeders who wish to conduct phenotypic selection within the early generations of their breeding programme.

At the speed of 5 km/h driven in the current study it was possible to image approximately 7,400 plots per hour. While this is already exceptionally high throughput, the system is capable of operating at higher speeds (with 10 km/h successfully tested). At higher speeds movement is introduced into the boom arms when travelling on uneven ground, and can result in plot images being off-centre. However, these issues could be easily addressed through modification to the boom or tractor, for example, auto-levelling boom arms or lower tractor tyre pressure to reduce boom arm and camera movement. The throughput of imaging observed in the current study becomes even more impressive when compared against the throughput of other systems. Recent work by Khan et al. (2018) compared the throughput of plot level RGB imaging from two systems; a low-cost Mobile Ground Platform (MGP) and an Unmanned Aerial Vehicle (UAV). In their study, throughputs of 120 plots per hour and 1200 plots per hour were achieved for the MGP and UAV, respectively. While these results show a clear advantage in the throughput of UAVs compared to ground platforms, the throughput achieved by the HIB in the current study is over six times greater than that achieved by Khan et al. (2018) with a UAV. This demonstrates that truly high-throughput ground based, plot level, imaging is achievable and, as described by Khan et al. (2018), can deliver high-fidelity images of crop canopies not currently achievable with UAVs.

Deployment of the HIB within a large-scale wheat breeding programme during the 2017 growing season allowed for images of individual plots to be captured with extremely high throughput. While data from a single site is presented for the assessment of canopy cover in the current study, the system was deployed at eight trial sites across southern Australia and used to collect 288,680 images from 74,880 unique field plots. Images acquired with the HIB are suitable for the application of the image analysis methods proposed in the current study, enabling wheat breeders to efficiently and objectively assess colour-based traits.

Though the current study has focused on images collected from RGB cameras mounted on the platform, it is possible to expand the system for the collection of a greater variety of data. Numerous sensors have been proposed as high-throughput field phenotyping tools, such as LiDAR (Deery et al., 2014; Bai et al., 2016; Underwood et al., 2017; Jimenez-Berni et al., 2018), multispectral and hyperspectral cameras (Busemeyer et al., 2013; Bai et al., 2016; Underwood et al., 2017), thermal sensors/cameras (Crain et al., 2016; Deery et al., 2016) and NDVI (Bai et al., 2016; Crain et al., 2016; Underwood et al., 2017), all of which could be integrated to the HIB.

CONCLUSION

The basic image analysis methods described in the current study are effectively able to produce digital scores that correlate well to visual scores for colour-based traits, with examples being presented for PY, senescence, STB and canopy cover. The methods described in the current study have a low barrier to entry and utilise commercially available digital cameras and open-source computer software. This, combined with the strong correlations observed between digital and visual data, the high heritability of assessments, and the associated time savings, make for an attractive set of methods for the assessment of colour-based traits within a wheat breeding programme. Furthermore, they show potential for application within other breeding programmes, particularly other cereals and field crops.

To further encourage the adoption of image analysis within plant breeding programmes, an effective system for the high-throughput collection of images has been described, including a clear pathway for integration into current field maintenance practises. This system was deployed within a wheat breeding programme and is capable of high-throughput large-scale image collection, providing images suitable for the analysis methods described in the current study. This ultimately provides a rapid and objective data collection methodology, enabling unprecedented levels of data collection from large-scale plant breeding field trials.

There is further potential to increase the value of collected images to breeding programmes, through the implementation of more complex image analysis methods – focusing on other applications such as seedling counting (Liu et al., 2016), ear counting and flowering detection (Sadeghi-Tehran et al., 2017; Virlet et al., 2017). High-throughput collection and processing of such data, from large-scale field trials, will only further strengthen the role of image analysis within plant breeding programmes.

AUTHOR CONTRIBUTIONS

JW, JE, JC, HK, and SM designed the High-Throughput Image Boom (HIB). JC wrote the image acquisition software with input from JW, JE, SM, and HK. JE and HK designed the experiments and managed the wheat breeding programme. JW established the data processing methods, and collected and analysed all the data. JW, JE, GM, and HK interpreted the analysed data. JW wrote the manuscript with contributions from JE, JC, GM, SM, and HK.

FUNDING

The authors wish to acknowledge the South Australian Grains Industry Trust (UA514), the Grains Research and Development Corporation (GRS11009), the Australian Research Council under its Linkage Project (LP150100055), The University of Adelaide School of Agriculture, Food and Wine, and the Australian Government Research Training Programme Scholarship for their funding support of this research.

ACKNOWLEDGMENTS

The authors wish to thank the following Australian Grain Technologies (AGT) staff for their assistance in effectively deploying the High-throughput Image Boom (HIB): Nathan Lloyd for his fabrication and engineering expertise; Darcy Moore, Rowan Prior, and Simeon Hemer for their logistical support. The authors wish to thank the two reviewers of this manuscript for their considered and constructive reviews.

SUPPLEMENTARY MATERIAL

The Supplementary Material for this article can be found online at: https://www.frontiersin.org/articles/10.3389/fpls.2019.00449/full#supplementary-material

REFERENCES

Adamsen, F. J., Pinter, P. J., Barnes, E. M., LaMorte, R. L., Wall, G. W., Leavitt, S. W., et al. (1999). Measuring wheat senescence with a digital camera. *Crop Sci.* 39, 719–724.

Andrade-Sanchez, P., Gore, M. A., Heun, J. T., Thorp, K. R., Carmo-Silva, A. E., French, A. N., et al. (2014). Development and evaluation of a field-based high-throughput phenotyping platform. *Funct. Plant Biol.* 41, 68–79. doi: 10.1071/fp13126

Araus, J. L., and Cairns, J. E. (2014). Field high-throughput phenotyping: the new crop breeding frontier. *Trends Plant Sci.* 19, 52–61. doi: 10.1016/j.tplants.2013.09.008

Atieno, J., Li, Y., Langridge, P., Dowling, K., Brien, C., Berger, B., et al. (2017). Exploring genetic variation for salinity tolerance in chickpea using image-based phenotyping. *Sci. Rep.* 7:1300. doi: 10.1038/s41598-017-01211-7

Australian Grain Technologies (2013). *Yellowing in Wheat [Online]. Roseworthy, South Australia, Australia*. Available at: http://www.agtbreeding.com.au/assets/docs/general/Yellowing-in-wheat.pdf (accessed January 29, 2018).

Australian Grain Technologies (2016). *Our understanding of yellowing in wheat (so far.) [Online]. Roseworthy, South Australia, Australia*. Available at: http://www.agtbreeding.com.au/assets/docs/general/Our-understanding-of-yellowing-in-wheat-so-far.pdf (accessed January 29, 2018).

Bai, G., Ge, Y. F., Hussain, W., Baenziger, P. S., and Graef, G. (2016). A multi-sensor system for high throughput field phenotyping in soybean and wheat breeding. *Comput. Electro. Agric.* 128, 181–192. doi: 10.1016/j.compag.2016.08.021

Brown, J. K. M., Chartrain, L., Lasserre-Zuber, P., and Saintenac, C. (2015). Genetics of resistance to *Zymoseptoria tritici* and applications to wheat breeding. *Fungal Genet. Biol.* 79, 33–41. doi: 10.1016/j.fgb.2015.04.017

Busemeyer, L., Mentrup, D., Moller, K., Wunder, E., Alheit, K., Hahn, V., et al. (2013). Breedvision - a multi-sensor platform for non-destructive field-based phenotyping in plant breeding. *Sensors* 13, 2830–2847. doi: 10.3390/s130302830

Butler, D., Cullis, B., Gilmour, A., and Gogel, B. (2009). *ASReml-R Reference Manual*. Brisbane, QLD: Queensland Department of Primary Industries.

Casadesús, J., Kaya, Y., Bort, J., Nachit, M. M., Araus, J. L., Amor, S., et al. (2007). Using vegetation indices derived from conventional digital cameras as selection criteria for wheat breeding in water-limited environments. *Anna. Appl. Biol.* 150, 227–236. doi: 10.1111/j.1744-7348.2007.00116.x

Cobb, J. N., DeClerck, G., Greenberg, A., Clark, R., and McCouch, S. (2013). Next-generation phenotyping: requirements and strategies for enhancing our understanding of genotype-phenotype relationships and its relevance to crop improvement. *Theor. Appl. Genet.* 126, 867–887. doi: 10.1007/s00122-013-2066-0

Coleman, R. D., Gill, G. S., and Rebetzke, G. J. (2001). Identification of quantitative trait loci for traits conferring weed competitiveness in wheat (*Triticum aestivum* L.). *Aust. J. Agric. Res.* 52, 1235–1246. doi: 10.1071/ar01055

Crain, J., Reynolds, M., and Poland, J. (2016). Utilizing high-throughput phenotypic data for improved phenotypic selection of stress-adaptive traits in wheat. *Crop Sci.* 57, 648–659. doi: 10.2135/cropsci2016.02.0135

Deery, D., Jimenez-Berni, J., Jones, H., Sirault, X., and Furbank, R. (2014). Proximal remote sensing buggies and potential applications for field-based phenotyping. *Agronomy* 4:349.

Deery, D. M., Rebetzke, G. J., Jimenez-Berni, J. A., James, R. A., Condon, A. G., Bovill, W. D., et al. (2016). Methodology for high-throughput field phenotyping of canopy temperature using airborne thermography. *Front. Plant Sci.* 7:1808. doi: 10.3389/fpls.2016.01808

Distelfeld, A., Avni, R., and Fischer, A. M. (2014). Senescence, nutrient remobilization, and yield in wheat and barley. *J. Exp. Bot.* 65, 3783–3798. doi: 10.1093/jxb/ert477

Guo, W., Zheng, B., Duan, T., Fukatsu, T., Chapman, S., and Ninomiya, S. (2017). EasyPCC: benchmark datasets and tools for high-throughput measurement of the plant canopy coverage ratio under field conditions. *Sensors* 17:798. doi: 10.3390/s17040798

Hafsi, M., Mechmeche, W., Bouamama, L., Djekoune, A., Zaharieva, M., and Monneveux, P. (2000). Flag leaf senescence, as evaluated by numerical image analysis, and its relationship with yield under drought in durum wheat. *J. Agron. Crop Sci.* 185, 275–280. doi: 10.1046/j.1439-037x.2000.00436.x

Halloran, G. M., McWhirter, K. S., and Sparrow, D. H. B. (1979). *A Course Manual in Plant Breeding*. Canberra: Australian Vice Chancellors' Committee, 3–26.

Jimenez-Berni, J. A., Deery, D. M., Rozas-Larraondo, P., Condon, A. G., Rebetzke, G. J., James, R. A., et al. (2018). High throughput determination of plant height, ground cover, and above-ground biomass in wheat with LiDAR. *Front. Plant Sci.* 9:237. doi: 10.3389/fpls.2018.00237

Khan, Z., Chopin, J., Cai, J., Eichi, V.-R., Haefele, S., and Miklavcic, S. (2018). Quantitative estimation of wheat phenotyping traits using ground and aerial imagery. *Remote Sens.* 10:950.

Kipp, S., Mistele, B., Baresel, P., and Schmidhalter, U. (2014). High-throughput phenotyping early plant vigour of winter wheat. *Eur. J. Agron.* 52, 271–278. doi: 10.1016/j.eja.2013.08.009

Lemerle, D., Verbeek, B., Cousens, R. D., and Coombes, N. E. (1996). The potential for selecting wheat varieties strongly competitive against weeds. *Weed Res.* 36, 505–513. doi: 10.1111/j.1365-3180.1996.tb01679.x

Li, Y., Chen, D., Walker, C. N., and Angus, J. F. (2010). Estimating the nitrogen status of crops using a digital camera. *Field Crops Res.* 118, 221–227. doi: 10.1016/j.fcr.2010.05.011

Liu, J., and Pattey, E. (2010). Retrieval of leaf area index from top-of-canopy digital photography over agricultural crops. *Agric. For. Meteorol.* 150, 1485–1490. doi: 10.1016/j.agrformet.2010.08.002

Liu, T., Wu, W., Chen, W., Sun, C., Zhu, X., and Guo, W. (2016). Automated image-processing for counting seedlings in a wheat field. *Precis. Agric.* 17, 392–406. doi: 10.1007/s11119-015-9425-6

Ludbrook, J. (1997). Special article comparing methods of measurement. *Clin. Exp. Pharmacol. Physiol.* 24, 193–203. doi: 10.1111/j.1440-1681.1997.tb01807.x

Ludbrook, J. (2012). A primer for biomedical scientists on how to execute model II linear regression analysis. *Clin. Exp. Pharmacol. Physiol.* 39, 329–335. doi: 10.1111/j.1440-1681.2011.05643.x

Lukina, E. V., Stone, M. L., and Rann, W. R. (1999). Estimating vegetation coverage in wheat using digital images. *J. Plant Nutr.* 22, 341–350. doi: 10.1080/01904169909365631

Morgounov, A., Gummadov, N., Belen, S., Kaya, Y., Keser, M., and Mursalova, J. (2014). Association of digital photo parameters and NDVI with winter wheat grain yield in variable environments. *Turkish J. Agric. For.* 38, 624–632. doi: 10.3906/tar-1312-90

Mullan, D. J., and Reynolds, M. P. (2010). Quantifying genetic effects of ground cover on soil water evaporation using digital imaging. *Funct. Plant Biol.* 37, 703–712. doi: 10.1071/FP09277

Oklahoma State University (2015). *CANOPEO: Rapid and Accurate Green Canopy Cover Measurement Tool [Online]*. Stillwater, OK: Oklahoma State University Department of Plant and Soil Sciences.

R-Core Team (2017). *R: A Language and Environment for Statistical Computing [Online]*. Vienna: R Foundation for Statistical Computing.

Rebetzke, G. J., Botwright, T. L., Moore, C. S., Richards, R. A., and Condon, A. G. (2004). Genotypic variation in specific leaf area for genetic improvement of early vigour in wheat. *Field Crops Res.* 88, 179–189. doi: 10.1016/j.fcr.2004.01.007

Sadeghi-Tehran, P., Sabermanesh, K., Virlet, N., and Hawkesford, M. J. (2017). Automated method to determine two critical growth stages of wheat: heading and flowering. *Front. Plant Sci.* 8:252. doi: 10.3389/fpls.2017.00252

Schindelin, J., Arganda-Carreras, I., Frise, E., Kaynig, V., Longair, M., Pietzsch, T., et al. (2012). Fiji: an open-source platform for biological-image analysis. *Nat. Methods* 9:676. doi: 10.1038/nmeth.2019

Schneider, C. A., Rasband, W. S., and Eliceiri, K. W. (2012). NIH Image to ImageJ: 25 years of image analysis. *Nat. Methods* 9, 671–675.

Schwenke, G. D., Simpfendorfer, S. R., and Collard, B. C. Y. (2015). Confirmation of chloride deficiency as the cause of leaf spotting in durum wheat grown in the Australian northern grains region. *Crop Pasture Sci.* 66, 122–134. doi: 10.1071/CP14223

Steinberg, G. (2015). Cell biology of *Zymoseptoria tritici*: pathogen cell organization and wheat infection. *Fungal Genet. Biol.* 79, 17–23. doi: 10.1016/j.fgb.2015.04.002

Stewart, E. L., and McDonald, B. A. (2014). Measuring quantitative virulence in the wheat pathogen *Zymoseptoria tritici* using high-throughput automated image analysis. *Phytopathology* 104, 985–992. doi: 10.1094/PHYTO-11-13-0328-R

Underwood, J., Wendel, A., Schofield, B., McMurray, L., and Kimber, R. (2017). Efficient in-field plant phenomics for row-crops with an autonomous ground vehicle. *J. Field Robot.* 34, 1061–1083. doi: 10.1002/rob.21728

Virlet, N., Sabermanesh, K., Sadeghi-Tehran, P., and Hawkesford, M. J. (2017). Field scanalyzer: an automated robotic field phenotyping platform for detailed crop monitoring. *Funct. Plant Biol.* 44, 143–153. doi: 10.1071/FP16163

Visscher, P. M., Hill, W. G., and Wray, N. R. (2008). Heritability in the genomics era — concepts and misconceptions. *Nat. Rev. Genet.* 9:255. doi: 10.1038/nrg2322

White, J. W., and Conley, M. M. (2013). A flexible, low-cost cart for proximal sensing. *Crop Sci.* 53, 1646–1649. doi: 10.2135/cropsci2013.01.0054

Zadoks, J. C., Chang, T. T., and Konzak, C. F. (1974). A decimal code for the growth stages of cereals. *Weed Res.* 14, 415–421. doi: 10.1111/j.1365-3180.1974.tb01084.x

Conflict of Interest Statement: JW, JE, and HK are affiliated with Australian Grain Technologies Pty Ltd, a commercial plant breeding company.

The remaining authors declare that the research was conducted in the absence of any commercial or financial relationships that could be construed as a potential conflict of interest.

Chapter 3

Photogrammetry for the Estimation of Wheat Biomass and Harvest Index

Statement of Authorship

Title of Paper	Photogrammetry for the estimation of wheat biomass and harvest index
Publication Status	☑ Published ☐ Accepted for Publication ☐ Submitted for Publication ☐ Unpublished and Unsubmitted w ork w ritten in manuscript style
Publication Details	Walter, J., Edwards, J., McDonald, G., Kuchel, H. (2018) Photogrammetry for the estimation of wheat biomass and harvest index. Field Crops Research 216, 165-174.

Principal Author

Name of Principal Author (Candidate)	James Walter
Contribution to the Paper	Designed the experiment, collected/analysed/interpreted data, wrote manuscript and acted as corresponding author.
Overall percentage (%)	85%
Certification:	This paper reports on original research I conducted during the period of my Higher Degree by Research candidature and is not subject to any obligations or contractual agreements with a third party that would constrain its inclusion in this thesis. I am the primary author of this paper.
Signature	Date: 29/05/2019

Co-Author Contributions

By signing the Statement of Authorship, each author certifies that:

i. the candidate's stated contribution to the publication is accurate (as detailed above);

ii. permission is granted for the candidate in include the publication in the thesis; and

iii. the sum of all co-author contributions is equal to 100% less the candidate's stated contribution.

Name of Co-Author	James Edwards
Contribution to the Paper	Supervised development of work, helped to design experiment, collect and interpret data, evaluate and edit the manuscript.
Signature	Date: 29/5/2019

Name of Co-Author	Glenn McDonald
Contribution to the Paper	Supervised development of work, helped to interpret data, evaluate and edit the manuscript.
Signature	Date: 31/5/19.

Name of Co-Author	Haydn Kuchel
Contribution to the Paper	Supervised development of work, helped to design experiment, interpret data, evaluate and edit the manuscript.
Signature	Date 29/5/19

Field Crops Research 216 (2018) 165–174

Contents lists available at ScienceDirect

Field Crops Research

journal homepage: www.elsevier.com/locate/fcr

Photogrammetry for the estimation of wheat biomass and harvest index

James Walter[a,*], James Edwards[b], Glenn McDonald[a], Haydn Kuchel[a,b]

[a] School of Agriculture, Food and Wine, University of Adelaide, Waite Campus, Glen Osmond, SA, Australia
[b] Australian Grain Technologies Pty Ltd, Perkins Building, Roseworthy Campus, Roseworthy, SA, Australia

ARTICLE INFO

Keywords:
Plant breeding
Phenotyping
Technology
Point cloud

ABSTRACT

Field-based next generation phenotyping has become of great interest to plant breeders and agricultural researchers in recent years, particularly for circumventing destructive or impractical phenotyping methods commonly used for certain traits. The non-destructive estimation of one such trait, above ground biomass (AGB), has been investigated repeatedly using 2D imagery, though little research has been conducted on 3D methods. The aims of the current study were to (i) investigate the use of readily-available consumer level digital cameras and software to estimate AGB, canopy height (CH) and harvest index (HI) of wheat plots, (ii) investigate the suitability of this data as a replacement for destructive sampling methods within a wheat breeding programme, and (iii) identify the point cloud density required for accurate estimation of AGB. To achieve this, a small plot trial of a single wheat cultivar was conducted in an irrigated nursery, at Roseworthy, South Australia. At physiological maturity plots were measured for CH and whole plots were harvested to attain AGB and threshed to measure grain yield and calculate HI. Prior to harvesting each plot was imaged using a digital camera, with these images being processed into 3D point clouds, which were subsequently used to estimate plot volume and CH. Strong correlations were observed between actual measurements of AGB, CH and HI to those estimated from point clouds. Images were processed in subset batches to determine an optimal number of images for processing. Stronger correlations between AGB and plot volume were observed when more images were processed, though as few as 48 images provided sufficiently accurate estimates of AGB. These methods were shown to be effective at estimating AGB, CH and HI and could be adopted by small scale research programmes. This study shows that a higher-throughput adaptation of this photogrammetry method could be used in phenotype intensive research such as plant breeding programmes.

1. Introduction

Above ground biomass (AGB) is a particularly troublesome trait to measure within breeding programmes due to the laborious and destructive methods needed to assess it. Despite this, AGB has been suggested as a potential trait of interest, for the improvement of grain yield, within cereal breeding programmes (Donald and Hamblin 1976; Damisch and Wiberg 1991; Sharma 1993; Richards 2000; Richards et al., 2002; Reynolds et al., 2012), particularly in relation to harvest index (HI) and radiation use efficiency.

With the rise in popularity of field-based next generation phenotyping, a number of studies have investigated commonly-available sensors, such as RGB cameras, multispectral cameras and LiDAR, to measure AGB non-destructively in field trials (Ehlert et al., 2009; Hosoi and Omasa 2009; Montes et al., 2011; Winterhalter et al., 2011; Bendig et al., 2014; Eitel et al., 2014; Amaral et al., 2015; Bendig et al., 2015; Li et al., 2015; Pittman et al., 2015; Schirrmann et al., 2016a; Schirrmann et al., 2016b).These studies have used a number of methods to estimate AGB, most commonly through canopy height or visual indices (VIs). While these studies have often shown strong relationships between AGB estimators and AGB, AGB is a complex trait and is three-dimensional (3D) in nature. Without taking account of this 3D information, estimating AGB from canopy height or VIs may be limited. It is also commonly agreed that the use of VIs can be limited due to saturation of the index (Tucker, 1977), and is therefore impractical to use at later crop growth stages or in very vigorously growing crops.

While many studies have focused on estimating AGB from two-dimensional spatial data, it is also possible to estimate AGB from 3D data. Airborne laser scanning (ALS) is a common method used in forestry research, where a LiDAR sensor is flown over the area of interest and laser returns are collected in a 3D point cloud. The point cloud can then be used for modelling and measuring, which has been successfully used as a tool to estimate forest AGB (Zolkos et al., 2013). With the success of LiDAR as a tool for measuring forest AGB, there is now keen interest in

* Corresponding author.
E-mail address: james.walter@adelaide.edu.au (J. Walter).

https://doi.org/10.1016/j.fcr.2017.11.024
Received 7 August 2017; Received in revised form 23 November 2017; Accepted 24 November 2017

using LiDAR for phenotyping in agricultural research; however, the implementation of LiDAR and other similar sensors is hampered by the lack of simple data collection methods and the complexity of creating data processing pipelines. The interest in LiDAR as a research tool is the point cloud data it generates, however, this data can be collected through multiple methods and is not exclusive to LiDAR. A limited number of studies have investigated the use of point cloud data within agricultural research. However, they have not focussed on the direct estimation of AGB, instead investigating the potential to identify ears (Saeys et al., 2009), or individual plant organ area (Hosoi and Omasa, 2009).

With the increased use of Unmanned Aerial Vehicles (UAVs) as a data collection tool in many industries, including agriculture, there are now a number of readily available software packages (*e.g.* Pix4Dmapper Pro, DroneDeploy, Agisoft PhotoScan) that are capable of using red, green and blue (RGB) images to create point clouds. This is an example of photogrammetry, a method of obtaining measurements through photographs. Photogrammetrically-derived point clouds have been demonstrated to be an effective alternative to LiDAR to create a digital surface model (DSM) for forestry research (Herrero-Huerta et al., 2016) and to create DSMs for agricultural field trials (Bendig et al., 2014, 2015). While these models have been successful in estimating canopy height and have been used as a predictor for AGB, images obtained from UAVs typically have a low spatial resolution (in the context of agricultural field plots) and may not sufficiently capture the fine details of cereal crop canopies.

Photogrammetry can be utilised for the creation of point clouds, not only from UAV obtained imagery, but also from ground based images. Due to the small area of coverage, these point clouds are high fidelity and could potentially be used to estimate AGB in research plots, based on the volume of the canopy.

The objectives of this study were (i) to investigate the use of readily-available consumer level digital cameras and photogrammetry software to estimate wheat plot AGB, canopy height (CH) and HI, (ii) to investigate the suitability of this high fidelity point cloud data for replacing destructive manual measurements, within a wheat breeding programme, (iii) and, as a prelude to scaling up this method, to identify the point cloud density required for accurate estimation of AGB.

2. Methods

2.1. Site/Plant material

The study took place at the University of Adelaide, Roseworthy Campus, Australia (34°31′52.8″S 138°41′9.8″E). Plots were grown in an irrigated nursery, between November 2015 and May 2016. Plots (12) of the Australian bread wheat (*Triticum aestivum* L.) cultivar Halberd were sown in a factorial completely randomised block design, with a single factor of four target plant densities (100, 200, 300 and 400 plants/m^2). Halberd was selected based on its phenotype, as it is a slow maturing, strongly photoperiod sensitive and vernalisation insensitive, tall variety with many tillers and large biomass.

Plots were sown as 5 rows with a 17 cm row spacing, at a length of 3m. To enhance the uniformity within each plot, plots were shortened to 1.5 m in length and the northern most row was removed (due to poor germination), which reduced the total plot area to 1.02m^2.

2.2. Image capture

Plots were imaged 7 days prior to harvest, using a Canon EOS 100D digital camera. Ninety-six RGB images were taken per plot, using a three-ringed pattern of 32 images per ring, as shown in Fig. 1, with the shutter being manually triggered while navigating the perimeter of the plot. Images were taken at a focal length of 18 mm with an aperture of F8.0, shutter speed was adjusted *ad-hoc* to counteract unavoidable changes in lighting caused by variable cloud cover. Images were captured in JPEG format at a resolution of 5184 × 3456 pixels. A generic clay brick, measuring 230 × 110 × 75 mm, was included in each set of plot images to provide a known scale. In circumstances where the clay brick did not render properly point clouds were scaled on the space between plant rows.

2.3. Image processing

Three-dimensional point clouds were created for each plot from the set of 96 RGB images, using Pix4Dmapper Pro (Pix4D, 2016) photogrammetric software, running on a Windows 10 P, with 32 GB of RAM and a quad-core 4.0GHZ processer. Images were imported to Pix4D and then optimised and matched to create 3D point clouds, using ½ scale images, optimal point density and a minimum of three required matches. Appropriate scales were applied to each cloud and results were re-optimised and processed. Finally, a digital surface model (DSM) was created for each point cloud, using Pix4D's DSM processing tool, using methods of inverse distance weighting with noise filtering and a 'sharp' surface smoothing filter.

In addition to the point clouds produced from the 96-image set, a further five sets of point clouds were created for each plot, using subsets of 80, 64, 48, 32 and 16 images from the full set. Image subsets of 32 and 64 comprised of a single, or two 32-image rings respectively, with the subsets of 16, 48 and 80 comprised of half, one and a half, and two and a half, 32-image rings respectively. To create the 16-image half rings, images were removed from one side of the plot, leaving 16 images along one side. This method was selected as systematic removal of every second image, resulted in poor processing results due to insufficient image overlap (data not shown).

As a substitute for AGB the volume of plant material within individual plots was calculated with Pix4D's inbuilt volume tool, hereafter referred to as point cloud volume (PCV). For this process, individual polygons were drawn approximately 5 cm above the base of each plot (Fig. 2), with volume between this and the previously computed DSM of the plot being calculated automatically. Polygons were drawn at a height of 5 cm to ensure they were located above the furrow ridges in each plot to eliminate potentially confounding objects, such as rocks and clods of soil, during volume estimation.

Canopy height (CH) was measured from point clouds created with the full 96-image set, using Pix4D's inbuilt measurement tool. Height was measured at four randomly selected points within the top layer of canopy, with the average of these points representing overall canopy height and being referred to as point cloud canopy height (PCH) for the remainder of the study.

2.4. Manual measurements and sampling

Canopy height was measured with a ruler one day prior to image capture. Four randomly selected representative plants were measured within each plot. Measurements were taken from the base of each plant to the uppermost spikelet, and averaged to best represent canopy height.

Entire plots were harvested and AGB measured after physiological maturity (Zadoks growth stage 92–93) (Zadoks et al., 1974), with plants being removed at ground level. Plant material from each plot was individually weighed to attain a dry AGB weight. Plots were harvested on a dry summer day, inducing low crop moisture levels and negating the need for oven drying of material.

Above ground biomass samples from each plot were individually threshed, with the grain being retained and weighed to determine grain yield and calculate HI for each plot. Harvest index was calculated as grain yield per plot (kg)/AGB per plot (kg). Predictions of HI were also calculated from PCV measurements, by converting these to an AGB estimate, using the equation of linear regression between the two, *i.e.*

$$\text{HI} = \text{grain yield per plot (kg)}/(M^{*}\text{AGB per plot (kg)} + C) \quad (1)$$

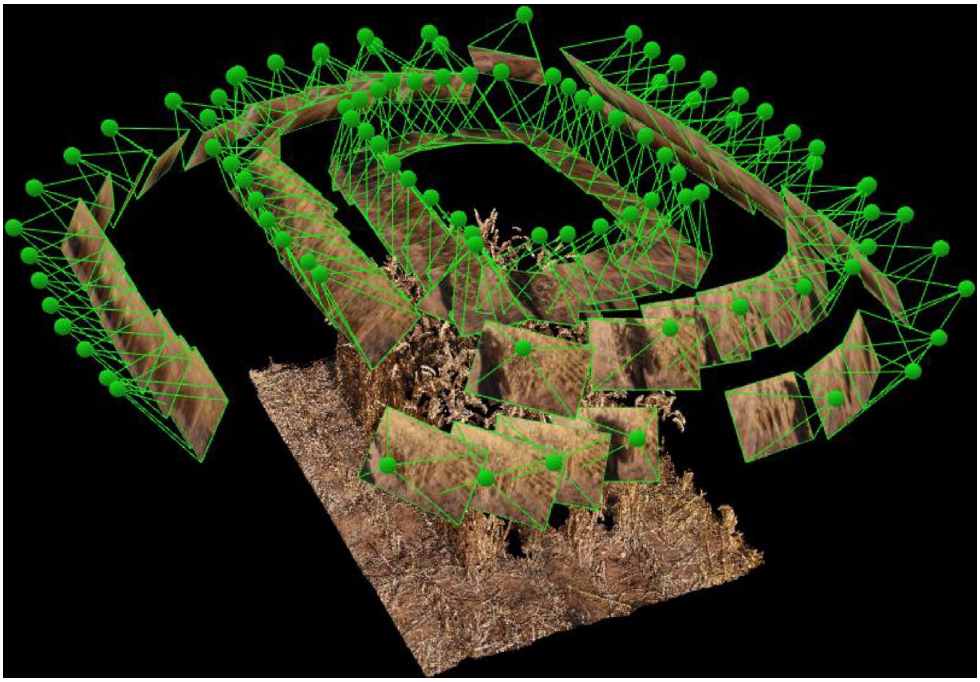

Fig. 1. Point cloud from a single plot of wheat created with Pix4D, showing the images used for construction.

Where M and C are the AGB and PCV regression slope and intercept.

Henceforth this will be referred to as point cloud volume predicted harvest index (PCV-HI).

2.5. Statistical analyses

Summary statistics, variance, and ANOVA of traits were conducted in the R statistical package (R-Core Team, 2015). Relationships between manual measurements and point cloud derived values were evaluated in R and RMA: Software for Reduced Major Axis Regression (Bohonak, 2004), using linear regression (Model II – Reduced Major Axis) (Ludbrook, 1997, 2012). Comparisons between linear regressions were conducted using the methods described in Zar (1984) for slope and elevation comparison.

3. Results

3.1. Point cloud creation

Mean initial processing times and mean points per cloud produced from each image set are shown in Table 1. Initial processing time includes image matching and processing, as well as point cloud densification. This accounted for the bulk of the processing required, with subsequent scaling of point clouds and generation of DSM's taking approximately a third of the original processing time. Mean points per cloud increased with the number of images in each set, however, point clouds produced from the 64-image set saw a spike in mean points per cloud, being greater than both the number of points in the 48 and 80-image sets, but still less than the 96-image sets.

Table 1
The mean processing time (to the nearest minute) and mean number of points within the point cloud of each plot (nearest thousand), for each image set processed.

Image Set	Mean Processing Time (min)	Mean Points Within Plot ($\times 10^3$)
16	6	180
32	15	321
48	28	485
64	49	917
80	65	881
96	80	952

While it was possible to produce point clouds using the sets of 16 and 32 images, the resulting point clouds contained a greatly reduced number of individual points and, upon visual inspection, appear to provide a poor representation of physical plots (Fig. 3). While the mean number of points was reduced when fewer images were processed, the distribution of these points within the plot was also reduced, with points only appearing as small clusters in the crop canopy.

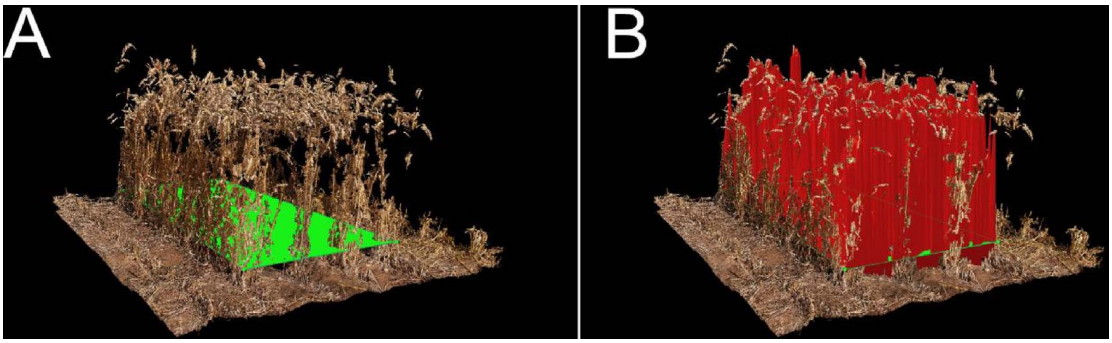

Fig. 2. Point cloud of a single plot of wheat showing, A) the polygon drawn at the plot base for volume estimation within Pix4D, and B) the volume estimation tool within Pix4D, showing the 3D volume measured.

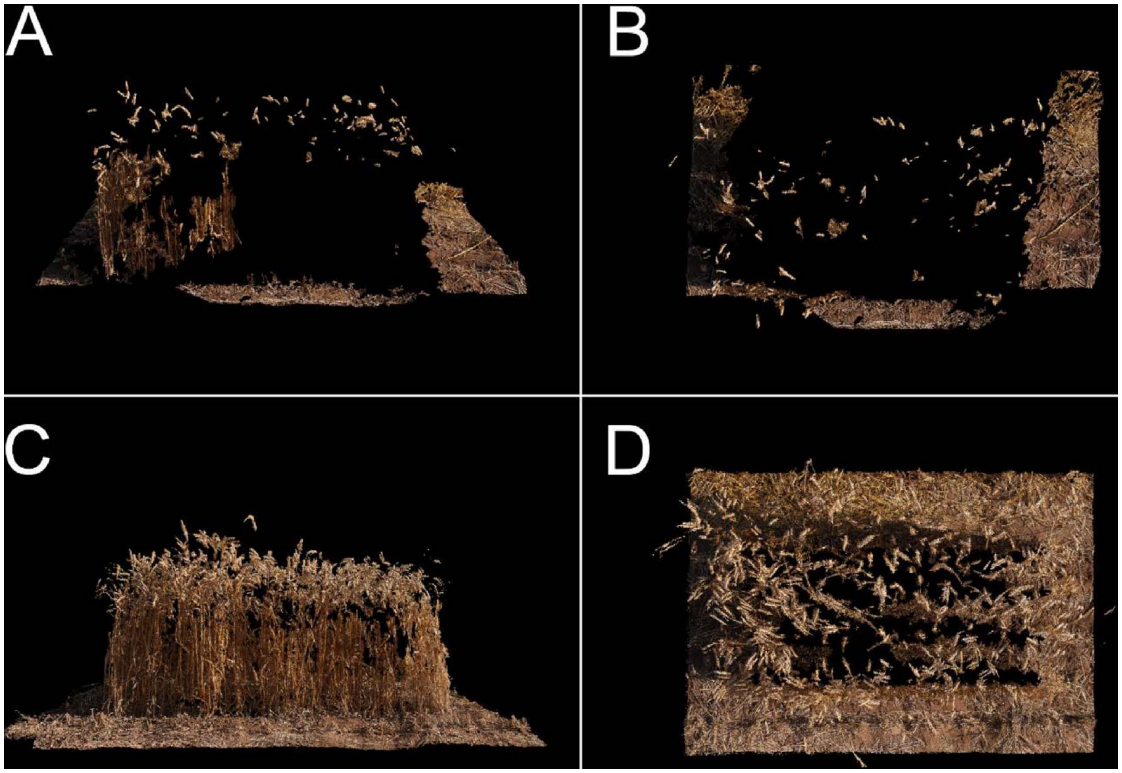

Fig. 3. Side (A, C) and top (B, D) views of plot point clouds (400 plants/m^2) processed using 16 (A, B) and 96 (C, D) images.

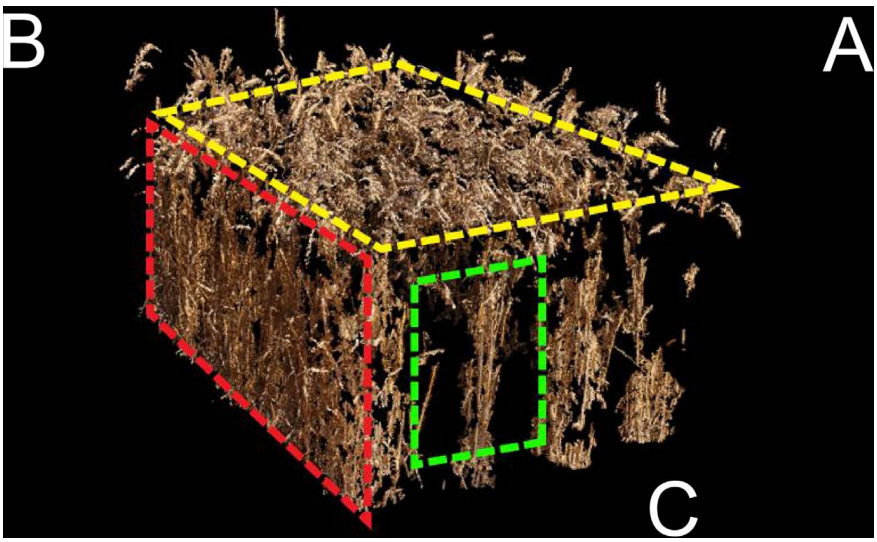

Fig. 4. Point cloud from a single plot of wheat showing points measured above the soil surface, for A) top of canopy B) side stems and leaves C) inner stems and leaves.

Within point clouds created from the 96-image sets, points were predominately located in the upper canopy. Plot edges were reasonably defined, with the majority of stems and leaves being modelled. In contrast, the inner canopy was poorly represented, with a distinct lack of points in this area of the cloud. An example of point distribution is displayed in Fig. 4, showing the upper canopy (A), plot edges (B), and inner canopy (C) for a plot produced from the 96-image set.

To investigate the disparity in the quality of point clouds created with fewer images, to those created with more images, correlation coefficients of regressions between AGB and PCV were plotted against the number of images used to produce each point cloud (Fig. 5). The plot of these correlation coefficients shows an increase in correlation strength, with an increase in the number of images contained in each image set.

Comparison of regression equations used to create Fig. 5 showed that a single slope could be applied to the majority of regressions, the exceptions being clouds created with the 16-image set having a significantly different slope to clouds created with the 96 and 80-image sets ($p > 0.05$).

For the remainder of this study results are presented from point clouds created using the 96-image set. From visual inspection of point clouds, as well as the regression in Fig. 5, it is apparent this is the most dense and best constructed set of point clouds, and will allow for the most rigorous data exploration in the remainder of the study.

3.2. Biomass vs volume

Above ground biomass of plots ranged from 0.86–1.82 kg, with a

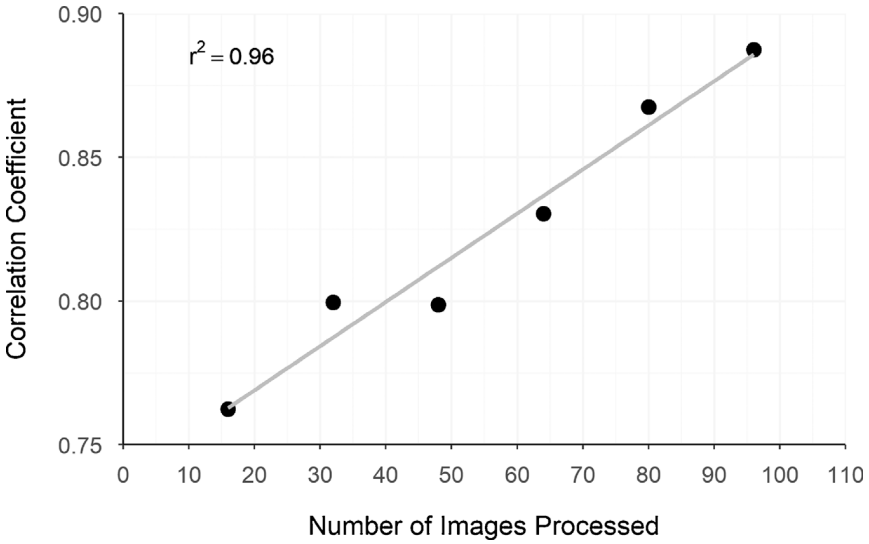

Fig. 5. The correlation coefficients of the linear regression between above ground biomass (AGB) and point cloud volume (PCV), for each image set.

mean of 1.38 kg per plot and a coefficient of variation (CV) of 0.23. Point cloud volume ranged from 0.04–0.57 m^3 per plot, with a mean of 0.28 m^3 per plot and a CV of 0.55.

Analysis of AGB and PCV with ANOVA showed no significant effect of seeding rate or replicate, on either set of measurements ($p > 0.05$).

Point cloud volume and AGB were analysed with simple linear regression. A strong positive relationship ($r^2 = 0.79$) was observed between the two traits (Fig. 6). Within Fig. 6, Point 1.8, 0.33 is considerably lower than point 1.82, 0.57 as a section of this plot had lodged. Lodging did not occur in any other plot.

3.3. Canopy height

Canopy height of plots ranged from 55 cm to 77.5 cm, with a mean of 68.33 cm and a CV of 11.50. Point cloud height ranged from 54 to 85.25 cm, with a mean of 69.23 cm and a CV of 15.10.

Point cloud height showed a strong positive relationship to CH (Fig. 7).

To investigate the role of height in the derivation of biomass and volume, manual height and PCH were compared against both AGB and PCV through simple linear regression (Fig. 8). The relationship between height measurements and AGB was strong, and similar regardless of whether CH ($r^2 = 0.84$) or PCH ($r^2 = 0.85$) was used. This was also observed in the regressions between height measurements and PCV, where a relatively strong relationship was present regardless of CH ($r^2 = 0.54$) or PCH ($r^2 = 0.61$) being used. Across these regressions, PCH showed a slightly stronger relationship to AGB and PCV than CH.

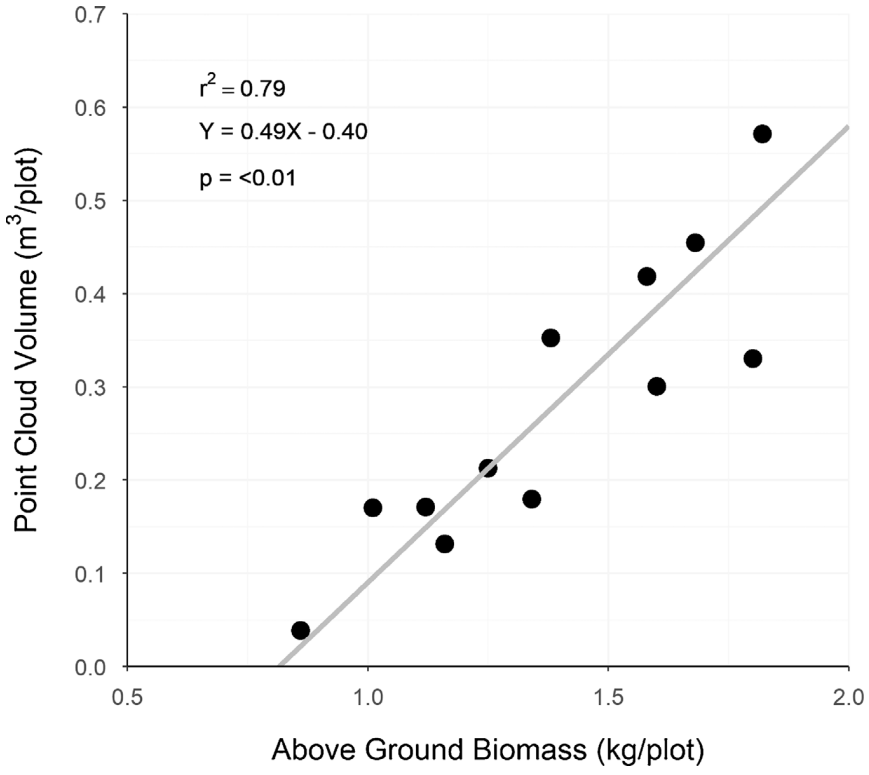

Fig. 6. Linear regression of manually measured above ground biomass and point cloud volume per plot (PCVP).

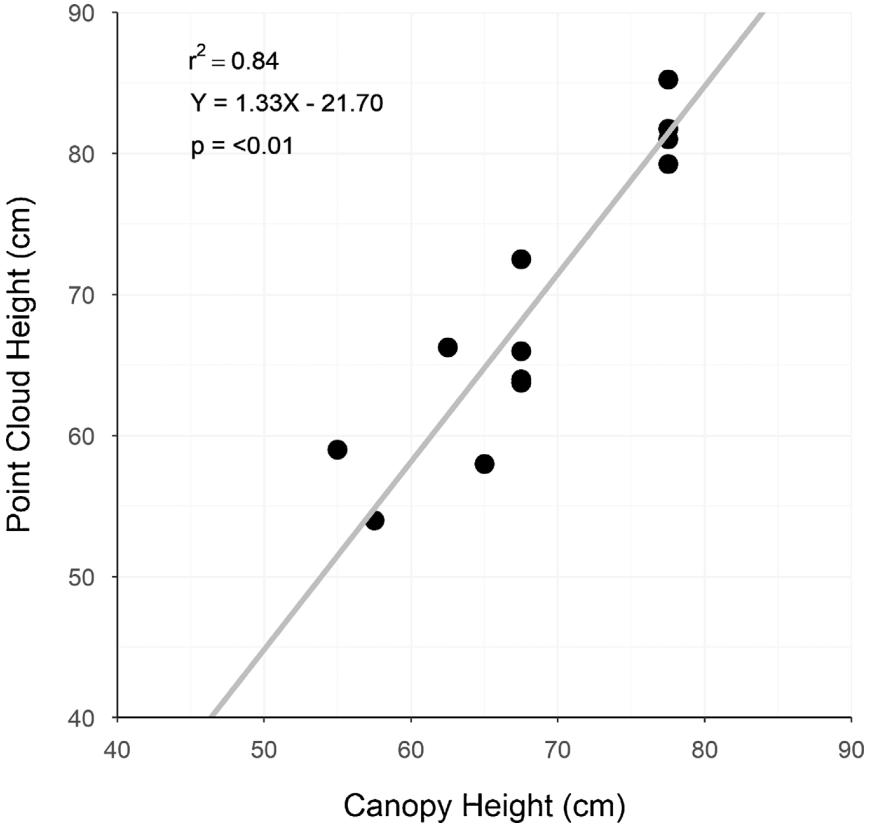

Fig. 7. Linear regression of manually measured canopy height (CH) and canopy height measured from point clouds (PCH).

3.4. Harvest index

To estimate HI using PCV, biomass per plot was predicted using the linear regression model shown in Fig. 6. From this, the trait PCV-HI was calculated and compared to HI. Predicted HI values had both a similar range and mean compared to measured HI. Harvest index values ranged from 0.17 to 0.44, with a mean of 0.30 and a CV of 26.69, and PCV-HI values ranged from 0.16 to 0.45, with a mean of 0.31 and a CV of 31.57.

Simple linear regressions were used to compare HI to PCV-HI (Fig. 9). Correlation between HI and PCV-HI was high (r = 0.94), with the regression model showing a significant correlation (p = < 0.01).

4. Discussion

4.1. Point cloud construction

Pix4D is designed for aerial mapping and 3D model creation of large-scale areas and objects, from Unmanned Aerial Vehicles (UAVs). Despite being designed for the processing of aerial imagery, it was easily and effectively used to create point clouds of wheat research plots from ground-based images in the current study.

One drawback of using a commercial digital camera for acquiring images in the current study, was the lack of any on-board coordinate or scaling system (such as GPS or IMU's) commonly found in UAVs. This resulted in all point clouds produced having an arbitrary scaling system, requiring correction based on known distances before data extraction could occur and thereby increasing the amount of processing time per model.

This small-scale modelling is also greatly influenced by environmental effects, particularly wind. Wind movement of plants within plots results in slightly different positioning of plants within images. This leads to poor co-localisation of points during point cloud processing, and results in missing sections of plants in the final point cloud.

Poor co-localisation of points was especially apparent in point clouds created with image sets containing fewer images. This is a fundamental limitation of using photogrammetry for the production of point clouds, where images must overlap sufficiently to effectively contribute to point cloud processing. The percentage of image overlap required is often suggested in the range of 60% (Schirrmann et al., 2016a) to 80% (Colomina and Molina, 2014), and is typically achieved when capturing images from UAVs with pre-planned flight paths and image capture points. The manual image capture methods of the current study did not allow for such precise pre-planning to obtain consistently large amounts of image overlap, though images were taken in a regular pattern for each plot, with an attempt to maximise overlap between images.

Processing point clouds using the 96-image set produced the best mean correlation between AGB and PCV across all plots, though it appears that reducing the number of images to 64, or perhaps as low as 48, may also be feasible for the estimation of plot AGB, as a common line of best fit can be shared between the majority of AGB and PCV regressions. However, this of course becomes a trade-off between the accuracy of AGB estimates and the image collection/processing time, and will be subjective to individual plant breeders and research scientists.

While correlation coefficients of the 16 and 32-image sets were still relatively high (0.76 and 0.80 respectively), it would be unreasonable to rely on these point clouds for volume calculation, due to the poor physical resemblance of these clouds to actual field plots.

It is also worth noting that while a trend in number of points increasing with number of images processed was observed, distribution of points within these clouds were vastly different. Point clouds processed from fewer images tended to have clumps of points at the canopy level, while point clouds processed from more images had a more homogenous spread of points across the canopy, with some points in the lower canopy as well as around the outer stems.

As previously mentioned, the photogrammetry methods of the current study are primarily designed for use with UAV obtained images.

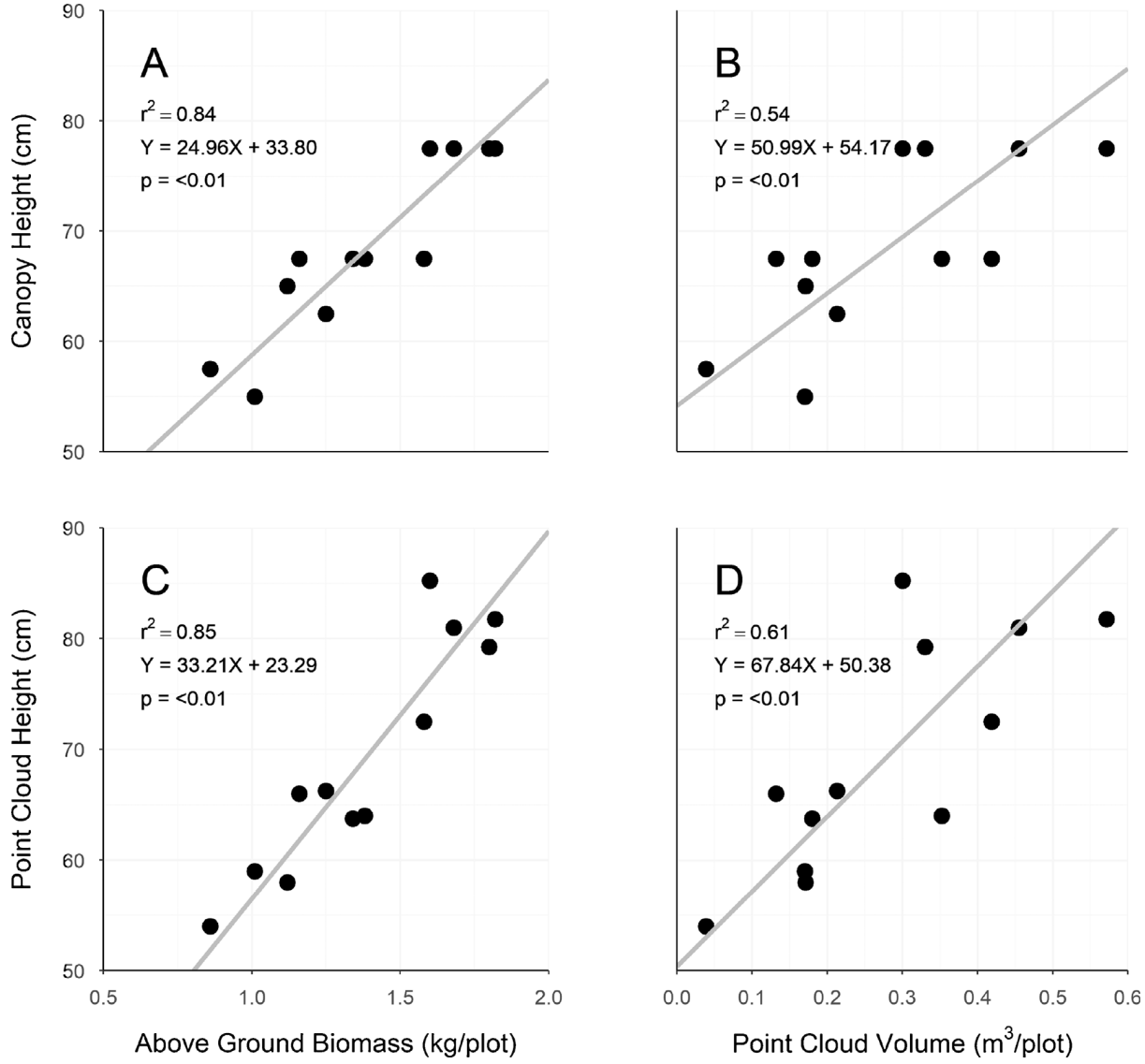

Fig. 8. Regressions for above ground biomass (AGB) and canopy height (CH) (A), point cloud volume (PCV) and CH (B), AGB and point cloud height (PCH) (C), and PCV and PCH (D).

The use of UAVs allows efficient data collection from large areas, an aspect desirable for field trials; however, the captured images and the subsequently processed point cloud have a low spatial resolution (in comparison to ground based imaging). While few studies have investigated the use of UAV collected images for volume based estimation of AGB from wheat plot point clouds, a large number of studies have investigated the use of such images for other agricultural research. In such studies, spatial resolution of UAV captured RGB images commonly ranges from ~1–10 cm per pixel (Rasmussen et al., 2013; Bendig et al., 2014; Geipel et al., 2014; López-Granados et al., 2016; Schirrmann et al., 2016a). In comparison, images from the current study have a spatial resolution of ~0.5 mm per pixel. This greater spatial resolution allows for a more accurate representation of field plots in the constructed point clouds and ultimately, may lead to a more accurate estimation of AGB from these point clouds.

While point clouds were generated through digital imaging and photogrammetry in the current study, they are also commonly generated through laser scanning sensors, such as LiDAR. Though the method of point cloud generation differs between these two sensors, the resulting 3D data is essentially the same. Despite this, LiDAR appears to offer the advantage of greater canopy penetration, to the extent that Li et al. (2015) were able to use it for the calculation of Leaf Area Index. In the current study there were few points within crop canopies (Fig. 4C), with points clustering around the outer edges of the plot. This may be due to slight movements in the canopy between pictures, resulting in only larger structures processing correctly, or it may be an inherent limitation of photogrammetry for this application, where the inner canopy is occluded by the exterior canopy. However, despite any limitation in canopy penetration, the methods employed by this study demonstrate the ability to use RGB cameras and photogrammetry for point cloud creation and the estimation of crop biomass.

4.2. Biomass estimation

Despite the limitations in point cloud construction, as described above, the methods of the current study were able to produce a strong positive relationship of $r^2 = 0.79$ between PCV and AGB (Fig. 6), similar to those reported by other research using point clouds for AGB estimation (Hosoi and Omasa, 2009; Eitel et al., 2014; Greaves et al., 2015). Point clouds have previously been used to estimate AGB in wheat (Hosoi and Omasa (2009); Eitel et al., 2014) and barley (Bendig et al., 2014), as well as leafy biomass of trees (Polo et al., 2009) and arctic shrubs (Greaves et al., 2015), with each of these studies finding strong correlations between dried AGB/leafy biomass and biomass

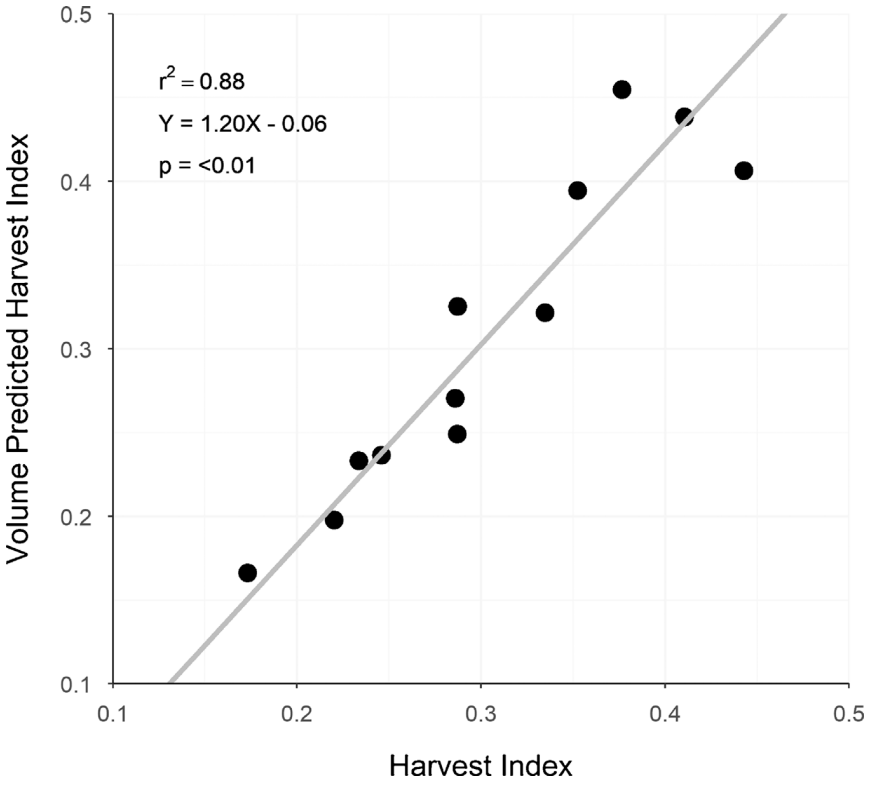

Fig. 9. The linear regression between harvest index and point cloud volume predicted harvest index.

estimators (*e.g.* volume) derived from point clouds. Of these studies, Greaves et al. (2015) used methods that were most similar to the current study; where biomass of arctic shrubs was estimated by using volume derived from a point cloud and mesh (similar to that created by the Pix4D volume tool). These methods resulted in strong relationships (r^2 = 0.92 and 0.91) between volume and dried biomass at two scanning distances. Greaves et al. (2015) also compared manual biomass samples to volume derived from point cloud voxelization (described by Hosoi and Omasa (2006)), again seeing strong relationships at two scanning distances (r^2 = 0.94 and 0.82). Voxel based methods were also used by Hosoi and Omasa (2009), during their investigation of point cloud calculated plant area density, for the comparison of LiDAR derived leaf and stem, and spike area, against manually measured dry weights (r^2 = 0.94 and 0.96 respectively). While the methods of Hosoi and Omasa (2009) are dissimilar from the current study, they still demonstrated a strong relationship between point cloud derived and manual measurements.

The methods of the current study are also similar to those used by Eitel et al. (2014) who observed a strong correlation between estimated volume and AGB. Eitel et al. (2014) used the difference between point cloud derived ground surface models and canopy surfaces models to estimate plot volume, whereas the volume measurement tool used in the current study was used to compare a canopy surface model to a flat surface slightly (~10 cm) above the soil surface.

The relationship between AGB and PCV observed in the current study showed a similar relationship to that observed by Eitel et al. (2014) (r^2 = 0.79) but slightly weaker than the study of Greaves et al. (2015) (r^2 = ~0.9). This may be due purely to natural variation between the data sets, however, one likely factor that may have contributed to this difference is the differing plant material measured. In the current study a single cultivar of wheat was sampled (as was conducted by Eitel et al., 2014), compared to a different plant species in Greaves et al. (2015).

4.3. Biomass height relationship

While volumetric methods of biomass estimation have been discussed, another potential method is the use of canopy height as a biomass predictor. This has been demonstrated by Ehlert et al. (2009) (laser rangefinders), Long and McCallum (2013) (LiDAR), and Bendig et al. (2014, 2015) (point cloud derived crop surface models), with these studies observing a strong correlation between canopy height and AGB. Point cloud derived canopy heights measured in the current study show a strong correlation to manual height as has been demonstrated in the literature (Long and McCallum, 2013; Bendig et al., 2014), indicating that they may be suitable as an estimator for AGB.

The relationship between plot canopy height and AGB (for both manual height and PCH) in the current study shows a strong correlation between the two, aligning with the work of Ehlert et al. (2009); and Bendig et al. (2014, 2015). This strong relationship is also echoed between PCV and canopy height, this being unsurprising as the volume calculations used in this study are heavily influenced by height.

4.4. Height estimation

While PCH measurements showed a strong relationship to canopy height, it is likely that this relationship could be improved with the development of alternate calculation methods. The methods of measuring canopy height from point clouds used in this study, are essentially the same as those used to manually measure canopy height, albeit at a computer rather than in the field. The estimation of canopy height could likely be improved with the application of custom algorithms that average the top layer of canopy points, or select a percentile of point height, allowing a much greater amount of points to be included than the four points used in the current study. However, to the Author's best knowledge it is not currently possible to implement such algorithms within Pix4D, though it may be possible to apply them to exported point clouds.

4.5. Harvest index estimation

The strong correlation observed between PCV-HI and HI indicate that PCV-HI would be a suitable substitute for HI where AGB was not measured. Deriving PCV-HI from plot point clouds offers breeders the opportunity to non-destructively calculate HI without manually collecting AGB data.

4.6. Application to wheat breeding

The techniques of point cloud creation and data extraction demonstrated in the current study provide a potential method for plant breeders to non-destructively estimate the AGB of breeding plots; allowing grain to be mechanically harvested for grain yield estimation, postharvest grain quality measurements and to provide seed for the next generation. However, while strong relationships between AGB and PCV, and HI and PCV-HI have been presented in this study, they were tested on a single genotype. Further testing of these methods across a wide array of genotypes is required, to observe a broad range of these relationships, as well as to test the suitability of these measurements for plant breeding. For this, the heritability (a common measure of genetic repeatability within breeding programmes) of these point cloud measurements will need to be assessed and compared to the heritability of manual measurements.

Though further testing of point cloud derived measurements is required before being incorporated into a wheat breeding programme, it is unlikely that the methods used in the current study are suitable for such a use. Throughput of these methods is extremely low, taking several minutes to image and in many instances over an hour (Table 1) to process each plot to extract AGB/PCV estimates, making it more efficient to physically harvest and measure AGB. This is especially true when considering hundreds, or more likely thousands, of plots may require sampling within a breeding programme. However, these methods would be suitable for small scale research projects where AGB estimates are desired and destructive sampling methods are not possible.

While the methods of the current study are low-throughput, they demonstrate the type of data extractable from point clouds, and the potential of this data to be used within plant breeding programmes. Non-destructive biomass estimation will provide plant breeders with a valuable data set that has previously been inaccessible. Current methods of AGB measurement or estimation are destructive and laborious (in the case of manual sampling), subjective (in the case of visual assessment), or prone to saturation after canopy closure (in the case of VIs). The use of point cloud data to estimate AGB will allow plant breeders to objectively estimate AGB from field trials, while maintaining the full integrity of yield plots for grain yield assessment. Though the methods of the current study are currently too impractical to apply to large scale field research, there are opportunities to help alleviate throughput challenges. For example, rigid frames with a large number of inexpensive cameras could be placed or driven over plots, allowing all images for any given plot to be collected at once. This would also remove any confounding effects of wind, as encountered in this study. Another example could be a motorised arm which pivots a camera around the centre of the plot and collects images as it travels, this again could be placed over each plot, or attached to a vehicle for easy transport.

Throughput of image processing could be improved through the use of computing clusters, however this would quickly become expensive when purchasing sufficient software licencing. While there is currently no open-source software capable of the processing conducted in the present study, there is promising open-source software in development (*e.g.* OpenDroneMap (http://opendronemap.org/)), which may offer an alternative to current licenced software options. Current software options take advantage of multi-thread and GPU processing of single machines, but do not allow for distributed parallel processing across multiple machines (Pix4D, 2016). Implementation of such processing may also allow for increased throughput, whether through processing speed or processing many projects simultaneously.

Despite the current throughput challenges, the main advantage of these methods is that they use inexpensive and intuitive sensors, making them easily accessible to plant breeders and research scientists. No specialist skills are required for digital camera operation, and the processing pipelines of software such as PiX4D are user-friendly. This is in contrast to other sensors of interest, such as LiDAR, which are expensive in comparison and require specific skill sets (*e.g.* software engineering) to initiate data collection and create in-house processing pipelines (Deery et al., 2014).

5. Conclusion

This study has demonstrated a set of methods, which can be conducted relatively cheaply, using commercially-available digital cameras and photogrammetry software, for the creation of point cloud data and the estimation of AGB, canopy height and HI. Point cloud derived volume estimates showed strong correlation to AGB, supporting the results from the few studies in this area of research. Multiple sets of point clouds were created from differing numbers of images to determine an optimal amount for processing, with a conclusion that biomass estimated from as few as 48 images per plot would be suitable to use for plant breeding and other research purposes. Estimates of both plot canopy height and HI derived from point clouds correlated well to manual measurements, both of which could be applied within breeding programmes or research projects. The current study demonstrates that high fidelity point cloud data can be a valuable tool for wheat research and breeding, when collected and processed with high-throughput methods.

Acknowledgements

The Authors wish to acknowledge the South Australian Grains Industry Trust (UA514), the Grains Research and Development Corporation (GRS11009), The University of Adelaide School of Agriculture Food and Wine and the Australian Government Research Training Program Scholarship for their funding support of this research.

References

Amaral, L.R., Molin, J.P., Portz, G., Finazzi, F.B., Cortinove, L., 2015. Comparison of crop canopy reflectance sensors used to identify sugarcane biomass and nitrogen status. Precis. Agric. 16, 15–28.

Bendig, J., Bolten, A., Bennertz, S., Broscheit, J., Eichfuss, S., Bareth, G., 2014. Estimating biomass of barley using crop surface models (CSMs) derived from UAV-based RGB imaging. Remote Sens. 6, 10395–10412.

Bendig, J., Yu, K., Aasen, H., Bolten, A., Bennertz, S., Broscheit, J., Gnyp, M.L., Bareth, G., 2015. Combining UAV-based plant height from crop surface models, visible, and near infrared vegetation indices for biomass monitoring in barley. Int. J. Appl. Earth Obs. Geoinf. 39, 79–87.

Bohonak, A., 2004. RMA: Software for Reduced Major Axis Regression. San Diego State University.

Colomina, I., Molina, P., 2014. Unmanned aerial systems for photogrammetry and remote sensing: a review. ISPRS J. Photogramm. Remote Sens. 92, 79–97.

Damisch, W., Wiberg, A., 1991. Biomass yield — a topical issue in modern wheat breeding programmes. Plant Breed. 107, 11–17.

Deery, D., Jimenez-Berni, J., Jones, H., Sirault, X., Furbank, R., 2014. Proximal remote sensing buggies and potential applications for field-based phenotyping. Agronomy 4, 349.

Donald, C.M., Hamblin, J., 1976. Biological yield and harvest index of cereals as agronomic and plant breeding criteria. Adv. Agron. 28, 361–405.

Ehlert, D., Adamek, R., Horn, H.-J., 2009. Laser rangefinder-based measuring of crop biomass under field conditions. Precis. Agric. 10, 395–408.

Eitel, J.U.H., Magney, T.S., Vierling, L.A., Brown, T.T., Huggins, D.R., 2014. LiDAR based biomass and crop nitrogen estimates for rapid, non-destructive assessment of wheat nitrogen status. Field Crops Res. 159, 21–32.

Geipel, J., Link, J., Claupein, W., 2014. Combined spectral and spatial modeling of corn yield based on aerial images and crop surface models acquired with an unmanned aircraft system. Remote Sens. 6, 10335.

Greaves, H.E., Vierling, L.A., Eitel, J.U.H., Boelman, N.T., Magney, T.S., Prager, C.M., Griffin, K.L., 2015. Estimating aboveground biomass and leaf area of low-stature Arctic shrubs with terrestrial LiDAR. Remote Sens. Environ. 164, 26–35.

Herrero-Huerta, M., Felipe-Garcia, B., Belmar-Lizaran, S., Hernandez-Lopez, D., Rodriguez-Gonzalvez, P., Gonzalez-Aguilera, D., 2016. Dense Canopy Height Model from a low-cost photogrammetric platform and LiDAR data. Trees-Struct. Funct. 30, 1287–1301.

Hosoi, F., Omasa, K., 2006. Voxel-based 3-D modeling of individual trees for estimating leaf area density using high-resolution portable scanning lidar. IEEE Trans. Geosci. Remote Sens. 44, 3610–3618.

Hosoi, F., Omasa, K., 2009. Estimating vertical plant area density profile and growth parameters of a wheat canopy at different growth stages using three-dimensional portable lidar imaging. ISPRS J. Photogramm. Remote Sens. 64, 151–158.

López-Granados, F., Torres-Sánchez, J., Serrano-Pérez, A., de Castro, A.I., Mesas-Carrascosa, F.-J., Peña, J.-M., 2016. Early season weed mapping in sunflower using UAV technology: variability of herbicide treatment maps against weed thresholds. Precis. Agric. 17, 183–199.

Li, W., Niu, Z., Huang, N., Wang, C., Gao, S., Wu, C.Y., 2015. Airborne LiDAR technique for estimating biomass components of maize: a case study in Zhangye City, Northwest China. Ecol. Indic. 57, 486–496.

Long, D.S., McCallum, J.D., 2013. Mapping straw yield using on-combine light detection and ranging (lidar). Int. J. Remote Sens. 34, 6121–6134.

Ludbrook, J., 1997. Special article comparing methods of measurement. Clin. Exp. Pharmacol. Physiol. 24, 193–203.

Ludbrook, J., 2012. A primer for biomedical scientists on how to execute Model II linear regression analysis. Clin. Exp. Pharmacol. Physiol. 39, 329–335.

Montes, J.M., Technow, F., Dhillon, B.S., Mauch, F., Melchinger, A.E., 2011. High-throughput non-destructive biomass determination during early plant development in maize under field conditions. Field Crops Res. 121, 268–273.

Pittman, J.J., Arnall, D.B., Interrante, S.M., Moffet, C.A., Butler, T.J., 2015. Estimation of biomass and canopy height in bermudagrass, alfalfa, and wheat using ultrasonic, laser, and spectral sensors. Sensors 15, 2920–2943.

Pix4D, 2016. Pix4Dmapper Pro. Available at: https://pix4d.com/product/pix4dmapper-pro/.

Polo, J.R.R., Sanz, R., Llorens, J., Arno, J., Escola, A., Ribes-Dasi, P., Masip, J., Camp, F., Gracia, F., Solanelles, F., Palleja, T., Pal, L., Planas, S., Gil, E., Palacin, J., 2009. A tractor-mounted scanning LIDAR for the non-destructive measurement of vegetative volume and surface area of tree-row plantations: a comparison with conventional destructive measurements. Biosyst. Eng. 102, 128–134.

R-Core Team, 2015. R: A Language and Environment for Statistical Computing. Available at: https://www.R-project.org/.

Rasmussen, J., Nielsen, J., Garcia-Ruiz, F., Christensen, S., Streibig, J.C., 2013. Potential uses of small unmanned aircraft systems (UAS) in weed research. Weed Res. 53, 242–248.

Reynolds, M., Foulkes, J., Furbank, R., Griffiths, S., King, J., Murchie, E., Parry, M., Slafer, G., 2012. Achieving yield gains in wheat. Plant Cell Environ. 35, 1799–1823.

Richards, R.A., Rebetzke, G.J., Condon, A.G., van Herwaarden, A.F., 2002. Breeding opportunities for increasing the efficiency of water use and crop yield in temperate cereals. Crop Sci. 42, 111–121.

Richards, R.A., 2000. Selectable traits to increase crop photosynthesis and yield of grain crops. J. Exp. Bot. 51, 447–458.

Saeys, W., Lenaerts, B., Craessaerts, G., De Baerdemaeker, J., 2009. Estimation of the crop density of small grains using LiDAR sensors. Biosyst. Eng. 102, 22–30.

Schirrmann, M., Giebel, A., Gleiniger, F., Pflanz, M., Lentschke, J., Dammer, K.H., 2016a. Monitoring agronomic parameters of winter wheat crops with low-cost UAV imagery. Remote Sens. 8, 19.

Schirrmann, M., Hamdorf, A., Garz, A., Ustyuzhanin, A., Dammer, K.H., 2016b. Estimating wheat biomass by combining image clustering with crop height. Comput. Electron. Agric. 121, 374–384.

Sharma, R.C., 1993. Selection for biomass yield in wheat. Euphytica 70, 35–42.

Tucker, C.J., 1977. Asymptotic nature of grass canopy spectral reflectance. Appl. Opt. 16, 1151–1156.

Winterhalter, L., Mistele, B., Jampatong, S., Schmidhalter, U., 2011. High-throughput sensing of aerial biomass and above-ground nitrogen uptake in the vegetative stage of well-watered and drought stressed tropical maize hybrids. Crop Sci. 51, 479–489.

Zadoks, J.C., Chang, T.T., Konzak, C.F., 1974. A decimal code for the growth stages of cereals. Weed Res. 14, 415–421.

Zar, J.H., 1984. Biostatistical Analysis. Prentice-Hall, Englewood Cliffs,N.J.

Zolkos, S.G., Goetz, S.J., Dubayah, R., 2013. A meta-analysis of terrestrial aboveground biomass estimation using lidar remote sensing. Remote Sens. Environ. 128, 289–298.

Chapter 4

Estimating Biomass and Canopy Height with LiDAR for Field Crop Breeding

Statement of Authorship

Title of Paper	Estimating Biomass and Canopy Height With LiDAR for Field Crop Breeding
Publication Status	☑ Published ☐ Accepted for Publication ☐ Submitted for Publication ☐ Unpublished and Unsubmitted work written in manuscript style
Publication Details	Walter JDC, Edwards J, McDonald G and Kuchel H (2019) Estimating Biomass and Canopy Height With LiDAR for Field Crop Breeding. Front. Plant Sci. 10:1145. doi: 10.3389/fpls.2019.01145

Principal Author

Name of Principal Author (Candidate)	James Walter
Contribution to the Paper	Developed data processing methods, collected/analysed/interpreted data, wrote manuscript and acted as corresponding author.
Overall percentage (%)	85%
Certification:	This paper reports on original research I conducted during the period of my Higher Degree by Research candidature and is not subject to any obligations or contractual agreements with a third party that would constrain its inclusion in this thesis. I am the primary author of this paper.
Signature	Date 14/10/19

Co-Author Contributions

By signing the Statement of Authorship, each author certifies that:

i. the candidate's stated contribution to the publication is accurate (as detailed above);

ii. permission is granted for the candidate in include the publication in the thesis; and

iii. the sum of all co-author contributions is equal to 100% less the candidate's stated contribution.

Name of Co-Author	James Edwards
Contribution to the Paper	Supervised development of work, helped to interpret data, evaluate and edit the manuscript.
Signature	Date 14/10/'19

Name of Co-Author	Glenn McDonald
Contribution to the Paper	Supervised development of work, helped to interpret data, evaluate and edit the manuscript.
Signature	Date 21/11/19

Name of Co-Author	Haydn Kuchel
Contribution to the Paper	Supervised development of work, contributed to analytical methodologies, helped to interpret data, evaluate and edit the manuscript.
Signature	Date 14/10/19

frontiers in Plant Science

ORIGINAL RESEARCH
published: 26 September 2019
doi: 10.3389/fpls.2019.01145

Estimating Biomass and Canopy Height With LiDAR for Field Crop Breeding

James D. C. Walter[1,2]*, *James Edwards*[1,2], *Glenn McDonald*[1] and *Haydn Kuchel*[1,2]

[1] School of Agriculture, Food and Wine, The University of Adelaide, Glen Osmond, SA, Australia, [2] Australian Grain Technologies Pty Ltd, Roseworthy, SA, Australia

Above-ground biomass (AGB) is a trait with much potential for exploitation within wheat breeding programs and is linked closely to canopy height (CH). However, collecting phenotypic data for AGB and CH within breeding programs is labor intensive, and in the case of AGB, destructive and prone to assessment error. As a result, measuring these traits is seldom a priority for breeders, especially at the early stages of a selection program. LiDAR has been demonstrated as a sensor capable of collecting three-dimensional data from wheat field trials, and potentially suitable for providing objective, non-destructive, high-throughput estimates of AGB and CH for use by wheat breeders. The current study investigates the deployment of a LiDAR system on a ground-based high-throughput phenotyping platform in eight wheat field trials across southern Australia, for the non-destructive estimate of AGB and CH. LiDAR-derived measurements were compared to manual measurements of AGB and CH collected at each site and assessed for their suitability of application within a breeding program. Correlations between AGB and LiDAR Projected Volume (LPV) were generally strong (up to r = 0.86), as were correlations between CH and LiDAR Canopy Height (LCH) (up to r = 0.94). Heritability (H^2) of LPV (H^2 = 0.32–0.90) was observed to be greater than, or similar to, the heritability of AGB (H^2 = 0.12–0.78) for the majority of measurements. A similar level of heritability was observed for LCH (H^2 = 0.41–0.98) and CH (H^2 = 0.49–0.98). Further to this, measurements of LPV and LCH were shown to be highly repeatable when collected from either the same or opposite direction of travel. LiDAR scans were collected at a rate of 2,400 plots per hour, with the potential to further increase throughput to 7,400 plots per hour. This research demonstrates the capability of LiDAR sensors to collect high-quality, non-destructive, repeatable measurements of AGB and CH suitable for use within both breeding and research programs.

Keywords: wheat, phenomics, high throughput phenotyping, field phenotyping, plant breeding

OPEN ACCESS

Edited by:
Andreas Hund,
ETH Zürich, Switzerland

Reviewed by:
Jorge E. Mayer,
Ag RD&IP Consult P/L, Australia
Alexandre Escolà,
Universitat de Lleida, Spain
Shangpeng Sun,
University of Georgia, United States

***Correspondence:**
James Walter
james.walter@agtbreeding.com.au

Specialty section:
This article was submitted to Technical Advances in Plant Science, a section of the journal Frontiers in Plant Science

Received: *19 May 2019*
Accepted: *22 August 2019*
Published: *26 September 2019*

Citation:
Walter JDC, Edwards J, McDonald G and Kuchel H (2019) Estimating Biomass and Canopy Height With LiDAR for Field Crop Breeding. Front. Plant Sci. 10:1145. doi: 10.3389/fpls.2019.01145

INTRODUCTION

In recent years there has been much discussion regarding the role of high-throughput phenotyping (HTP) technologies within field crop breeding programs, focused primarily on the potential of these technologies to reduce the current disparity between the amount of phenotype and genotype data available to breeders (Cobb et al., 2013; Araus and Cairns, 2014). There are three key aspects

of these technologies which interest field crop breeders: i) the ability to collect data faster than traditional methods; ii) the ability to collect higher-quality objective data than traditional methods; and (iii) the ability to collect data which cannot be collected through existing methods. With these three aspects in mind, the trait of above-ground biomass (AGB) is a prime candidate to benefit from the potential advantages offered by HTP technologies.

Above-ground biomass is traditionally measured through laborious and destructive methods, requiring crop cuts to be collected from field plots and dried in an oven before being weighed to assess the dry biomass of each sample. This multi-step process is prone to error, from variability in the area within the plot sampled, to the potential loss of material while cutting, transporting, and handling samples. Furthermore, the destructive nature of crop cuts is undesirable within field crop breeding programs due to the loss of plot area and edge effects that influence plot yield. Despite the inconvenience of phenotyping AGB, it is an important trait of interest in many field crop breeding programs. For bread wheat (*Triticum aestivum* L.), AGB has been identified as a trait with much potential to exploit within breeding programs, particularly in relation to yield improvements through harvest index and radiation use efficiency (Reynolds et al., 2012), water use efficiency (Richards et al., 2002), drought tolerance (Fischer and Wood, 1979), as well as potential advantages in crop competitiveness (Zerner et al., 2016).

Of the sensors investigated to estimate AGB with HTP to date, one of the most promising is LiDAR, a laser-based sensor, from which raw data can be transformed into a three-dimensional (3D) point cloud. As AGB is a 3D trait in nature, point cloud data provides a logical advantage compared to two-dimensional sensors such as digital or multispectral cameras, to accurately account for and estimate AGB of field crops. Although there are other methods and technologies that can be used to generate point cloud data, such as digital images and photogrammetry techniques (Walter et al., 2018), LiDAR-based systems offer not only a high-throughput and high-density method of collecting such data, but also the possibility of penetrating and collecting measurements from within the crop canopy.

To date, few studies have investigated the use of LiDAR, or similar technologies, to estimate the AGB of field crops. Those that have, often used LiDAR-derived canopy height (CH) as a proxy of AGB (Long and McCallum, 2013; Pittman et al., 2015; Eitel et al., 2016). This approach may be suitable for large-scale biomass estimation, such as in commercial crops, but in cereal breeding programs there is often little variation in CH among breeding lines. Investigations into processing methods which utilize the 3D nature of LiDAR-derived point cloud data have been undertaken, with volume measurements of point clouds (Jimenez-Berni et al., 2018; Sun et al., 2018; Walter et al., 2018), and 3D indices (Jimenez-Berni et al., 2018) shown to correlate strongly to manually measured AGB. While the findings of these studies are promising, they have not fully investigated how these methods and data may be applied to field crop breeding programs. One particular shortcoming of these previous studies is that they were limited to a single environment and a relatively small number of plots, in contrast to commercial breeding programs, which operate across many environments and require many plots to be evaluated.

The current study investigates the deployment of a LiDAR-based system for the non-destructive estimation of AGB and CH across multiple environments, with this system based on the High-throughput Imaging Boom (HIB) described by Walter et al. (2019). The logistics of integrating such a system within a breeding program are discussed, along with the relevance of the data to breeding programs, particularly focusing on trait heritability and genetic and residual correlations. Though the current study takes place within a wheat breeding program, we believe this discussion is relevant to a wide variety of field crop breeding and research programs.

METHODS

Site and Trial Design

To investigate the application of LiDAR sensors within a wheat breeding program, field trials were run across eight sites in southern Australia, encompassing a range of environments with differences in yield potential. The trial sites selected are used for the evaluation of germplasm by a commercial wheat breeding program and are representative of the environmental range over which wheat is grown in the region. Location and details of the eight sites are shown in **Table 1**.

Each trial consisted of eight bread wheat (*Triticum aestivum* L.) cultivars, grown in small plots and designed as a completely

TABLE 1 | Location and details of the eight field trial sites present in the current study. Latitude and longitude are presented in the WGS84 datum.

Site		Latitude (°)	Longitude (°)	Mean crop above-ground biomass at ZGS 65 (t/ha)	Mean crop canopy height at ZGS 65 (cm)
Angas Valley	(AV)	–34.758645	139.241074	6.7	76.5
Booleroo	(BL)	–32.801685	138.296129	5.5	63.5
Kaniva	(KV)	–36.436664	141.197603	14.6	87.7
Minnipa	(MN)	–32.841374	135.156289	1.4	39.6
Pinnaroo	(PN)	–35.350264	141.066939	7.9	81.4
Roseworthy	(RS)	–34.526346	138.665595	11.1	92.8
Rudall	(RD)	–33.656549	136.141373	5.0	49.4
Winulta	(WT)	–34.253630	137.884995	12.4	88.2

randomized factorial design, with factors of genotype and sample time and three replicates (192 plots total). More sampling times were allocated during experimental design than were ultimately utilized in the current study. Trials were uniquely randomized at each site and were specifically designed to provide large amounts of phenotypic variation for plant height and above-ground biomass. Cultivars selected for this purpose were: Axe, Beckom, Halberd, Krichauff, Scepter, Shield, Wyalkatchem, and Yitpi. Trials were located within large-scale wheat breeding sites (approximately 6 ha and 8,000 plots per site) and managed by Australian Grain Technologies (AGT). Plots were 3.2 × 1.32 m and consisted of five rows spaced at 25 cm.

Manual Measurements

Manual measurements were collected across all sites during the growing season. Sample times differed between sites (**Table 2**), though all sites were sampled at anthesis — Zadoks growth scale 65 [ZGS 65 (Zadoks et al., 1974)] — as a measurement of maximum leaf biomass. Developmental rate differs between the varieties used in the current study, with flowering time spread approximately across a two week window. As such ZGS values assigned are nominal, and sample dates were determined when 50% of varieties were at, or had surpassed, the designated ZGS. This does not impact on the processing or analysis methods used for the purpose of comparing manual and digital measurements in the current study. At each sample time CH was measured in each plot, while AGB was measured in plots of the corresponding sample time. Canopy height was measured with a ruler at four randomly-selected points within each plot, with an average of these heights recorded to provide a representative CH. Above-ground biomass was collected from individual plots as two linear meters of plant material (1m from two adjacent rows) cut at ground level. Cuts were taken from the inner seed rows to avoid edge effects. Cuts from each plot were bundled, dried at 45°C for two weeks, then weighed to obtain AGB. Due to the small size of plots sown in the trial it was impractical to take multiple AGB samples from individual plots. To circumvent this, sampling time was allocated as a factor within the trial design, such that each sampling time was undertaken within unique plots.

TABLE 2 | Sample times and associated Zadoks growth scale for each of the sites in the current study.

Site	Sample time				
	ZGS 31	*ZGS 49*	*ZGS 59*	*ZGS 65*	*ZGS 96*
AV		✓		✓	
BL				✓	
KV				✓	
MN				✓	
PN				✓	
RS	✓	✓	✓	✓	✓
RD				✓	
WT	✓	✓		✓	

LiDAR Measurements

The LiDAR sensors used in the current study were SICK LMS400-2000 (SICK AG, Waldkirch, Germany). These 2D sensors have a 70° field of view and are capable of scanning between 270–500 Hz at an angular resolution of 0.1°–1.0°, with a ± 4 mm systematic measurement error and a 3–10 mm statistical error, depending on remission distance. For the purpose of the current study, two sensors were mounted on a boom of adjustable height and attached to a tractor as shown in **Figure 1**. The sensors are mounted at a nadir angle, with scans occurring along the crop row. Measurements are collected across the crop rows as the tractor moves. Detailed information on the boom and its implementation within field plot trials is provided in Walter et al. (2019). For the current study all LiDAR measurements were collected from a single direction of travel, as opposed to the serpentine manner described in Walter et al. (2019). To investigate the repeatability of LiDAR measurements at Roseworthy, three scans were conducted at each timepoint. Two scans were collected from the same direction of travel, to observe the repeatability of duplicate scans, with the third scan

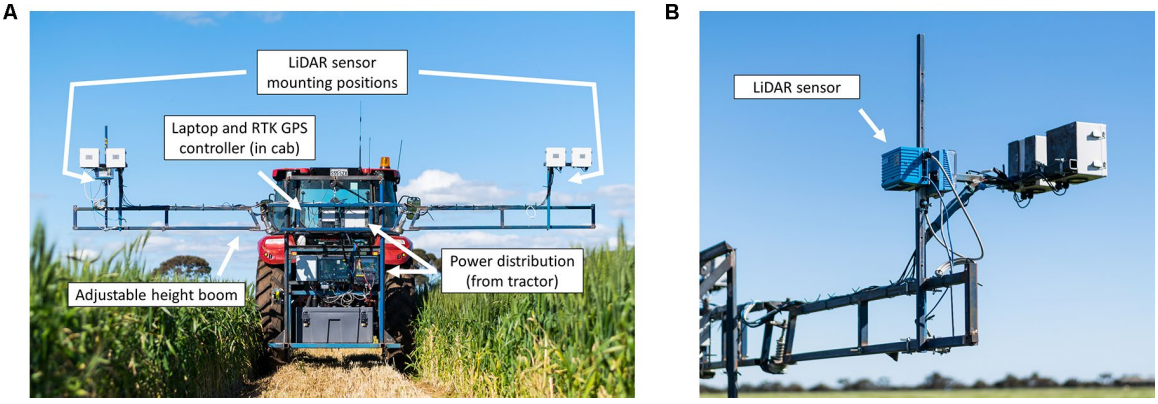

FIGURE 1 | The tractor mounted LiDAR system used in the current study showing the boom system and LiDAR sensor mounting positions, with major components annotated **(A)** and a closer view of one of the mounted LiDAR sensors **(B)**.

collected from the opposite direction of travel, to observe any effects of travel direction on scan data.

Scans were captured at a speed of 2 km/h with the LiDAR sensor capturing data in a 70° nadir field of view, at 300 Hz, with an angular resolution of 0.133° and a theoretical scanning resolution of 1.5 mm between consecutive scans. Sensors were configured to output data to laptop computers in the tractor cab. Data capture was triggered by a 1.5 V pulse, output from a Trimble FM1000 RTK GPS unit (Trimble Inc., Sunnyvale, California, USA). This allowed individual plots to be identified *in-situ* using shapefiles created using GIS software MiniGIS (geo-konzept GmbH, Adelschlag, Germany) loaded onto the Trimble FM1000. LiDAR sensors were mounted at a height of 230 cm above the ground throughout all scans, allowing for an approximate field of view of 2 m at 80 cm above-ground level (estimated average wheat canopy height). All data collection occurred on the same day, within each sample time, with manual measurements taken immediately after plots were scanned by the LiDAR system.

LiDAR Processing

Raw scan data was processed in the R software package (R-Core Team, 2017). Scan data was cleaned to remove false returns through a process of removing negative height values and filtering each scan line through a 98th percentile check to remove excessively high points. To better extract data from each plot, scanlines of two plot rows within each plot were processed, with ends of each scan trimmed to give a total plot length of 1 m (i.e. 0.5 m either side of the sensor), equating to the area of plot to be manually sampled. Points with a height less than 5 cm were re-assigned a height of 0 cm to eliminate returns from raised soil along seeding furrows, rocks or other miscellaneous objects. Visualization of these point cloud processing steps are shown in **Figure 2**. Similar procedures, for the removal of ground-level points, when dealing with fixed-height LiDAR data, have been demonstrated by Friedli et al. (2016); Sun et al. (2017) and Jimenez-Berni et al. (2018).

Canopy height was extracted through percentile algorithm in R (R-Core Team, 2017). Firstly, identifying the 98th percentile of maximum returned height in each scan line (**Figure 3A**), and secondly taking the 86th percentile of these values to provide an estimate of overall canopy height, henceforth referred to as LiDAR Canopy Height (LCH) (**Figure 3B**). The 86th percentile was selected through optimization of Pearson's correlation coefficient and RMSE between LCH and CH for all sample times at Roseworthy (**Supplementary Material**).

As a surrogate to AGB, plot volume estimates were produced by calculating the distance between each point in a scan line, the distance between scan lines and the height of each point. Using these three variables, a rectangular prism was created for each point in the point cloud, and volume of this prism calculated. A two-dimensional representation of these prisms for a single scan line is presented in **Figure 3C** with the *z* axis distance for these prisms provided by the movement of the LiDAR sensor. The summation of all prism volumes from within the point cloud was used as an estimate of plot volume. This measure will henceforth be referred to as LiDAR Projected Volume (LPV), as it encompasses all space below the LiDAR returns, rather than purely the area occupied by plant material. In the current study this volume is calculated as m^3/m^2, as this can be directly compared to plant material per square meter of plot, as measured in kg/m^2 for AGB. A single automated script was written in R to clean raw data and simultaneously calculate LCH and LPV, with processing taking approximately 13 s per plot.

In addition to the LPV calculations, point clouds for the Roseworthy data set were processed using the formulas described

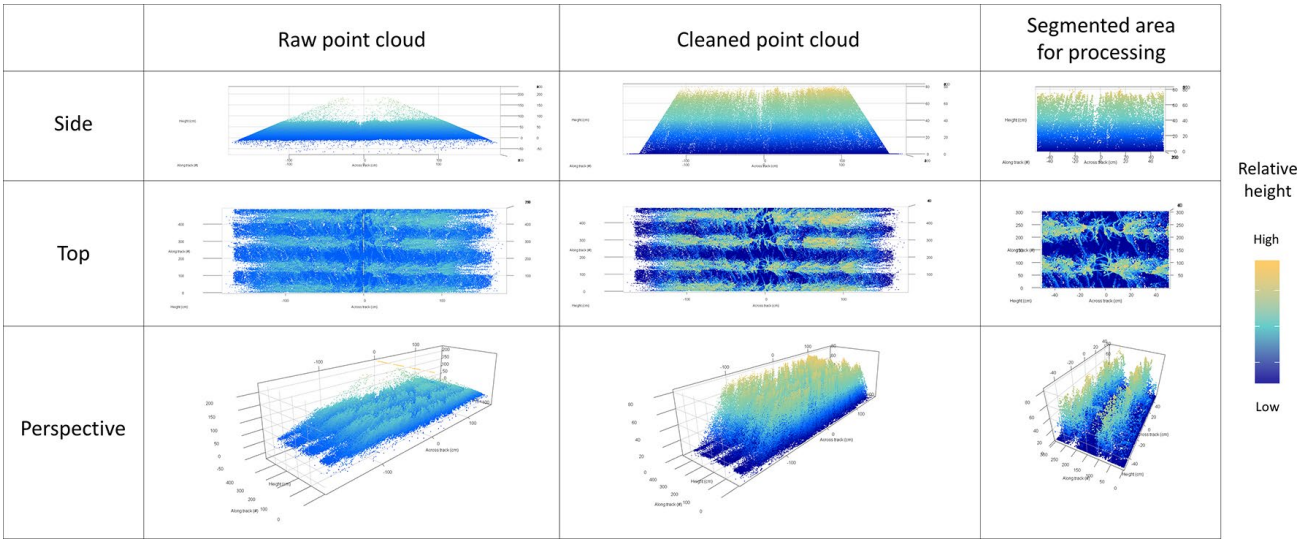

FIGURE 2 | Visualisation of a point cloud collected in the current study (at Zadoks growth scale 65), showing the three steps of data processing; raw point cloud, cleaned point cloud, and segmented area used for processing of measurements, from a side, top and perspective view.

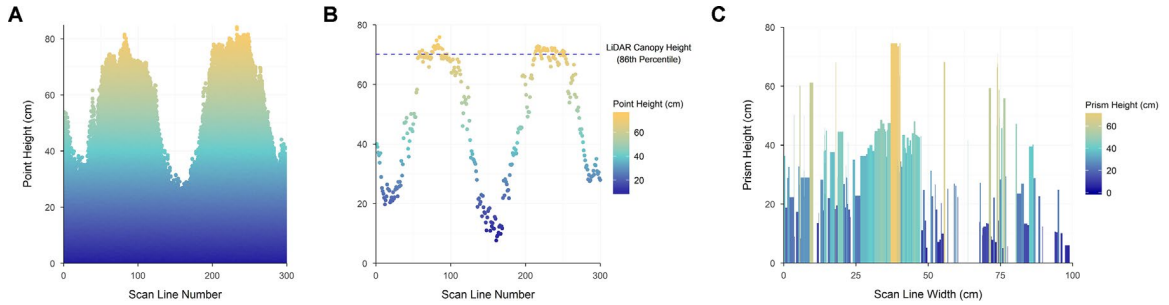

FIGURE 3 | The height of all laser returns present in each scan line of a point cloud segmented for processing **(A)**, a visualization of the LiDAR Canopy Height calculation process **(B)** showing the 98th percentile of processed points within each scan line and the over-all LiDAR Canopy Height value, represented with a dashed blue line, as calculated by the 86th percentile of these points, and a two-dimensional representation of LiDAR Projected Volume calculated for a single scan line of the point cloud **(C)**; the width and height of each prism being represented by the *x* axis (scan line width) and the *y* axis (prism height) respectively. The depth of each prism is calculated from the distance between scan lines as the LiDAR sensor moves, producing the unplotted *z* axis (prism depth).

by Jimenez-Berni et al. (2018) to calculate their 3D profile index (3DPI) used to estimate AGB. This index is based around the fraction of points present throughout the point cloud, rather than a volume-based measurement. It requires splitting the point cloud into layers, applying a correction factor to each layer and finally taking a summation of the corrected point fractions present in each later. This process, and the required formula, are described in detail by Jimenez-Berni et al. (2018). The processing and AGB estimation methods of Jimenez-Berni et al. (2018) were followed, using the separate equations for pre- and post-anthesis measurements presented, and finally estimating AGB through transforming LiDAR data with the linear regression equation between AGB and 3DPI at each measurement time.

Statistical Analysis

All statistical analyses were conducted in the R software package (R-Core Team, 2017). Mixed linear models were used for multivariate analyses, comparing traits and trait collection methods, using ASREML (Gilmour et al., 2015). From multivariate analyses Pearson's correlation coefficients were calculated between traits (raw correlations), along with genetic and residual correlations, accounting for the proportion of variance observed between the two traits based on genetic and residual components, respectively (Falconer, 1960). Outputs of multivariate analyses were also used for the calculation of broad-sense heritability (Equation 1), which can be described as the proportion of observed trait variation attributable to genetics (Visscher et al., 2008), for the traits CH, LCH, and LPV. Outputs from a randomized complete block analysis with ASREML were used to calculate broad-sense heritability for AGB.

$$H^2 = \frac{\sigma_G^2}{\sigma_G^2 + \sigma_E^2} \qquad \text{(Equation 1.)}$$

where H^2 is broad-sense heritability, σ_G^2 is the variance attributable to genetic effects and σ_E^2 the variance attributable to environmental effects (residual variance).

Due to the small sample size and large spatial spread of AGB measurements collected within trials at each sample time, genetic and residual correlations were not calculated between AGB and other traits.

RESULTS

LiDAR Repeatability

Repeatability of multiple measurements taken at Roseworthy was generally high for both LCH and LPV measurements at both individual sample times (**Table 3**) and when pooling sample times (**Figure 4**). Scans taken in the same direction of travel show greater repeatability than scans taken in opposite directions of travel.

Repeatability of height measurements was seen to be extremely high at three of the five sample times, ZGS 49, 65, and 96, when scanned in the same direction of travel, with high r^2 values, linear regression coefficients nearing one and intercepts nearing zero (**Table 3**). In contrast repeatability of samples taken at ZGS 31 and 59 showed much greater variation, with lower linear regression coefficients and intercepts further away from zero (**Table 3**, **Figure 4A**). Repeatability of measurements in opposite directions of travel was less accurate than the same direction of travel (**Figure 4C**). Generally, measurements of LCH from opposite directions had linear regression coefficients nearing one and intercepts nearing zero, though lower r^2 values than scans from the same direction (**Table 3**), with differences between timepoints being less pronounced. A similar trend for repeatability of LPV measurements was also observed, though overall LPV showed greater reproducibility than LCH. High repeatability was observed between LPV measurements in the same direction of travel (**Figure 4B**) and good repeatability in opposite directions of travel (**Figure 4D**).

Canopy Height

A wide range in canopy height was observed between site locations and sample timepoints, with this being especially apparent between environments. Strong raw correlations were observed between LCH and manually measured height for all sites (r = 0.56–0.94), and at the majority of sample times (**Table 4**). However, individual sample times at some sites showed poorer correlation compared to the rest of the data set.

TABLE 3 | Coefficient of determination (r^2) and components (slope ± standard error, and intercept ± standard error) for linear regression models between repeated scans in the same and opposite directions, processed for the traits LiDAR Canopy Height (LCH) and LiDAR Projected Volume (LPV), at each sample time (ZGS) at Roseworthy.

Trait	Scan 1 vs Scan 2 (Same direction)				Scan 1 vs Scan 3 (Opposite Direction)			
	ZGS	r^2	Slope ± s.e.	Intercept ± s.e.	ZGS	r^2	Slope ± s.e.	Intercept ± s.e.
LCH	31	0.08	0.31 ± 0.08	31.98 ± 3.67	31	0.31	0.71 ± 0.08	17.73 ± 3.21
	49	0.99	0.97 ± 0.01	1.32 ± 0.46	49	0.88	0.97 ± 0.03	1.76 ± 1.50
	59	0.61	0.72 ± 0.04	20.02 ± 3.28	59	0.76	0.93 ± 0.04	5.58 ± 2.84
	65	0.95	0.94 ± 0.02	5.15 ± 1.28	65	0.86	0.95 ± 0.03	2.45 ± 2.26
	96	0.95	0.98 ± 0.02	1.38 ± 1.36	96	0.68	0.87 ± 0.04	11.14 ± 3.47
LPV	31	0.82	0.92 ± 0.03	0.01 ± 0.00	31	0.75	0.93 ± 0.01	0.01 ± 0.01
	49	0.99	0.99 ± 0.01	0.00 ± 0.00	49	0.79	0.82 ± 0.04	0.04 ± 0.01
	59	0.99	0.99 ± 0.01	0.00 ± 0.00	59	0.91	0.88 ± 0.04	0.04 ± 0.01
	65	0.96	0.94 ± 0.01	0.02 ± 0.00	65	0.89	0.82 ± 0.05	0.05 ± 0.01
	96	0.95	0.95 ± 0.02	0.01 ± 0.00	96	0.84	0.81 ± 0.05	0.05 ± 0.00

All models are significant at the level of $p < 0.001$.

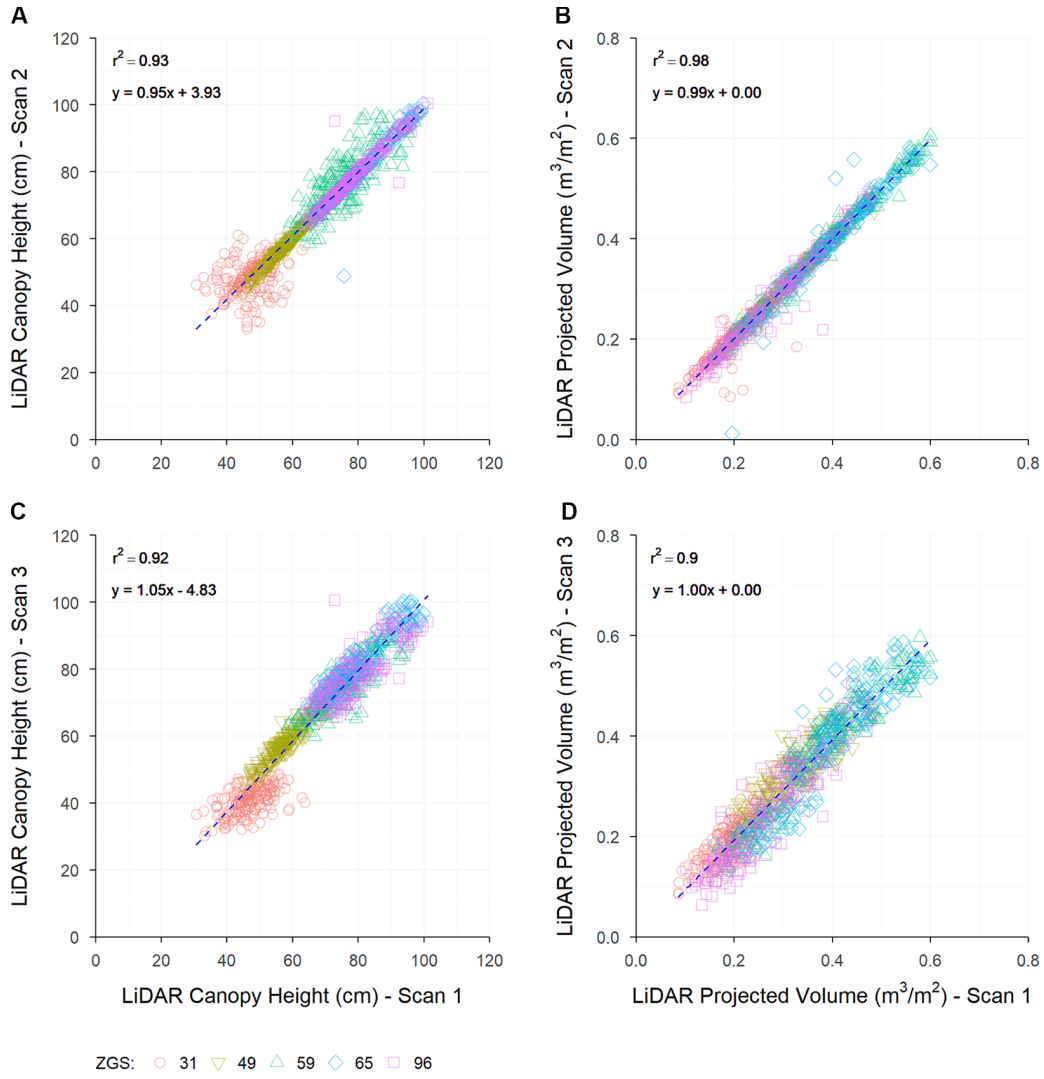

FIGURE 4 | The repeatability of LiDAR-based measurements collected at Roseworthy throughout the season, comparing scans collected from the same direction **(A**, **B)** and the opposite direction **(C**, **D)** for the measurement of LiDAR canopy height **(A**, **C)** and LiDAR projected volume **(B**, **D)**. Dashed lines indicate the line of best fit, coloured shapes indicate measurements collected at Zadoks growth scales (ZGS) as follows, red circles at ZGS 31, yellow triangles at ZGS 49, green triangles at ZGS 59, blue diamonds at ZGS 65 and pink squares at ZGS 90.

TABLE 4 | Correlations between traits, plus or minus standard error, at each site and sample time (ZGS), measured in the current study.

Site	ZGS	Correlation											
		Raw			Raw		Genetic		Residual		Raw	Genetic	Residual
		AGB	AGB	AGB	LPV	LPV	LPV	LPV	LPV	LPV	CH	CH	CH
		LPV	*CH*	*LCH*	*CH*	*LCH*	*CH*	*LCH*	*CH*	*LCH*	*LCH*	*LCH*	*LCH*
AV	49	0.86 ± 0.11 ***	0.64 ± 0.16 ***	0.68 ± 0.16 ***	0.52 ± 0.06 ***	0.87 ± 0.04 ***	0.68 ± 0.24 ***	0.92 ± 0.08 ***	0.48 ± 0.06 ***	0.87 ± 0.02 ***	0.58 ± 0.06 ***	0.88 ± 0.10 ***	0.48 ± 0.06 ***
	65	0.64 ± 0.16 ***	0.16 ± 0.21	0.28 ± 0.20	0.67 ± 0.06 ***	0.76 ± 0.05 ***	0.89 ± 0.09 ***	0.92 ± 0.06 ***	0.44 ± 0.07 ***	0.73 ± 0.04 ***	0.90 ± 0.03 ***	0.98 ± 0.01 ***	0.67 ± 0.04 ***
BL	65	0.69 ± 0.16 ***	-0.15 ± 0.21	0.21 ± 0.21	0.30 ± 0.07 ***	0.62 ± 0.06 ***	0.84 ± 0.13 ***	0.81 ± 0.14 ***	0.17 ± 0.07 ***	0.63 ± 0.05 ***	0.76 ± 0.05 ***	1.00 ± 0.01 ***	0.42 ± 0.06 ***
KV	65	0.45 ± 0.19 *	0.25 ± 0.20	0.22 ± 0.21	0.67 ± 0.05 ***	0.80 ± 0.04 ***	0.88 ± 0.09 ***	0.89 ± 0.08 ***	0.33 ± 0.07 ***	0.67 ± 0.04 ***	0.91 ± 0.03 ***	1.00 ± < 0.01 ***	0.51 ± 0.06 ***
MN	65	0.70 ± 0.15 ***	0.71 ± 0.15 ***	0.69 ± 0.15 ***	0.29 ± 0.07 ***	0.80 ± 0.04 ***	0.64 ± 0.25 ***	0.88 ± 0.10 ***	0.04 ± 0.08	0.74 ± 0.03 ***	0.56 ± 0.06 ***	0.91 ± 0.08 ***	0.08 ± 0.08
PN	65	0.66 ± 0.16 ***	0.39 ± 0.20	0.42 ± 0.20 *	0.77 ± 0.05 ***	0.86 ± 0.04 ***	0.90 ± 0.07 ***	0.92 ± 0.06 ***	0.55 ± 0.05 ***	0.88 ± 0.02 ***	0.94 ± 0.03 ***	1.00 ± < 0.01 ***	0.58 ± 0.05 ***
RD	65	0.66 ± 0.16 ***	0.58 ± 0.17 **	0.72 ± 0.15 ***	0.58 ± 0.06 ***	0.82 ± 0.04 ***	0.74 ± 0.18 ***	0.80 ± 0.14 ***	0.26 ± 0.07 ***	0.72 ± 0.04 ***	0.77 ± 0.05 ***	0.99 ± 0.01 ***	0.45 ± 0.06 ***
RS	31	0.86 ± 0.11 ***	0.58 ± 0.17 **	0.71 ± 0.15 ***	0.70 ± 0.05 ***	0.83 ± 0.04 ***	0.45 ± 0.34 ***	0.62 ± 0.26 ***	0.53 ± 0.06 ***	0.86 ± 0.02 ***	0.83 ± 0.04 ***	0.97 ± 0.04 ***	0.62 ± 0.05 ***
	49	0.73 ± 0.15 ***	0.70 ± 0.15 ***	0.70 ± 0.15 ***	0.76 ± 0.05 ***	0.90 ± 0.03 ***	0.93 ± 0.06 ***	0.97 ± 0.03 ***	0.50 ± 0.06 ***	0.87 ± 0.02 ***	0.90 ± 0.03 ***	1.00 ± < 0.01 ***	0.64 ± 0.05 ***
	59	–0.05 ± 0.21	0.21 ± 0.21	0.04 ± 0.21	0.60 ± 0.07 ***	0.72 ± 0.06 ***	0.64 ± 0.23 ***	0.83 ± 0.12 ***	0.20 ± 0.08 ***	0.64 ± 0.05 ***	0.77 ± 0.05 ***	0.95 ± 0.04 ***	0.28 ± 0.07 ***
	65	0.62 ± 0.17 **	0.35 ± 0.2	0.51 ± 0.18 *	0.65 ± 0.07 ***	0.73 ± 0.06 ***	0.82 ± 0.13 ***	0.77 ± 0.16 ***	0.25 ± 0.09 ***	0.71 ± 0.05 ***	0.94 ± 0.02 ***	1.00 ± < 0.01 ***	0.29 ± 0.07 ***
	96	0.47 ± 0.19 *	–0.01 ± 0.21	0.06 ± 0.21	0.22 ± 0.10 *	0.31 ± 0.10 **	0.18 ± 0.37 *	0.19 ± 0.37 **	0.25 ± 0.11 ***	0.28 ± 0.11 ***	0.90 ± 0.03 ***	1.00 ± < 0.01 ***	0.27 ± 0.07 ***
	31	0.75 ± 0.14 ***	0.44 ± 0.19 *	0.27 ± 0.21	0.63 ± 0.06 ***	0.56 ± 0.06 ***	0.82 ± 0.13 ***	0.84 ± 0.11 ***	0.31 ± 0.07 ***	0.70 ± 0.04 ***	0.58 ± 0.06 ***	0.96 ± 0.03 ***	0.24 ± 0.07 ***
WT	49	0.55 ± 0.18 **	0.70 ± 0.15 ***	0.66 ± 0.16 ***	0.74 ± 0.05 ***	0.86 ± 0.04 ***	0.84 ± 0.11 ***	0.91 ± 0.07 ***	0.29 ± 0.08 ***	0.81 ± 0.03 ***	0.91 ± 0.03 ***	0.99 ± 0.01 ***	0.41 ± 0.07 ***
	65	0.47 ± 0.19 *	0.22 ± 0.21	0.37 ± 0.20	0.65 ± 0.06 ***	0.74 ± 0.06 ***	0.82 ± 0.13 ***	0.81 ± 0.13 ***	0.44 ± 0.07 ***	0.71± 0.04 ***	0.93 ± 0.03 ***	1.00 ± < 0.01 ***	0.56 ± 0.05 ***

*Raw correlations shown for Above-ground Biomass (AGB), LiDAR Projected Volume (LPV), Canopy Height (CH) and LiDAR Canopy Height (LCH); raw, genetic and residual correlations between LiDAR Projected Volume, Canopy Height and LiDAR Canopy Height; and raw genetic and residual correlations between Canopy Height and LiDAR Canopy Height. Significance of each correlation is indicated as *p < 0.05, **p <0.01 and ***p < 0.001.*

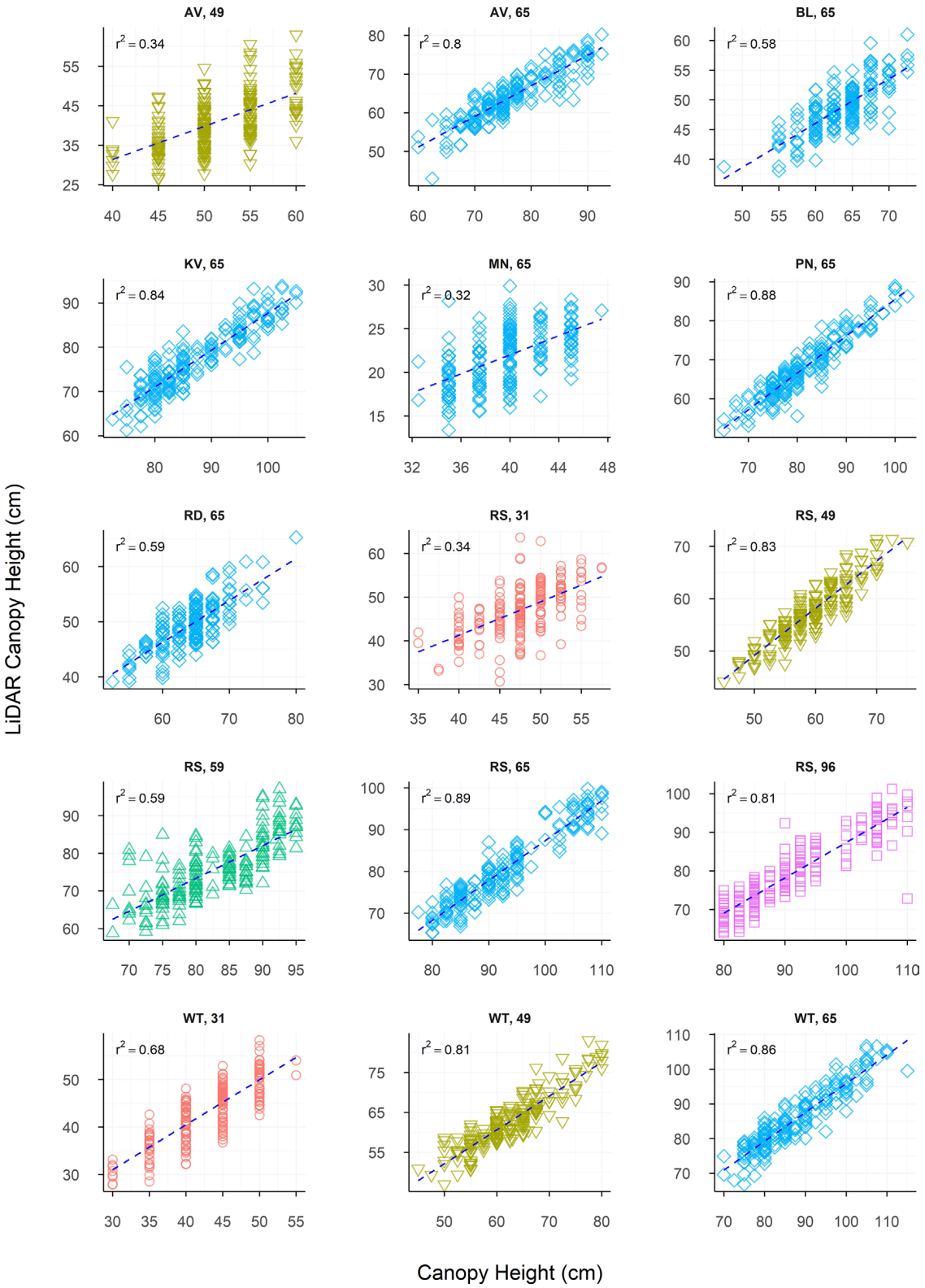

FIGURE 5 | The relationship between LiDAR Canopy Height and Canopy Height, presented individually for each site and sample time (ZGS). Dashed lines indicate the line of best fit, coloured shapes indicate measurements collected at Zadoks growth scales (ZGS) as follows, red circles at ZGS 31, yellow triangles at ZGS 49, green triangles at ZGS 59, blue diamonds at ZGS 65 and pink squares at ZGS 90.

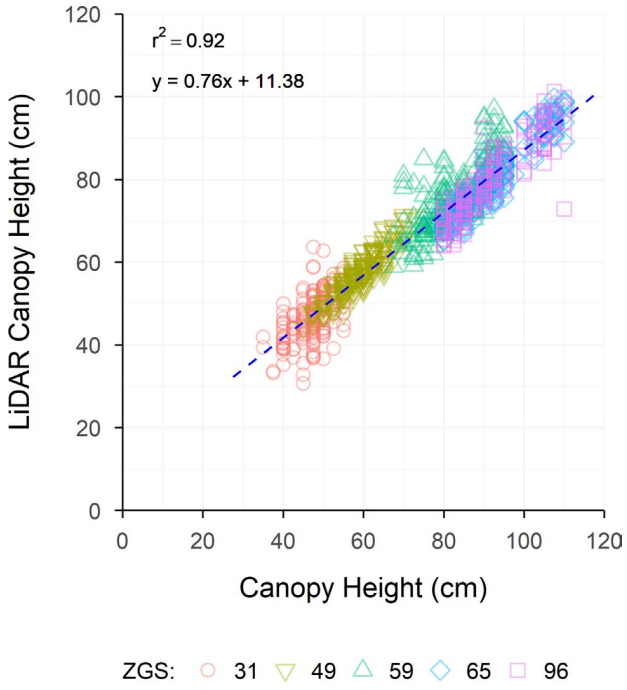

FIGURE 6 | The relationship between LiDAR Canopy Height and Canopy Height for all sample times measured at Roseworthy. Dashed lines indicate the line of best fit, coloured shapes indicate measurements collected at Zadoks growth scales (ZGS) as follows, red circles at ZGS 31, yellow triangles at ZGS 49, green triangles at ZGS 59, blue diamonds at ZGS 65 and pink squares at ZGS 90.

Strong linear relationships were observed between CH and LCH at the majority of sites (**Figure 5**), though weaker relationships were observed for some early growth stages (Roseworthy at ZGS 31 and Angas Valley at ZGS 49), or when CH was low (Minnipa ZGS 65). Pooling measurements throughout the season showed strong continuity of data and strong linear relationships between CH and LCH, such as presented in **Figure 6** for Roseworthy.

Raw ($r = 0.56$ to 0.94) and genetic ($r_g = 0.91$ to 1.00) correlations between CH and LCH were strong across all sample times, while residual correlations ranged from 0.08 to 0.67 (**Table 4**). For repeated measures there were no apparent trends for raw, genetic or residual correlations over time. Both CH and LCH had high heritability at all times of measurement, excluding Winulta at ZGS 31. Heritability tended to increase over time at sites where repeated measurements were taken (**Table 5**).

Above-Ground Biomass

Above-ground biomass samples collected showed large amounts of variation between sites, with LPV showing similar amounts of variation. Raw correlations between AGB and LPV were predominantly strong and positive, though some weaker correlations were observed, with one weak negative correlation (**Table 4**). **Figure 7** shows the linear nature of the relationship between AGB and LPV within each sample. The relationships between measurements of AGB and LPV collected over the growing season at Angas Valley, Roseworthy and Winulta are displayed in **Figure 8**. Both Angas Valley and Winulta showed an increase of AGB and LPV over time. This was also observed at Roseworthy for most sample times. However, samples collected at ZGS 65 and 96 showed increased AGB (compared to previous samples) but did not show any increase in LPV, with slight decreases in LPV being observed.

Above-ground biomass correlated most strongly to LPV for much of the raw data, though a number sites showed stronger, or similar, correlations to CH and LCH (**Table 4**). LiDAR projected volume correlated strongly to LCH for most measurements. Similar but generally weaker correlations were observed between LPV and CH.

The heritability of AGB measurements was generally lower than that of LPV measurements, although this was reversed in some instances. Heritability of AGB appears to show no trend across repeated measures, though heritability of LPV appears to generally increase over time, with the exception of Roseworthy at ZGS 96.

To assess the effectiveness of the LPV measurements calculated in the current study as an AGB estimator, LPV was compared to 3DPI, as described by Jimenez-Berni et al. (2018), for the Roseworthy data set. Except for ZGS 31, LPV was strongly correlated with 3DPI and, in general, showed slightly greater correlations to AGB (**Table 6**). A strong relationship between AGB and 3DPI-predicted AGB was observed throughout the season (**Figure 9**), excluding the ZGS 49 measurement which did not fit this trend. A similar relationship was observed by Jimenez-Berni et al. (2018).

TABLE 5 | Broad-sense heritability of each trait, at each site and sample time (ZGS), measured in the current study.

Trait	Site and sample time														
	AV		BL	KV	MN	PN	RD	RS					WT		
	49	*65*	*65*	*65*	*65*	*65*	*65*	*31*	*49*	*59*	*65*	*96*	*31*	*49*	*65*
Above-ground biomass	0.47	0.22	0.46	0.32	0.67	0.26	0.48	0.52	0.12	0.42	0.78	0.59	0.63	0.33	0.45
LiDAR projected volume	0.32	0.79	0.48	0.76	0.61	0.78	0.75	0.58	0.80	0.89	0.90	0.83	0.33	0.57	0.76
Canopy height	0.76	0.90	0.76	0.97	0.82	0.94	0.76	0.89	0.91	0.97	0.98	0.98	0.49	0.86	0.95
LiDAR canopy height	0.67	0.86	0.78	0.93	0.84	0.95	0.82	0.87	0.95	0.97	0.98	0.96	0.41	0.84	0.94

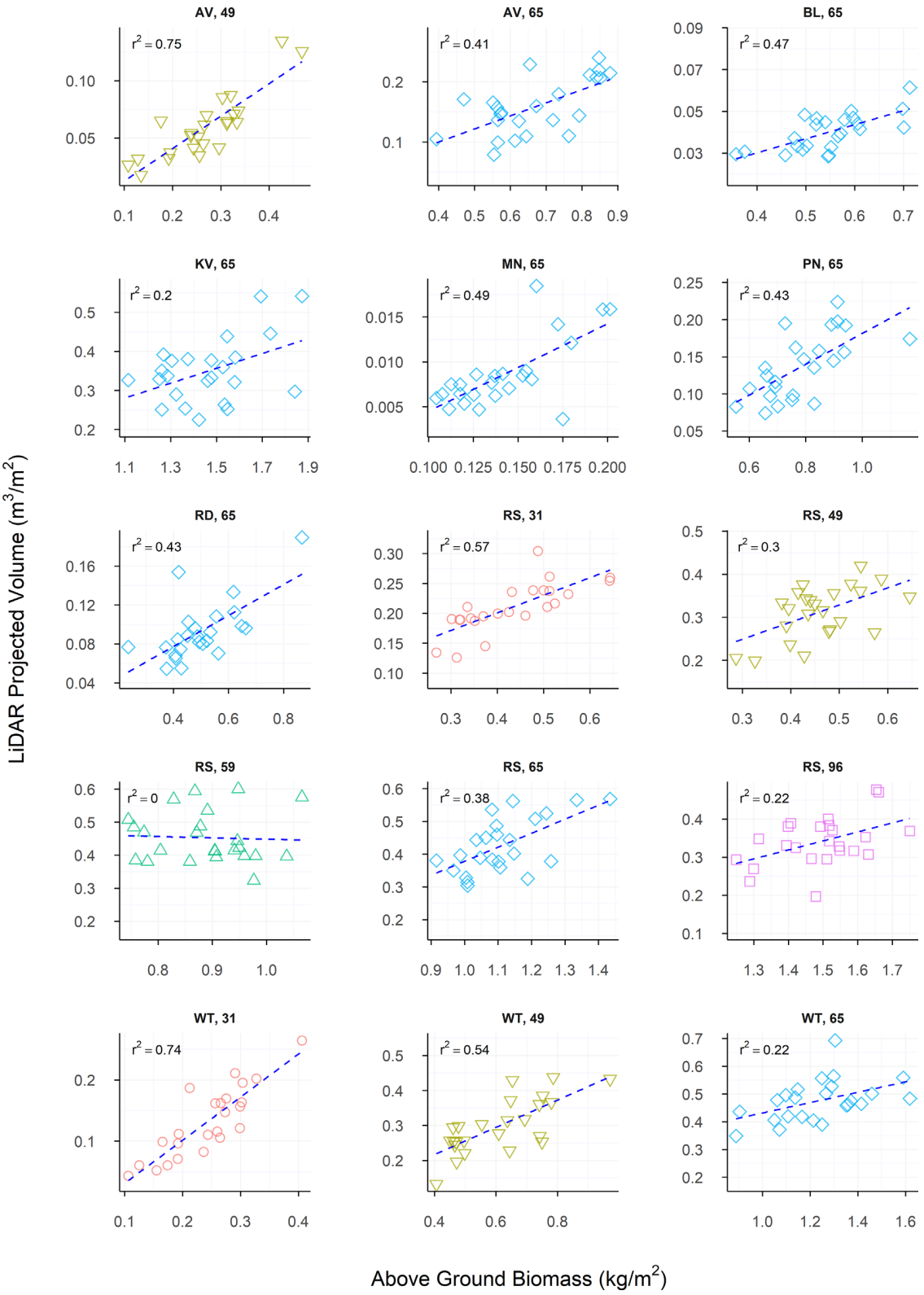

FIGURE 7 | The relationship between LiDAR Projected Volume and Above-ground Biomass, presented individually for each site and sample time measured in the current study. Dashed lines indicate the line of best fit, coloured shapes indicate measurements collected at Zadoks growth scales (ZGS) as follows, red circles at ZGS 31, yellow triangles at ZGS 49, green triangles at ZGS 59, blue diamonds at ZGS 65 and pink squares at ZGS 90.

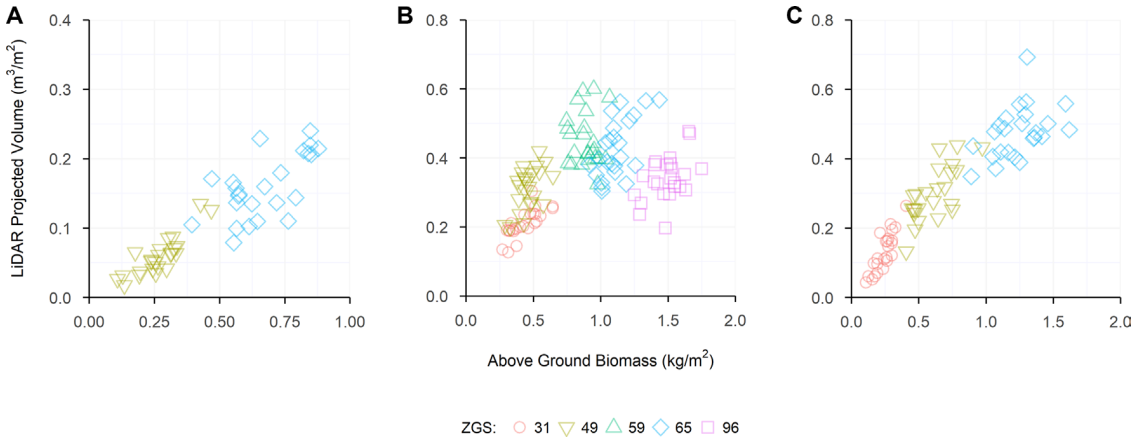

FIGURE 8 | The relationship between LiDAR Projected Volume and Above-ground Biomass for each sample time collected at Angas Valley **(A)**, Roseworthy **(B)** and Winulta **(C)**. Coloured shapes indicate measurements collected at Zadoks growth scales (ZGS) as follows, red circles at ZGS 31, yellow triangles at ZGS 49, green triangles at ZGS 59, blue diamonds at ZGS 65 and pink squares at ZGS 90.

TABLE 6 | Pearson's correlation coefficients (r), between LiDAR Projected Volume (LPV), 3DPI and Above-ground Biomass (AGB), for each sample time (ZGS) at Roseworthy.

ZGS	LPV: AGB		3DPI: AGB		LPV: 3DPI	
31	0.75 ± 0.14	***	0.17 ± 0.21		0.05 ± 0.07	
49	0.55 ± 0.18	**	0.42 ± 0.19	*	0.82 ± 0.04	***
59	–0.05 ± 0.21		–0.07 ± 0.75		0.88 ± 0.03	***
65	0.62 ± 0.17	**	0.44 ± 0.19	*	0.90 ± 0.03	***
96	0.47 ± 0.19	*	0.48 ± 0.19	*	0.95 ± 0.02	***

*Values are shown as ± standard error. Significance of each correlation is indicated as *p < 0.05, **p <0.01 and ***p < 0.001.*

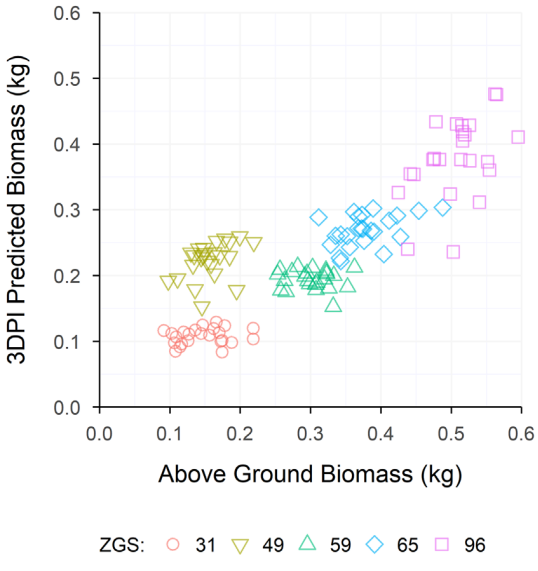

FIGURE 9 | The relationship between 3DPI Biomass and manually measured Above-ground Biomass, for each sample time at Roseworthy. Coloured shapes indicate measurements collected at Zadoks growth scales (ZGS) as follows, red circles at ZGS 31, yellow triangles at ZGS 49, green triangles at ZGS 59, blue diamonds at ZGS 65 and pink squares at ZGS 90.

DISCUSSION

The adoption of LiDAR and terrestrial laser scanners (TLS) as field-based sensors for the non-destructive phenotyping of AGB and canopy height has been discussed and demonstrated numerous times in the literature (Deery et al., 2014; Tilly et al., 2014; Eitel et al., 2016; Friedli et al., 2016; Kronenberg et al., 2017; Sun et al., 2017; Virlet et al., 2017; Jimenez-Berni et al., 2018; Sun et al., 2018), ultimately contributing towards a solution to the phenotyping bottleneck present in large-scale research and plant breeding programs (Cobb et al., 2013; Araus and Cairns, 2014). Despite the different approaches to the deployment of these sensors, there are still many questions left unanswered, particularly with regard to the robustness and reliability of the data collected and its application and value within research or field crop breeding programs.

In the current study, adaption of the imaging boom described in Walter et al. (2019) to accommodate a dual LiDAR system allowed for LiDAR sensors to be efficiently deployed across eight large-scale wheat breeding trial sites in a range of environments, and for large amounts of point cloud data to be collected at multiple growth stages.

Data Repeatability

Objective and repeatable data collection is of key importance within breeding and research programs but can be difficult to obtain through traditional in-field measurements. Thus, the

overall high repeatability and objective nature of point cloud data collected with LiDAR sensors in the current study shows great potential for integration within field-based research programs.

Repeated LiDAR scans from the same direction of travel were capable of producing near identical LCH measurements for three of the five physiological growth stages measured (ZGS 49, 65, and 96). The remaining two growth stages (ZGS 31 and 59) still showed sound repeatability of LCH measurements, though not to the extent seen at other growth stages. Interestingly, the repeatability of LPV across all physiological growth stages showed a strong relationship, with few outlying points, similar to that observed for LCH at ZGS 49, 65, and 96. There is no apparent cause of the variation observed between LCH measurements at ZGS 31 and 59 and we can only speculate that this is an artefact of the LCH calculation process, as the variation between LPV measurements for these samples is much lower than for LCH and is similar to that observed for other LPV measurements.

Measurements of both LCH and LPV were less repeatable when measured with opposite directions of travel, however repeatability was still strong. The discrepancies observed between measurements collected in opposite directions likely arise for two reasons; firstly, despite endeavors to mount LiDAR sensors identically on each side of the boom, there are likely to be small differences between the two, altering the laser emission and return pattern of each unit. Secondly, triggering of the LiDAR sensors relative to shapefiles on the RTK GPS unit requires calibration, which if not precise may result in small variations to the area of plot measured. Towards addressing these issues, LiDAR sensor and direction of travel could be fitted as random terms within spatial analyses, which may help to account for variation between measurements.

To the authors' best knowledge, repeatability of data derived from LiDAR plot scans has yet to be described in the literature, however Busemeyer et al. (2013) have reported very high repeatability of canopy height measurements collected with a light-curtain (r^2 = 0.99, Mean Relative Error = 0.01). Given the similarities between the type of data obtained from these two sensors, the high repeatability of LiDAR data observed in the current study is a positive, but not unexpected, result.

Canopy Height

Point cloud data collected through the LiDAR system was able to accurately and repeatedly estimate canopy height of wheat grown in field plots across multiple growth stages and environments. Strong raw correlations were observed at the majority of locations and growth stages measured, ranging from r = 0.56 at the weakest, to r = 0.94 at the strongest. Similar results have been previously reported for wheat and other field crops, with r^2-values of 0.99 (Jimenez-Berni et al., 2018), 0.99 (Kronenberg et al., 2017), 0.99 (Virlet et al., 2017), 0.97 (Sun et al., 2018), 0.91 (Tilly et al., 2014), 0.87 (Eitel et al., 2016), 0.84 (Walter et al., 2018) and 0.73 to 0.93 (Friedli et al., 2016). The current study and those of Jimenez-Berni et al. (2018) and Sun et al. (2018) collected data with mobile LiDAR systems deployed in field; Virlet et al. (2017) used a dual 3D laser scanner system mounted on the Field Scanalyzer gantry; Kronenberg et al. (2017) used a cable suspended laser scanner mounted on the ETH field phenotyping platform; Tilly et al. (2014); Eitel et al. (2016) and Friedli et al. (2016) used TLS systems; and Walter et al. (2018) used digital cameras and photogrammetry. Though each of these systems differ, comparable results have been achieved from each, reinforcing the concept that 3D data collected in the form of point clouds is highly suitable for the derivation of canopy height.

While the correlations presented in the current study do not appear to be as strong as some previously reported in the literature, it is important to consider the way in which the data has been collated for presentation. Data from the current study has been collected from eight wheat varieties across eight locations and in some circumstances at multiple time points. This contrasts with the data presented by Jimenez-Berni et al. (2018), where three replicates of 18 genotypes were measured at a single location and time point, with the mean values of each genotype being presented and used for correlation. The results presented by Jimenez-Berni et al. (2018) are more similar to those from **Table 4**, of genetic correlations between CH and LCH at each site, which showed improved correlations compared to raw data.

The weakest correlation between CH and LCH in the current study occurred at Minnipa, where severe drought conditions occurred during most of the 2017 growing season. Very little variation was observed between canopy heights, with varieties ranging from 32.5 to 47.5 cm, much less than the variation observed at other sites. A similar explanation is likely for the weaker correlations present at Roseworthy at ZGS 31 and Angas Valley at ZGS 49, where plants measured early in the growing season had short canopies and little variation in CH. These correlations, as well as all correlations in the current study, could likely be improved through optimisation of the percentile algorithm used to process the data. A similar process has been described by Friedli et al. (2016), with data in **Supplementary Material** reinforcing this work, and showing the variability in selecting an algorithm based on maximizing the correlation and reducing the RMSE. The authors believe the use of a single algorithm is suitable in large-scale breeding or research programs as it is generally not feasible to collect ground truth data for each site and timepoint to optimize this process. Moreover, the implications of taking physical measurements are counterintuitive to the aims of deploying these sensor systems for rapid collection of large amounts of data.

The similarity in the heritabilities calculated for CH and LCH gives great confidence in LiDAR-derived canopy height, showing that in terms of accuracy/repeatability within a breeding program it is as good as, or in some cases superior to, manual measurements. In addition to the high heritability of LCH demonstrated in the current study, a similarly high heritability of LiDAR-derived CH has previously been reported by Kronenberg et al. (2017) for a diverse set of European bread wheat cultivars (H^2 = 0.96), though this was not compared to the heritability of manual measurements. While in the current study, and in that of Kronenberg et al. (2017), heritabilities were calculated for material containing greater variation in CH than often present within breeding populations, it is expected these results are still directly applicable as CH is known to be a highly heritable trait. The strong genetic correlations observed between CH and LCH in the current study further support that LCH will be suitable for estimating CH within breeding populations, as similar genetic components are measured by both methods. The moderately

strong residual correlations between CH and LCH would seem to indicate the ability of LCH to capture differences in CH resulting from environmental variance across the experimental area. This makes sense from a physiological perspective, as plant height can be influenced by a number of biotic and abiotic factors, which may result in uneven growth throughout the trial. While the variation observed in CH within the current study was typically greater than would be observed within modern breeding populations, the results of current study suggest that LiDAR sensors would be suitable for measuring relative CH, or for measuring absolute CH if required. The slopes of lines of best fit for **Figures 5** and **6** show that as CH increased LCH underestimated CH, generally by around 10 cm. This is likely due to the data cleaning process and LCH algorithm function, and though it is not an issue if relative CH is desired, if an absolute measurement of CH is required this discrepancy will need to be accounted for.

Above-Ground Biomass

The LPV measurement in the current study has been shown capable of estimating a wide range of AGB, across different varieties, phenological stages and environments. To date, very few studies have investigated the use of point cloud data for the type of bio-volume measurements presented here. The few that have presented data for different plant species, such as cotton (Sun et al., 2018), arctic shrubs (Greaves et al., 2015) and trees (Rosell Polo et al., 2009), or for wheat which was grown in a single environment (Jimenez-Berni et al., 2018; Walter et al., 2018), except for one study by Eitel et al. (2014), where two adjacent fields of wheat plots with differing micro-climates were investigated. The collection of the point cloud data across eight different environments in the current study is an important addition to the current understanding of AGB estimation from point cloud bio-volume measurements.

The multi-location measurements presented in the current study provide a unique set of results, where large ranges in AGB were observed across a single phenological growth stage. At each location there was a moderately strong correlation between AGB and LPV, with each of these relationships (excluding Roseworthy at ZGS 59) being suitably explained by a linear regression model (**Figure 7**).

Combining repeated measurements from within sites at Angas Valley, Roseworthy and Winulta showed heteroscedastic relationships, which appear to be curvilinear. This is most apparent at Roseworthy, where AGB increases with time, however LPV plateaus and declines following ear emergence (ZGS 59). This trend also appears to be occurring at Angas Valley and Winulta, where AGB seems to be increasing more than LPV, though the final sample occurring at ZGS 65 for these sites prevents confirmation of this. This can likely be explained by the senescence of the crop. As the crop senesces, leafy volume is lost through leaves drying out and contracting, however, overall AGB continues to increase due to grain fill. Though this curvilinear relationship can be explained, it does highlight the limitation of using volume as an estimator for AGB at later growth stages. A further limitation of using LPV for AGB estimation may be present in dense canopies, where laser penetration within the canopy is poor. In such cases an over-estimation of volume will occur, as only points collected from the top of the canopy will be used to compute LPV. While this did not appear to be a limitation in the current study, with the laser sufficiently penetrating the canopy at maximum leafy biomass, it should be noted as a potential limitation of LiDAR-based volume measurements in high AGB environments. Furthermore, different relationships are observed over time at Angas Valley, Roseworthy and Winulta, suggesting that unique curvilinear relationships may be required for each environment. Considering geographical differences as a predictor of seasonal differences, it is likely these relationships will also alter from year to year as a result of the differing abiotic and biotic factors which occur between seasons and environments. This in turn may affect numerous aspects of crop morphology, which may alter the relationship between volume-based measurements and AGB. This introduces the question of how breeders will use such data. Will it be used to measure AGB over time within trials, comparing relative AGB at a single time point between trials, or for comparing relative AGB at individual time points? To better understand the interactions occurring between volume-based measurements and AGB, and how these interactions may influence a breeder's use of these measurements, a series of multi-year, multi-environment trials would be beneficial.

The moderately strong correlations observed between AGB and LPV within individual measurement points, align with the results of Walter et al. (2018) and Jimenez-Berni et al. (2018), where linear regressions provided a suitable explanation for the relationship between AGB and point cloud bio-volume estimates. The work of Jimenez-Berni et al. (2018) is the most comparable to the current study, and their results indicate a strong linear relationship between AGB of wheat and their 3D Indices of processed LiDAR data for numerous physiological growth stages. However, optimization of equations was conducted for the processing of these 3D Indices, based on developmental stage, which were further transformed using separate equations for pre and post-anthesis measurements for comparison to measured AGB. These processes of optimisation require ground-truth data, which as discussed previously, are not likely to be collected within a breeding program. It is also worth noting that in the current study, and that of Jimenez-Berni et al. (2018), as AGB increases, digital measurements obtained with LiDAR sensors correlate less strongly to manual measurements, with the pooling of measurements showing a heteroscedastic relationship. This is likely a limitation imposed by the LiDAR sensors used in these studies, which return only a single discrete point, compared with units capable of returning multiple discrete points or a full wave form. Capturing multiple discrete returns or the full wave form, may overcome this issue and allow for deeper penetration within the crop canopy. However, such systems are currently prohibitively expensive for their deployment within plant breeding programs, both from an upfront cost and from a data processing perspective.

Processing LiDAR data from Roseworthy using 3DPI as described by Jimenez-Berni et al. (2018), yielded a positive linear relationship across all sample times (**Figure 9**). The results presented here align with those of Jimenez-Berni et al. (2018), and show the robustness of their 3DPI when applied to an alternate data set, even in the absence of optimisation. The sample at ZGS 49 did fall outside of the linear relationship observed for 3DPI, however, similar results were observed for ZGS 49 in the processing methods of the current study, where samples at ZGS 49 did not increase in projected volume but did increase in AGB. Values of 3DPI at individual sample times correlated strongly with LPV, with the exception of the ZGS 31 sample, which showed a weak correlation (**Table 6**). 3DPI also

showed similar, but slightly weaker, correlations to AGB compared to LPV (**Table 6**). It is likely these correlations could be improved through the optimization of the *k* value within the 3DPI equation. However, as described for canopy height, continued optimization of such equations runs contrary to the benefits of implementing such phenotyping systems within field crop breeding programs. For this reason, we believe the performance of the LPV measurement used within the current study is applicable to field crop breeding programs, providing sound estimates of AGB and requiring no optimization for deployment within breeding programs. Similar volume based measurements to those used in the current study were successfully utilized to estimate cotton AGB by Sun et al. (2018), who observed manually-measured biomass to correlate strongly to volume measurements across a small number of plots.

Above-ground biomass of cereal crops is highly variable (Sharma, 1993); which was confirmed in the current study where H^2 ranged from 0.12 to 0.78. Despite this broad range, only at two measurement times (Roseworthy at ZGS 31 and Angas Valley at ZGS 49) did AGB have a substantially greater heritability than LPV, while for all other measurements LPV showed similar, or substantially greater heritability than AGB. This generally high heritability of LPV, combined with the moderate correlations to AGB, indicates that it could be used as an effective tool for making genetic gain if selecting for AGB.

Application of Data

Past studies investigating the use of LiDAR sensors as a phenotyping tool have shown strong correlations to manually-collected data for multiple traits and have suggested potential applications of such data. Despite these often strong relationships, practical applications have yet to be published. For this point cloud generated phenotype data to be used effectively within wheat breeding programs, data collection and processing needs to be quick and largely automated, reducing the manual labor and time required. While the travel speed of the LiDAR system was relatively slow in the current study (2 km/h) this can be easily increased with alterations to the system hardware, specifically the path from GPS signal to LiDAR sensor trigger. Despite this, throughput of the system allows two unique plots to be scanned every 3 s, allowing for 2,400 plots to be scanned per hour. To the author's knowledge the throughput of similar ground-based LiDAR systems has not previously been reported in the literature, with the exception of Sun et al. (2018) who reported an approximate throughput of 600 plots per hour for cotton field plots of similar size to the plots measured in the current study. While the current reported throughput of 2,400 plots per hour is high, there is still potential to improve upon this by increasing the travel speed of the system in conjunction with alterations to the system hardware. It is expected this could increase throughput to approximately 7,400 plots per hour, as reported for the HIB described by Walter et al. (2019). However, it should be noted that were travel speed to be increased, longitudinal resolution of collected point clouds would decrease. As such, further validation for correlations between LiDAR-based and manual measurements would be required at greater speeds of travel. Processing of the data takes approximately 13 s per plot (though this could potentially be optimized for greater speed) resulting in a total time of approximately 15 s to collect and convert raw data into LCH and LPV measurements for a single plot. This is an immense increase in throughput compared to manual methods, with CH measurements taking approximately 10 s per plot and AGB cuts several minutes per plot, not including time required for handling, drying and weighing samples post collection. Further to this, all measurements taken with the system are non-destructive, allowing for repeated measurements in season and for AGB to be estimated without impacting upon plot grain yield. This now provides the opportunity for breeders to collect large-scale data sets for AGB, which were previously impossible to collect due to the destructive nature of manual measurements.

Even though in the current study, the LiDAR system was effectively able to provide large increases in throughput and decreases in manual labor for the collection of CH and AGB measurements, it is likely that within a large-scale breeding program, collection of this data would only occur at one or two key physiological time points throughout the season. Examples of this could be; once the greater part of a site has reached first node (ZGS 31) for estimating early AGB, or at anthesis (ZGS 65) for estimating maximum AGB, though these timepoints would be driven by the specific trait of interest. For routine integration within a wheat breeding program, these measurements would ideally be combined with another field operation, such as herbicide or fungicide spraying. Combining data collection with routine field maintenance practices would allow for repeated measurements during the season, while also reducing the logistical burden of transporting equipment between field sites. Alternatively, a more focused set of measurements could be conducted at a single site, allowing many repeated measures throughout the season. However, this would fail to assess the genotype-by-environment interaction effects which need to be considered by breeders. Ultimately the field campaign undertaken will depend on the breeding objectives of the program and consequently the specific data desired by the breeder. The data presented on LiDAR data repeatability in the current study suggests that LiDAR sensors could be used to measure absolute values of CH and to a lesser extent AGB. However, it seems the most apparent fit for such data within breeding programs is for the relative measurement of these traits, which could be used to select within populations to achieve the desired breeding objective.

The LiDAR-based data generated in the current study shows great promise for application within breeding programs, particularly as the heritability of LCH and LPV assessments were generally comparable to, or greater than, manual measurements, indicating that genetic gain can be made through selection of each trait. There are many examples as to how the type of data collected within the current study could be applied within wheat breeding programs: one example is the selection of breeding lines based on early AGB accumulation at first node (ZGS 31). Some programs may wish to select for this trait, or against it, depending on the desired purpose of the material, e.g. for dual-purpose wheats (i.e. those producing large amounts of grazeable biomass prior to ZGS 31) or for weed competitiveness. A second example is for breeders wishing to select for increased AGB independently of CH. Currently to achieve this, breeders must manually collect measurements of CH and AGB. However, this process can be greatly simplified as LCH and LPV are calculated from the same data, and a combination of the two measurements could be used for the selection of increased AGB while maintaining lower CH. Broadening the scope of potential

application, there are many other field crop breeding programs which could take advantage of the type of data presented in the current study, prime examples being biomass heavy crops, such as those used for hay or silage, as well as horticultural breeding programs where leafy biomass or volume may be key traits.

CONCLUSION

Through the deployment of a mobile ground-based LiDAR system across multiple environments within a large-scale commercial wheat breeding program, it has been shown that the collection and processing of 3D point cloud data is highly repeatable, strongly correlated to manual measurements of CH and AGB, and highly heritable. This combination makes LiDAR sensors a promising and valuable tool for wheat or other field crop breeders who wish to non-destructively measure CH and or AGB within their breeding programs.

Discussion on the application of LiDAR sensors to breeding programs in the current study has been based around the direct or indirect selection of specific traits within breeding programs, however there are also the exciting possibilities of fitting LiDAR data in multivariate analyses of yield trials, or within crop physiological models, in both cases to improve upon current techniques of data analysis and variety performance prediction. The authors suggest that the possibilities listed above are the logical progression for future work investigating LiDAR sensors, either for use in breeding or research programs.

DATA AVAILABILITY

The datasets generated for this study are available on request to the corresponding author.

AUTHOR CONTRIBUTIONS

JW, JE and HK: designed and oversaw the management of experiments; JW: established data processing methods, collected and analyzed all data; JW, JE, GM and HK: interpreted analyzed data; JW: wrote the manuscript with contributions from JE, GM and HK.

FUNDING

The authors wish to acknowledge the South Australian Grains Industry Trust (UA514), the Grains Research and Development Corporation (GRS11009), The University of Adelaide School of Agriculture, Food and Wine, and the Australian Government Research Training Program Scholarship for their funding support of this research.

ACKNOWLEDGMENTS

The authors wish to thank Piet Reyns, Eva Ampe and Jan Sentjens of Limagrain Netherlands for their guidance and support in deploying and troubleshooting the LiDAR system used in the current study, as well as Jose Jimenez-Berni for his discussions around 3DPI. Thanks also go to the three reviewers of this manuscript for their considered and constructive reviews.

SUPPLEMENTARY MATERIAL

The Supplementary Material for this article can be found online at: https://www.frontiersin.org/articles/10.3389/fpls.2019.01145/full#supplementary-material

REFERENCES

Araus, J. L., and Cairns, J. E. (2014). Field high-throughput phenotyping: the new crop breeding frontier. *Trends Plant Sci.* 19 (1), 52–61. doi: 10.1016/j.tplants.2013.09.008

Busemeyer, L., Mentrup, D., Moller, K., Wunder, E., Alheit, K., Hahn, V., et al. (2013). BreedVision — A multi-sensor platform for non-destructive field-based phenotyping in plant breeding. *Sensors* 13 (3), 2830–2847. doi: 10.3390/s130302830

Cobb, J. N., DeClerck, G., Greenberg, A., Clark, R., and McCouch, S. (2013). Next-generation phenotyping: requirements and strategies for enhancing our understanding of genotype-phenotype relationships and its relevance to crop improvement. *Theor. Appl. Genet.* 126 (4), 867–887. doi: 10.1007/s00122-013-2066-0

Deery, D., Jimenez-Berni, J., Jones, H., Sirault, X., and Furbank, R. (2014). Proximal remote sensing buggies and potential applications for field-based phenotyping. *Agronomy* 4 (3), 349. doi: 10.3390/agronomy4030349

Eitel, J. U. H., Magney, T. S., Vierling, L. A., Brown, T. T., and Huggins, D. R. (2014). LiDAR based biomass and crop nitrogen estimates for rapid, non-destructive assessment of wheat nitrogen status. *Field Crops Res.* 159, 21–32. doi: 10.1016/j.fcr.2014.01.008

Eitel, J. U. H., Magney, T. S., Vierling, L. A., Greaves, H. E., and Zheng, G. (2016). An automated method to quantify crop height and calibrate satellite-derived biomass using hypertemporal lidar. *Remote Sens. Environ.* 187, 414–422. doi: 10.1016/j.rse.2016.10.044

Falconer, D. S. (1960). *Introduction to quantitative genetics*. New York: Ronald Press Co.

Fischer, R., and Wood, J. (1979). Drought resistance in spring wheat cultivars. III.* Yield associations with morpho-physiological traits. *Aust. J. Agric. Res.* 30 (6), 1001–1020. doi: 10.1071/AR9791001

Friedli, M., Kirchgessner, N., Grieder, C., Liebisch, F., Mannale, M., and Walter, A. (2016). Terrestrial 3D laser scanning to track the increase in canopy height of both monocot and dicot crop species under field conditions. *Plant Methods* 12, 15. doi: 10.1186/s13007-016-0109-7

Gilmour, A. R., Gogel, B. J., Cullis, B. R., Welham, S. J. and Thompson, R. (2015). ASReml User Guide Release 4.1 Functional Specification, VSN International Ltd, Hemel Hempstead, HP1 1ES, UK www.vsni.co.uk

Greaves, H. E., Vierling, L. A., Eitel, J. U. H., Boelman, N. T., Magney, T. S., Prager, C. M., et al. (2015). Estimating aboveground biomass and leaf area of low-stature Arctic shrubs with terrestrial LiDAR. *Remote Sens. Environ.* 164, 26–35. doi: 10.1016/j.rse.2015.02.023

Jimenez-Berni, J. A., Deery, D. M., Rozas-Larraondo, P., Condon, A. G., Rebetzke, G. J., James, R. A., et al. (2018). High throughput determination of plant height, ground cover, and above-ground biomass in wheat with LiDAR. *Front. Plant Sci.* 9 (237). doi: 10.3389/fpls.2018.00237

Kronenberg, L., Yu, K., Walter, A., and Hund, A. (2017). Monitoring the dynamics of wheat stem elongation: genotypes differ at critical stages. *Euphytica* 213 (7), 157. doi: 10.1007/s10681-017-1940-2

Long, D. S., and McCallum, J. D. (2013). Mapping straw yield using on-combine light detection and ranging (lidar). *Int. J. Remote Sens.* 34 (17), 6121–6134. doi: 10.1080/01431161.2013.793869

Pittman, J. J., Arnall, D. B., Interrante, S. M., Moffet, C. A., and Butler, T. J. (2015). Estimation of biomass and canopy height in bermudagrass, alfalfa, and wheat

using ultrasonic, laser, and spectral sensors. *Sensors* 15 (2), 2920–2943. doi: 10.3390/s150202920

R-Core Team. (2017). *R: A Language and Environment for Statistical Computing [Online]*. Vienna, Austria: R Foundation for Statistical Computing. Available: https://www.R-project.org/ [Accessed 2017].

Reynolds, M., Foulkes, J., Furbank, R., Griffiths, S., King, J., Murchie, E., et al. (2012). Achieving yield gains in wheat. *Plant Cell Environ.* 35 (10), 1799–1823. doi: 10.1111/j.1365-3040.2012.02588.x

Richards, R. A., Rebetzke, G. J., Condon, A. G., and van Herwaarden, A. F. (2002). Breeding opportunities for increasing the efficiency of water use and crop yield in temperate cereals. *Crop Sci.* 42 (1), 111–121. doi: 10.2135/cropsci2002.1110

Rosell Polo, J. R., Sanz, R., Llorens, J., Arno, J., Escola, A., Ribes-Dasi, P., et al. (2009). A tractor-mounted scanning LIDAR for the non-destructive measurement of vegetative volume and surface area of tree-row plantations: a comparison with conventional destructive measurements. *Biosyst. Eng.* 102 (2), 128–134. doi: 10.1016/j.biosystemseng.2008.10.009

Sharma, R. C. (1993). Selection for biomass yield in wheat. *Euphytica* 70 (1), 35–42. doi: 10.1007/BF00029638

Sun, S., Li, C., Paterson, A. H., Jiang, Y., Xu, R., Robertson, J. S., et al. (2018). In-field high throughput phenotyping and cotton plant growth analysis using LiDAR. *Front. Plant Sci.* 9 (16). doi: 10.3389/fpls.2018.00016

Sun, S. P., Li, C. Y., and Paterson, A. H. (2017). In-field high-throughput phenotyping of cotton plant height using LiDAR. *Remote Sens.* 9 (4), 21. doi: 10.3390/rs9040377

Tilly, N., Hoffmeister, D., Cao, Q., Huang, S., Lenz-Wiedemann, V., Miao, Y., et al. (2014). Multitemporal crop surface models: accurate plant height measurement and biomass estimation with terrestrial laser scanning in paddy rice: SPIE. 23. *J. App. Remote Sens.* 8 (1), 1–23. doi: 10.1117/1.JRS.8.083671

Virlet, N., Sabermanesh, K., Sadeghi-Tehran, P., and Hawkesford, M. J. (2017). Field Scanalyzer: an automated robotic field phenotyping platform for detailed crop monitoring. *Funct. Plant Biol.* 44 (1), 143–153. doi: 10.1071/FP16163

Visscher, P. M., Hill, W. G., and Wray, N. R. (2008). Heritability in the genomics era — concepts and misconceptions. *Nat. Rev. Genet.* 9, 255. doi: 10.1038/nrg2322

Walter, J., Edwards, J., Cai, J., McDonald, G., Miklavcic, S. J., and Kuchel, H. (2019). High-throughput field imaging and basic image analysis in a wheat breeding programme. *Front. Plant Sci.* 10 (449). doi: 10.3389/fpls.2019.00449

Walter, J., Edwards, J., McDonald, G., and Kuchel, H. (2018). Photogrammetry for the estimation of wheat biomass and harvest index. *Field Crops Res.* 216, 165–174. doi: 10.1016/j.fcr.2017.11.024

Zadoks, J. C., Chang, T. T., and Konzak, C. F. (1974). A decimal code for the growth stages of cereals. *Weed Res.* 14 (6), 415–421. doi: 10.1111/j.1365-3180.1974.tb01084.x

Zerner, M. C., Rebetzke, G. J., and Gill, G. S. (2016). Genotypic stability of weed competitive ability for bread wheat () genotypes in multiple environments. *Crop Pasture Sci.* 67 (7), 695–702. doi: 10.1071/CP15198

Conflict of Interest Statement: JW, JE, and HK are affiliated with Australian Grain Technologies Pty Ltd, a commercial plant breeding company. The remaining author declares that the research was conducted in the absence of any commercial or financial relationships that could be construed as a potential conflict of interest.

Chapter 5

General Discussion

The concept for this project arose from a knowledge gap surrounding next generation phenotyping technologies (NGP) and high-throughput field phenotyping (HTFP), and the speculation that these technologies would be one of the next frontiers to advance genetic gain in plant breeding. Here the term NGP is used rather than High-throughput Phenotyping (HTP), and subsequently HTFP, as NGP encompasses all technologies which may offer breeding programmes improvement through increased accuracy, throughput or efficient resource allocation. While HTP and HTFP technologies also aim to improve accuracy and resource allocation, intrinsically they must be higher throughput than traditional methods. However, it may be possible to deploy a new technology in a breeding programme which provides improvements to accuracy and resource allocation of traditional phenotyping methods but is no higher throughput. Though there are many studies investigating these technologies, and how they can be applied within field trials, as of the date of thesis submission there is still little literature exploring the context of how data collected with these technologies can be adopted by breeding programmes, nor the value of such data from a breeding perspective.

The objectives of the current study were to investigate the deployment of commercially available proximal remote sensing technologies, in this case digital cameras and LiDAR sensors, within the large-scale small-plot field trials run by wheat breeding programmes, and to determine the suitability of collected data for routine breeding use.

5.1 Key Findings and Contributions

From the original research articles contained within this thesis, the following key findings were identified in regard to specific sensors and their suitability for adoption within breeding programmes:

- Digital cameras are a versatile tool suitable for imaging small-plot field trials at either low or high throughput
- Digital images can be processed to measure colour-based traits of interest (such as canopy cover and senescence), with outputs being suitable for use in routine breeding analyses due to their high heritability and strong genetic correlation to manually measured traits
- Colour-based traits can be simply measured using open-source image processing software, making this a readily available and deployable tool for breeders and researchers
- Ground-based digital images can be collected and processed into a three-dimensional point cloud, using commercial photogrammetry software, for the estimation of canopy height, above-ground biomass (AGB) and harvest index when grain yield data is available
- High-fidelity point clouds show great potential as a non-destructive measurement tool within breeding programmes, though currently photogrammetric methodologies are low throughput and resource intensive
- LiDAR sensors offer a high-throughput method to collect three-dimensional point clouds, with this data being processable in open-source scripting and programming languages
- LiDAR-acquired point clouds are suitable for the estimation of canopy height and AGB of field plots; LiDAR-derived measurements have similar or higher heritability compared to manual measurements and are suitable for inclusion in routine breeding analyses

Furthermore, insights into ground-based phenotyping platforms and strategies for their deployment were identified as follows:

- Ground-based platforms provide the opportunity to collect high fidelity and high-spatial resolution data, with few limitations to the type of sensors which can be deployed through these means
- These platforms can be designed to utilise equipment and management strategies already in place within breeding programmes, such as tractors used for field maintenance and predefined GPS pathways for traversing field trials, allowing for a more streamline deployment
- It is important to consider the design and layout of breeding trial sites to ensure suitable platforms are deployed to maximise efficiency of data collection and minimise any disruption resulting from deployment to the breeding programme
- The deployment of ground-based platforms can be limited by transportation logistics and unfavourable weather conditions, such as wind, rain and waterlogged soil

The findings outlined above provide field-crop breeders confidence in the data collected by next generation phenotyping technologies, with the articles contained within describing the objective, repeatable and genetically significant nature (in terms of heritability and genetic/residual correlations) of this data. Each of these characteristics is of great importance for inclusion within breeding analyses, and until now have not been examined critically within the literature. Furthermore, it has been demonstrated how a novel high-throughput field phenotyping platform, designed from the ground-up for deployment within the small-plot field trials of breeding programmes, can take advantage of existing equipment and infrastructure within said programmes to achieve unprecedented throughput of ground-based image and point cloud collection.

Further advancements in technology and data processing methods which have occurred since the commencement of this project will be discussed, along with efforts to date of deploying NGP technologies within breeding programmes. Furthermore, potential avenues for future research are identified, and a strategic framework for choosing when to deploy new technologies within a breeding programme is presented.

5.2 Ongoing Technological Advancements

Technology is a field in which improvements occur exponentially, with this notion popularised as Moore's law (Moore, 1965). This holds true for sensors used in next generation phenotyping, which continue to get smaller and lighter, while simultaneously new sensors are developed which are of higher resolution or provide new methods of measurement compared to sensors currently in use. The image sensors utilized by digital cameras are a prime example of this, clearly showing an adherence to Moore's law. Early work investigating the use of digital images for measuring traits of interest within field plots was undertaken with sensors in the range of 0.4 (Lukina et al., 1999) to 0.7 (Adamsen et al., 1999) megapixels (MP); less than 20 years later, digital cameras with image sensors containing 18 or more MP are commonly available, such as those used in Chapters 2 and 3. Today, high-end image sensors of 150 MP are commercially available (PhaseOne), which in future will likely be readily and cheaply available in small, lightweight camera bodies. Such advancements in technology are impressive, though one must question at what point more data is being captured than can be efficiently utilized? For example, Hu et al. (2019) demonstrated the effect spatial resolution plays when calculating percentage canopy cover from digital images, where reduced spatial resolution resulted in exaggeration of canopy cover estimates compared to a reference value. While this work focused on the effect of reducing spatial resolution, an alternative thought process is that there may be a theoretical limit to actionable spatial resolution, beyond which there is no significant gain in useful information, especially when considered in the context of a breeding programme.

Continued advancement of technology has also been observed for phenotyping platforms , with perhaps the most impressive being the progress of Unmanned Aerial Vehicles (UAVs), which have transitioned from specialist equipment through to readily deployable consumer items. While UAVs now provide an attractive platform to enable NGP within breeding programmes, they are still limited to lightweight sensors and as such generally lack the spatial resolution desired for image analysis of field plots. There are, of course, exceptions to this, for example, a large hexacopter (e.g. DJI Matrice 600) fitted with a digital camera containing a 100+ megapixel sensor (e.g. PhaseOne XF series). Such a system

could achieve spatial resolutions nearing that observed from the High-throughput Imaging Boom (HIB) in Chapter 2, however the small, easy to deploy nature of consumer UAVs would subsequently be lost.

With this in mind, there will likely be a place for multiple platform types within the field of NGP research, and perhaps within breeding programmes, for the foreseeable future. Though ground-based platforms may bare a logistical burden in regard to deployment at remote sites, and hence potentially a low scalability to large-scale breeding programmes, their advantages stem from the lack of limitations regarding sensor payload and high-spatial resolution of collected data. To put this in perspective, the HIB described in Chapter 2 was designed and developed with two specific ideas in mind:

i To produce a platform which seamlessly integrated into current field maintenance practices used within field-crop breeding programmes

ii To facilitate the collection of high-spatial resolution data from desired sensors, regardless of their weight or size

By developing a platform based around these concepts, sensors can be deployed with relative ease to rigorously evaluate data captured from field plots and its potential use in breeding programmes. Sensors identified as valuable to breeding programmes can then be deployed on more scalable platforms, as technology advances and sensor size and weight are reduced.

The above section has discussed advancements to physical NGP technologies, however, advancements in analytical methods are expected to contribute as much as, or more than, advancements in sensors and platforms toward the implementation of NGP within breeding programmes. Traditional image analysis methods, such as those described in Chapter 2, which look at individual pixel values have a limited application, for which the information of interest must be contained within each pixel. These approaches are well suited to analysing images based upon pixel colour values but are ill-suited to identifying shapes and patterns within images. Computer vision and machine learning (ML) algorithms are able to overcome this limitation, identifying objects of interest within images learned from user defined training data. Over the past few years the barrier to entry for ML has been

greatly lowered, with ML modules and packages being made available to object-oriented programming languages such as Python and R. This has facilitated the investigation of ML as a set of analytical tools for NGP, where great potential has already been identified for the identification of wheat heads (Hasan et al., 2018; Sadeghi-Tehran et al., 2017, 2019) and anther extrusion (Sadeghi-Tehran et al., 2017), determining heading date and head/awn morphology (Wang et al., 2019), as well as improving upon traditional methods for estimating canopy cover of field plots (Guo et al., 2017). Further-more ML can be applied to a variety of data types and is not limited purely to images. One interesting avenue of exploration would be to develop and test a ML model in an attempt to improve upon the point cloud derived estimates of aboveground biomass of wheat, as described in Chapters 3 and 4.

Though the barrier to entry for ML has been lowered, specialist skill sets are still required to understand the theory behind the function of each algorithm, and for writing the base code required to train and run these models. While, in its current state, it is unlikely that ML is to be adopted by the average plant breeder to analyse NGP data, efforts have been made to make ML more accessible to the average breeder and researcher. For example, the decision tree segmentation model for evaluating canopy cover *EasyPCC* developed by Guo et al. (2017) was built into an easy to use graphical user interface, and the wheat spike detecting neural network *DeepCount* developed by Sadeghi-Tehran et al. (2019) was published with all required Python scripts. It is encouraging to see researchers making such tools freely available as this will help foster the uptake of NGP and the realisation of its potential application within breeding programmes.

5.3 Progress Towards the Integration of Next Generation Phenotyping Data

From the current study, it has been demonstrated that NGP technologies can be deployed in a high-throughput manner within the large-scale field trials of wheat breeding programmes, to collect phenotype data suitable for inclusion within routine breeding analyses. While the methods for collecting this data were demonstrated and suggestions on

how this data could be integrated within breeding programmes were raised, the true fit and value of this data within breeding programmes was not investigated. To date there has been little literature published regarding the integration of NGP data within breeding programmes, with efforts so far focused on the fitting of proxy traits, i.e. spectral readings which may be associated with traits, into multi-variate models for pedigree and genomic prediction (Rutkoski et al., 2016; Sun et al., 2017; Krause et al., 2019).

Rutkoski et al. (2016) showed the accuracy of grain yield prediction for breeding lines within a univariate analysis could be significantly improved upon by fitting proxy traits (canopy temperature and NDVI) into the analysis, along with pedigree (A) or marker (K) relationship matrices. Sun et al. (2017) continued this line of work, investigating different models (simple repeatability, multitrait and random regression) for the analysis of proxy trait (canopy temperature and NDVI) data collected across time, subsequently to be included in pedigree and genomic prediction models. Again, fitting proxy traits into multi-variate prediction models with either A or K matrices was shown to improve upon univariate analyses of grain yield.

A slightly different approach to the application of proxy traits to genomic prediction has been investigated by Krause et al. (2019), where collected proxy trait (hyperspectral) data was used to generate relationship matrices (H), as an alternative to A or K matrices. H matrices were shown to provide similar increases to grain yield prediction accuracy as A and K matrices when predicting within and between sites, and combining A or K with H matrices further improved prediction accuracy. The use of H matrices as part of genomic prediction models may be particularly beneficial to breeding programmes where genotypic data is limited, though in breeding programmes where genotypic data is readily available it is likely K matrices will continue to be used, though perhaps in multi-kernel models including H matrices as described by Krause et al. (2019). If H matrices were to provide a true alternative to K matrices, the collection of phenotypic data to generate these H matrices must provide a better economic proposition than collecting genotypic data.

Given the potential to increase the accuracy of genomic prediction models for grain yield through fitting genetically correlated proxy traits, the next course of action should be to fit 'known' traits with strong genetic correlations to grain yield. A prime example of this

would be to use NGP-derived yield component traits such as AGB (demonstrated in Chapters 3 and 4), plant number per plot and spike number per plot (both of which are showing great potential to be measured using a combination HTFP platforms, such as described in Chapter 2, and ML analyses as described above). Theoretically, accounting for these components should provide a large proportion of the variability driving yield, allowing for improved genomic prediction and selection models. This will of course require further research to determine whether fitting these 'known' NGP-derived traits provides this expected benefit, though given the strong heritability of NPG-derived traits and their strong genetic correlation to their manually measured counterparts (as demonstrated in Chapters 2 and 4), breeders and researchers can fit these into multi-variate models with confidence. An alternative course of action, which may be 'higher risk' than that described above, would be to investigate fitting NGP data *per se* into statistical or ML analysis. In this instance no 'known' trait would be measured, but rather NGP data *per se* would be investigated for its predictive ability of a breeding objective. This could incorporate data from a multitude of sensor types, either individually or in combination. The caveat to this being that with so many unknown variables involved, a great deal of research may be required to find potential benefits from such methods.

The above outlines currently suggested paths for NGP-derived data, and two potential paths of investigation moving forward, though further to this, there is the question of when NGP technologies can be most effectively deployed within breeding programmes to collect this data and optimise their implementation. The works of Rutkoski et al. (2016), Sun et al. (2017) and Krause et al. (2019) are all conducted on field plots where grain yield is able to be measured. However, each of these studies, as well as the review of Rebetzke et al. (2019), suggest that the fit of these technologies may be in the earlier stages of breeding programmes, where plot sizes are generally smaller, population sizes are larger and grain yield data may not always be collected efficiently. This question of when to apply NGP technologies within a breeding programme, along with the question of how best to utilise the data, is key to efficiently deploying NGP technologies within functional breeding programmes and is perhaps best discussed in regards to the fundamentals of plant breeding.

5.4 A Strategic Approach for New Technology in Wheat Breeding

The goal of plant breeding, as a whole, is to improve the performance of economically valuable plant species through the use of genetic principles. As such, it can be thought of as the amount of genetic gain that is made for the economic trait of interest. In wheat breeding this is generally focused on grain yield, albeit not exclusively.

The concept of genetic gain is fundamental to plant breeding and can be described as the response to selection over time (Falconer, 1960), i.e. the measurable increase in genetic performance over time. This response can be calculated using the equation for genetic gain, colloquially known as the 'breeder's equation':

$$R_t = \frac{ih\sigma_A}{t} \tag{5.1}$$

Where R_t represents genetic gain per unit time (response to selection), i selection intensity, h selection accuracy, σ_A genetic variance (standard deviation of breeding values), and t generation interval.

Each component of this equation can be influenced by the breeder in an attempt to increase genetic gain. For example, selection intensity can be increased with larger population size, selection accuracy can be increased through more accurate measurement of the trait of interest, genetic variance can be increased through wider crossing strategies, and generation interval can be reduced by identifying parents at earlier generations within the programme.

Looking at the equation for genetic gain, there are two apparent avenues through which NGP technology can most assist:

i Selection intensity can be increased as a factor of population size, due to the increased capacity of phenotyping available with NGP and HTFP technologies, as opposed to traditional methods

ii Selection accuracy can be increased through more accurate, repeatable and objective measurements of traits, as opposed to traditional methods. Or through providing additional information for inclusion in statistical modelling.

A third potential option, suggested by Rebetzke et al. (2019), is that NGP technologies may allow for greater genetic variance, as larger populations can be grown and phenotyped to accommodate wider crossing strategies.

In essence, this equates to: i) 'can it measure the trait faster?', and ii) 'can it measure the trait more accurately?'. When considering the practical application of this technology to a breeding programme there is also the question of iii) 'what is the cost compared to traditional methods?'. With these three core questions it is possible to examine where these technologies are best deployed within a breeding programme. This could be examined in minute detail for any given breeding programme, though the overall concepts of questions i, ii and iii are broad and fundamental to the application of any technology within any breeding programme. As such, for the purpose of this discussion, a strategy agnostic of technology and programme structure will be presented to aid breeders' decision in adopting new technology.

Figure 5.1 outlines a decision tree for determining whether a new technology should be deployed within a breeding programme, irrespective of the trait, technology or stage of breeding programme considered. The only assumption of this decision tree is that the technology is capable of being deployed within the programme, i.e. this tree cannot be used for a technology which has a physical limitation preventing its deployment.

As shown in Figure 5.1 it can be a complex process deciding whether a new technology should be deployed. Interestingly this decision is much simpler when considering the merits of measuring a new trait, rather than when considering altering methods for a trait routinely measured. For a new trait, provided it can be measured by the new technology and it is a breeding objective for the programme, all that need be considered is whether the value of genetic gain achievable for the trait will offset the cost of deploying the technology. This is a concept that is often overlooked within the literature, as not only the cost deploying the technology needs to be considered, but also the cost-benefit ratio in terms of genetic gain. In cases where the trait is not a breeding objective, the question changes to whether collecting and analysing this data (in a cost efficient manner) could be used to increase the accuracy for a trait which is a breeding priority, through multi-variate statistical analyses, which will be measured regardless of this new trait. This also applies when

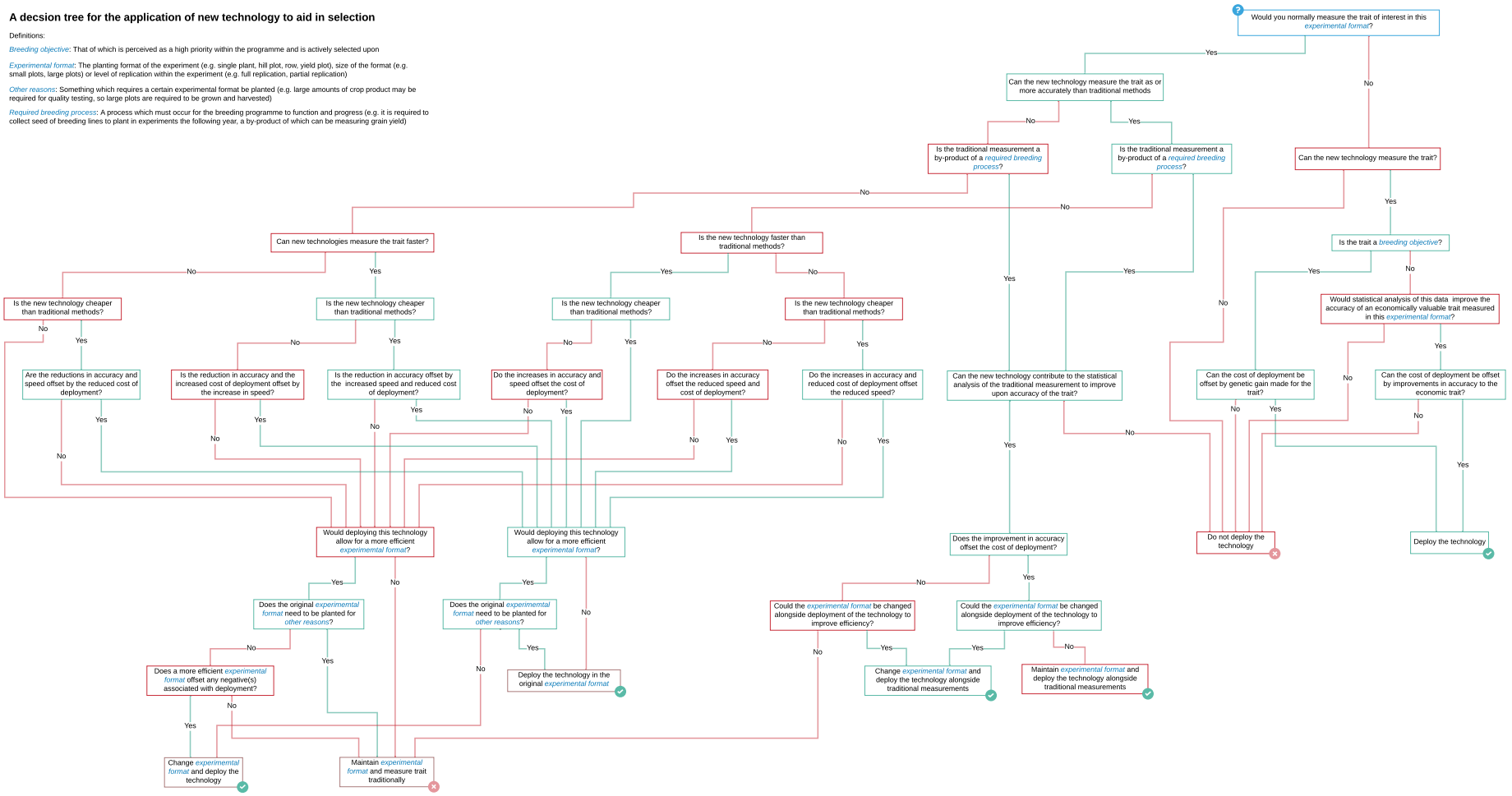

FIGURE 5.1: A decision tree for the application of new technology to aid selection in a breeding programme. Blue italicised terms are described within the figure. The blue circle with a question mark indicates the start point, green circles with ticks indicate an outcome where the new technology will be deployed, red circles with crosses indicate an outcome where the new technology will not be deployed. Green and red lines follow yes and no answers respectively.

considering measuring a trait for the purpose of indirect selection (Falconer, 1960), where accuracy and speed contribute toward genetic gain of the breeding objective, which must be considered in relation to the cost of deployment.

For traits which are traditionally measured within the breeding programme, it can be a more complicated decision as to whether new technology should replace, or be used in conjunction with, traditional methods. While the key questions of accuracy, speed and cost are still present, the context in which the trait is measured, as well as how it fits in the experimental format need to be considered. Firstly, it is important to understand whether the trait is measured as a by-product of a required breeding process, as this will alter how new technology may be deployed. For example, grain yield is an important trait to assess wheat breeding line performance, however, measuring grain yield can also be a by-product of seed multiplication, a required breeding process. Secondly, it needs to be considered whether deploying this technology would allow for a more efficient experimental format to be planted. Efficiency could be gained from miniaturisation of the planting format (e.g. small plot to row), or through reducing replication within the trial, such as using sparse (partially replicated) experimental designs across multiple locations (Cullis et al., 2006). In instances where experimental format can be changed, the breeder has the option to free up resources that can either be reallocated within the programme or held on to, to run a leaner, cheaper, programme. In some circumstances, while the deployment of new technology may allow a more efficient experimental format to be planted, the original format may still be required for other reasons within the programme. For example, multiple replicates of yield plots may be required to harvest grain for quality testing and reducing replication would produce insufficient amounts of grain. Given the number of flow-on effects which may occur from simply changing a method of trait assessment, it is unsurprising that plant breeders can be hesitant to change from current practices or adopt new technology within their programmes, even when from the outside it appears that only a small change is occurring. In reality, implementing a simple change may result in the reassessment of the overall programme structure.

Further to its potential use by plant breeders, this tree can also be used by researchers either developing new technologies, or investigating current technologies for use within breeding programmes. Every yes/no question which cannot currently be answered lends

itself to further research. As an example of this, the use of LiDAR to measure wheat AGB in a yield plot format could be investigated. In a situation where AGB is not generally measured and not being directly selected for, it could be measured with LiDAR for input into multi-variate analyses with grain yield. However, it is not known how this would affect the accuracy of the of grain yield estimate from the trial, it may be improved, but it may also have no effect. This then opens a research question, which when answered would allow breeders to decide if this is a technology worth considering. Following this line of enquiry, it is possible to look further down the tree and address a question to which the previous question does not yet have a clear answer. In the example of wheat AGB and grain yield, it is possible to skip this currently unanswered question and instead question whether a theoretically large improvement in grain yield accuracy would offset the deployment cost of the technology? Should the answer to this question be 'no', research into the deployment of this technology would not be considered a high priority by breeders.

When considering deploying NGP technology it is important to ask how well the technology can measure the trait of interest, as well as whether the technology has a logistically and economically sound data processing pipeline to generate data for that trait, with these questions being encapsulated within the broad questions posed within Figure 5.1, regarding accuracy and cost respectively. It is difficult to give broad recommendations on the application of NGP technologies to wheat breeding programmes as there are so many variables at play. Even after the in-depth work conducted in Chapters 2 through 4, broad recommendations of how digital cameras and LiDAR can be utilised within programmes cannot be made, only suggestions as to how breeders may choose to consider their application. Every programme is structured differently, with different objectives and different resources available to reach those objectives. Decision trees such as Figure 5.1 will aid in the strategic implementation of NGP within breeding programmes, though ultimately it is at the discretion of each breeder as to what is best suited for their programme.

5.5 Future Considerations for Next Generation Phenotyping in Wheat Breeding

Using the decision tree described in Figure 5.1 it is easy to imagine how NGP technology could be deployed within a wheat breeding programme, however there are still challenges to be addressed before this can be realised. Phenotyping platform development and deployment are still an issue for many breeding programmes, with progress in this area being hindered due to the diversity of breeding programme structures and the inability, so far, to apply a 'one size fits all' solution. In Chapter 2 we proposed and developed the high-throughput imaging boom (HIB), a ground-based phenotyping platform, specifically to meet needs of a single wheat breeding programme. While we achieved this goal, challenges in the deployment of the system still arose. Being tractor-based, the logistics of transporting such a system between remote sites are complex, requiring two people be present for safe loading, unloading and transport of the system on a truck. While this may be somewhat location specific (i.e. dependent on local workplace safety laws), in this case large amounts of time (and hence cost to the breeding programme) were required to transport the system between sites. Aside from the physical logistics of transporting equipment to remote sites, it is also difficult to match phenotyping activities to desired physiological growth stages at remote sites. This is where a team of trained technical staff and a fleet of phenotyping systems would be beneficial, though this would be expensive for the programme. Furthermore, there are limitations in deployment of the system after large rainfall events, as soil beneath the tractor tyres is churned and trial sites are damaged when excessive moisture is present. This is particularly limiting during the beginning of the southern Australian cropping season where large amounts of rain can generally be expected, yet traits such as plant number, canopy cover and early vigour are desirable to assess.

To overcome this logistical burden of transporting NGP systems it may be feasible to fuse NGP technologies with equipment required for routine trial maintenance procedures. For example, sensors could be attached to spray booms (or a secondary boom used in conjunction with a spray boom) and data collected while herbicides, fungicides or pesticides are being applied to the trial site. As these booms are typically larger than that used for the

HIB, a greater number of sensors could be attached, increasing the number of plots simultaneously measured. While this solution would reduce time and labour in transporting a dedicated phenotyping system, it does not solve limitations to deployment on excessively moist soil, and adds a new limitation; that of limiting data collection to growth stages at which herbicides, fungicides and pesticides are applied. This may be suitable for some breeding programmes, but likely not all.

For the obstacle of field access, the most apparent solution is to switch from a ground-based platform to an aerial platform, such as UAVs, for the collection of phenotype data. As discussed previously UAV platform and sensor technology technology is constantly improving, and while UAVs may not currently be able to efficiently and routinely obtain the phenotype data desired by breeders, it is likely they will be able to in future. Though the transport and deployment of UAVs can be much simpler than a ground-based system, a minimum of a single operator is still required to be present to conduct the phenotyping activities. An optimal solution to this would be a UAV base station which could be established at, or prior to, the sowing of each trial site. From here the UAV would autonomously deploy (or be remotely activated) to collect phenotype data and return to the base station for battery charging and data transmission. This would allow breeders to collect phenotypic data routinely from multiple field sites with minimal effort. Such a system may seem like a blue sky concept, however, similar 'drone in a box' services have been developed for mining and security applications (Airobotics, 2019; Percepto, 2019).

Even with a clear idea of what an optimal phenotyping platform may look like within a particular wheat breeding programme, the deployment of these technologies still hinges on the ability to demonstrate their value to breeders. Current and potential future research efforts have been discussed previously, however, it is worth reiterating that a high priority for future research should be placed on demonstrating the use of NGP measurements to advance genetic gain for common breeding objectives. Given that grain yield is often the primary objective of breeding programmes, demonstrating significant advancements in genetic gain for this trait should be a high priority. Specifically the work of Rutkoski et al. (2016) and Sun et al. (2017) should be expanded upon to investigate the potential of improving grain yield accuracy through using a range of NGP derived traits within genomic selection and multi-variate models. Ideally this would not focus on fitting single

traits, but rather suites of traits expected to account for genetic variation in grain yield and for residual variation within field trials.

Further to the improvement of genomic selection and multi-variate models, another high priority avenue of research should be the use of NGP derived phenotype data, in combination with site-specific environmental and dense genomic data, for the inclusion within crop growth models (CGMs) to simulate genotype performance. Crop growth models can be used to predict phenotype based upon genetic-by-environment-by-management interactions (Hammer et al., 2019) and as such can be a useful tool for increasing genetic gain within breeding programmes (Cooper et al., 2014). While CGMs have not traditionally handled large-scale phenotype data, Messina et al. (2018) have proposed the concept of second generation crop growth models (SGCGMs) capable of incorporating large-scale phenotypic data generated from HTFP platforms, for the improvement of physiological models (such as the genotype-to-phenotype model (Messina et al., 2011)) as well as the training of CGM-whole genome prediction models (Technow et al., 2015; Messina et al., 2018). Deployment of such models within a wheat breeding programme could improve the way in which variety performance is evaluated and allow for increased genetic gain. With grain yield as an example, the use of SGCGMs could allow for improved performance prediction for genotypes absent from the population, or for genotypes absent from specific locations. This could also allow for better understanding of varietal adaption within specific environments, and the investigation of the value of specific traits or trait combinations within certain environments. In turn, this may allow targeted deployment of NGP within environments, focusing on the traits best associated with adaption and performance. Furthermore, with deployment of these models it may also be feasible to gain useful information from field sites abandoned mid-season due to environmental conditions such as drought and frost. This would negate the lost opportunity cost of an abandoned site and greatly improve efficiency within the breeding programme.

Going forward, provided research demonstrates the value of NGP measurements to breeding programmes, and sensor, platform and data processing technology improves to a point where it can be reliably and conveniently deployed within breeding programmes, these tools will find their fit within breeding programmes and will become valuable assets for

breeders to deploy. The prospect of being able to collect grain yield data along with NGP-derived traits such as above-ground biomass, plants per plot and spikes per plot, and seed traits such as thousand grain weight and kernel size within a wheat breeding programme is an exciting one. This information could contribute a great deal towards understanding how these components define grain yield in specific environments, providing the opportunity to increase its genetic gain.

5.6 Conclusion

Next generation phenotyping is an exciting frontier for wheat and other field-crop breeders, offering to revolutionise the way in which phenotype data is collected from large-scale field trials. Herein it has been shown how digital cameras and LiDAR sensors can be deployed within large-scale field trials for the non-destructive, accurate and repeatable measurement of numerous traits commonly measured within wheat breeding programmes. All traits measured were shown to be highly suitable for inclusion in routine breeding analyses, providing breeders confidence in deploying these technologies, should they choose, or for inclusion in future research on how these measurements can best benefit breeding programmes. Furthermore, the data produced using these technologies can be of great value to researchers, particularly in regard to recording phenotypic differences observed in agronomic and crop physiologic research, as well as broad genetic studies aimed at the dissection of traits. As phenotyping and associated technologies continue to improve and future research demonstrates how these technologies can contribute towards improving genetic gain within breeding programmes, the decision tree framework proposed herein can be used by breeders to find the appropriate fit of these technologies.

Bibliography

ADAMSEN, F. G., PINTER, P. J., BARNES, E. M., LAMORTE, R. L., WALL, G. W., LEAVITT, S. W., & KIMBALL, B. A. (1999). Measuring wheat senescence with a digital camera. *Crop Science* **39**, 719–724.

AIROBOTICS (2019). Automated industrial drones [online]. Available at: https://www.airoboticsdrones.com/ [Accessed 10th November 2019].

COOPER, M., MESSINA, C. D., PODLICH, D., TOTIR, L. R., BAUMGARTEN, A., HAUSMANN, N. J., WRIGHT, D., & GRAHAM, G. (2014). Predicting the future of plant breeding: complementing empirical evaluation with genetic prediction. *Crop & Pasture Science* **65**, 311–336.

CULLIS, B. R., SMITH, A. B., & COOMBES, N. E. (2006). On the design of early generation variety trials with correlated data. *Journal of agricultural, biological, and environmental statistics* **11**, 381.

FALCONER, D. S. (1960). *Introduction to quantitative genetics*. Ronald Press Co, New York.

GUO, W., ZHENG, B., DUAN, T., FUKATSU, T., CHAPMAN, S., & NINOMIYA, S. (2017). Easypcc: Benchmark datasets and tools for high-throughput measurement of the plant canopy coverage ratio under field conditions. *Sensors* **17**, 798.

HAMMER, G., MESSINA, C., WU, A., & COOPER, M. (2019). Biological reality and parsimony in crop modelswhy we need both in crop improvement! *in silico Plants* **1**. diz010.

HASAN, M. M., CHOPIN, J. P., LAGA, H., & MIKLAVCIC, S. J. (2018). Detection and analysis of wheat spikes using convolutional neural networks. *Plant Methods* **14**, 100.

HU, P., GUO, W., CHAPMAN, S. C., GUO, Y., & ZHENG, B. (2019). Pixel size of aerial imagery constrains the applications of unmanned aerial vehicle in crop breeding. *ISPRS Journal of Photogrammetry and Remote Sensing* **154**, 1–9.

KRAUSE, M. R., GONZÁLEZ-PÉREZ, L., CROSSA, J., PÉREZ-RODRÍGUEZ, P., MONTESINOS-LÓPEZ, O., SINGH, R. P., DREISIGACKER, S., POLAND, J., RUTKOSKI, J., SORRELLS, M., ET AL. (2019). Hyperspectral reflectance-derived relationship matrices for genomic prediction of grain yield in wheat. *G3: Genes, Genomes, Genetics* **9**, 1231–1247.

LUKINA, E. V., STONE, M. L., & RANN, W. R. (1999). Estimating vegetation coverage in wheat using digital images. *Journal of Plant Nutrition* **22**, 341–350.

MESSINA, C., TECHNOW, F., TANG, T., TOTIR, R., GHO, C., & COOPER, M. (2018). Leveraging biological insight and environmental variation to improve phenotypic prediction: Integrating crop growth models (cgm) with whole genome prediction (wgp). *European Journal of Agronomy* **100**, 151 – 162. Recent advances in crop modelling to support sustainable agricultural production and food security under global change.

MESSINA, C. D., PODLICH, D., DONG, Z. S., SAMPLES, M., & COOPER, M. (2011). Yield-trait performance landscapes: from theory to application in breeding maize for drought tolerance. *Journal of Experimental Botany* **62**, 855–868.

MOORE, G. E. (1965). Cramming more components onto integrated circuits. *Electronics* **38**, 114.

PERCEPTO (2019). Solving operational challenges from above [online]. Available at: https://percepto.co/ [Accessed 10th November 2019].

REBETZKE, G., JIMENEZ-BERNI, J., FISCHER, R., DEERY, D., & SMITH, D. (2019). High-throughput phenotyping to enhance the use of crop genetic resources. *Plant Science* **282**, 40–48.

RUTKOSKI, J., POLAND, J., MONDAL, S., AUTRIQUE, E., PÉREZ, L. G., CROSSA, J., REYNOLDS, M., & SINGH, R. (2016). Canopy temperature and vegetation indices from high-throughput phenotyping improve accuracy of pedigree and genomic selection for grain yield in wheat. *G3: Genes, Genomes, Genetics* **6**, 2799–2808.

SADEGHI-TEHRAN, P., SABERMANESH, K., VIRLET, N., & HAWKESFORD, M. J. (2017). Automated method to determine two critical growth stages of wheat: Heading and flowering. *Frontiers in Plant Science* **8**, 252.

SADEGHI-TEHRAN, P., VIRLET, N., AMPE, E. M., REYNS, P., & HAWKESFORD, M. J. (2019). Deepcount: In-field automatic quantification of wheat spikes using simple linear iterative clustering and deep convolutional neural networks. *Frontiers in Plant Science* **10**, 1176.

SUN, J., RUTKOSKI, J. E., POLAND, J. A., CROSSA, J., JANNINK, J.-L., & SORRELLS, M. E. (2017). Multitrait, random regression, or simple repeatability model in high-throughput phenotyping data improve genomic prediction for wheat grain yield. *The plant genome* **10**.

TECHNOW, F., MESSINA, C. D., TOTIR, L. R., & COOPER, M. (2015). Integrating crop growth models with whole genome prediction through approximate bayesian computation. *PloS one* **10**, e0130855.

WANG, X., XUAN, H., EVERS, B., SHRESTHA, S., PLESS, R., & POLAND, J. (2019). High-throughput phenotyping with deep learning gives insight into the genetic architecture of flowering time in wheat. *bioRxiv* .

Appendix A

Chapter 2 Supplementary material

A.1 Supplementary Material 1

Basic Colour Segmentation of Digital Images.

Detailed methods for the basic image analysis of colour-based traits from digital images.

Also available online:

https://www.frontiersin.org/articles/10.3389/fpls.2019.00449/full#supplementary-material

frontiers

Supplementary Material

Basic Colour Segmentation of Digital Images

Using:

FiJI – https://fiji.sc/

Threshold_Colour Plugin – http://www.mecourse.com/landinig/software/software.html

1. Import images as a stack

- File > Import > Image Sequence…
- Navigate to the folder containing your images and select the first image

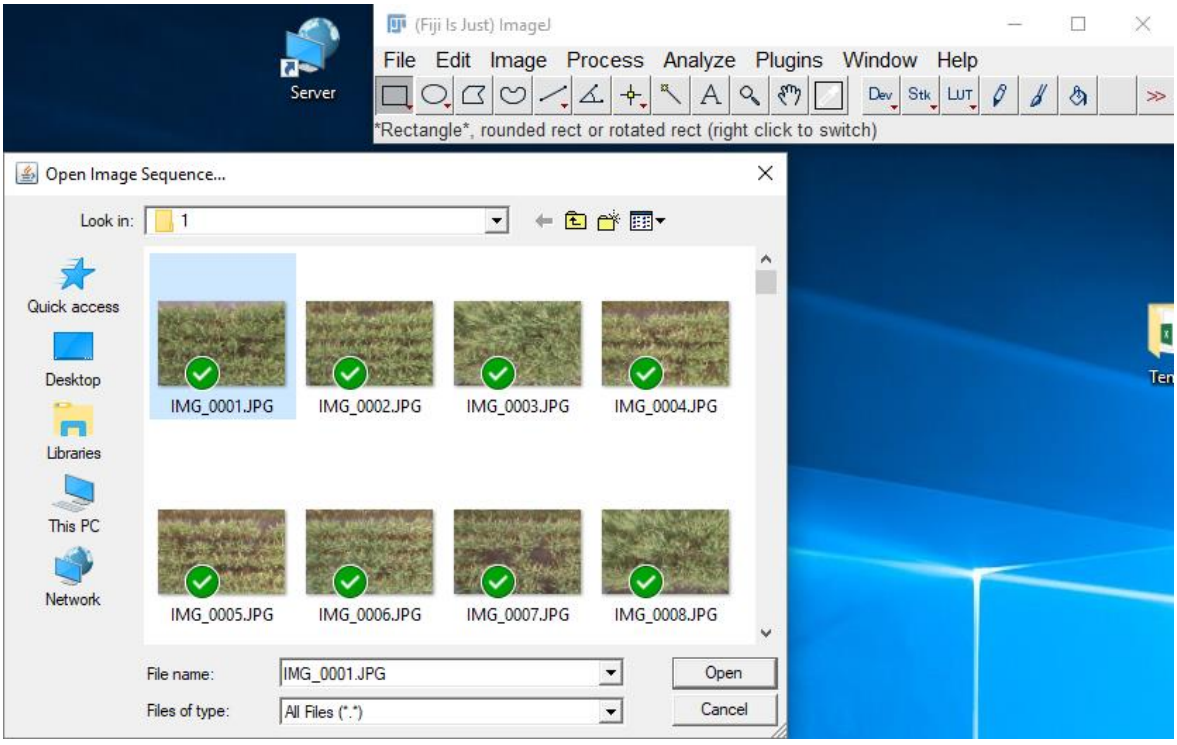

- Specify number of images (if default is incorrect) in the Sequence Options Window*
    - *Depending on RAM limitations of the computer, images may need to be resized before loaded into image-J, especially when dealing with a large number of files.

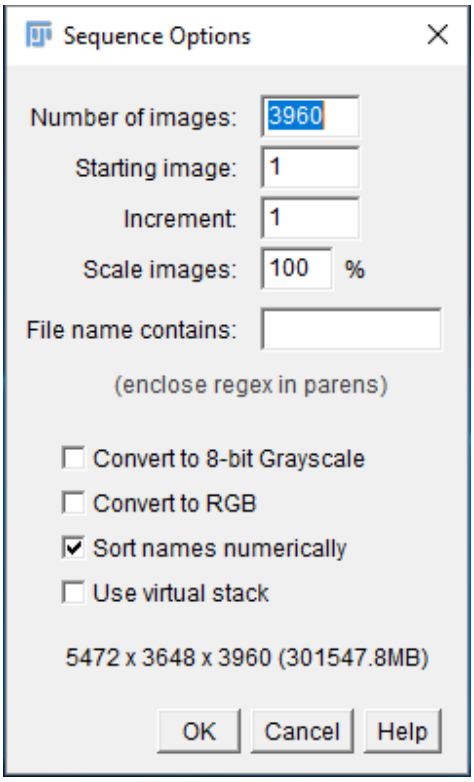

2. Define Regions of Interest (ROI) in images (if required)

- Analyze > Tools > ROI manager
- Using the cursor, select the area of your image you wish to perform the analysis on*

- Once the area is selected, press the ‘Add’ button in the ROI manager
    - *You can cycle through images using the scroll bar at the bottom, to ensure the ROI is suitable across your image set

3. Convert images to ROI stack

- Ensure that the ROI you have created is selected (highlighted) in the ROI manager

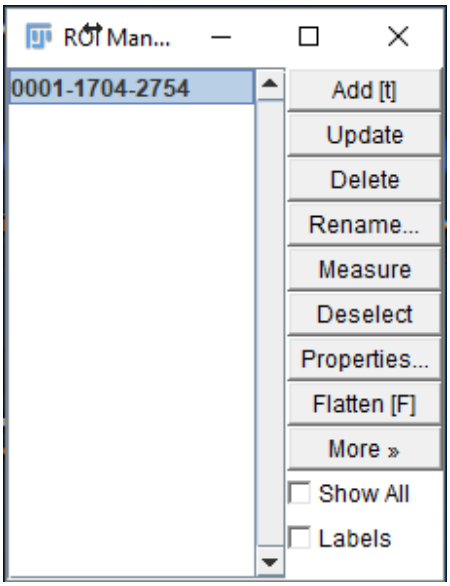

- Image > Duplicate (make sure the 'Duplicate stack' box is checked)

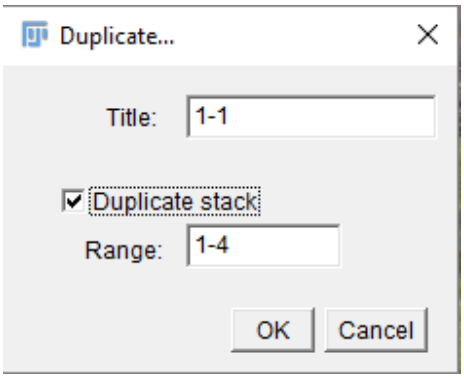

- A new window will appear with all the ROI from your image stack. This may take a moment to process, especially for large image sets
- At this point, the original image stack and the ROI manager window can be closed (if desired)
- The ROI image stack can also be saved by navigating to File > Save As > Image sequence

4. Duplicate the ROI stack

- Duplicate the ROI image stack, one stack will be used for measuring Total Leaf Area, while the other will measure Leaf Area Yellow
- Image > Duplicate (make sure the 'Duplicate stack' box is checked)
- A second window containing the ROI stack will appear

5. Threshold for Total Leaf Area

- Select one of the ROI stacks
- Navigate to Plugins > Threshold Colour > Threshold Colour
- Use the scroll bars in the Threshold Colour window to select the desired threshold
- Hue values should remove reds and blues from the image, keeping yellows and greens. This will likely be in the range of 15 – 100
- Thresholding on Brightness may be useful to remove dark and shadowy patches of soil, but it is important not to remove large areas of dark leaves.
- Saturation values may or may not be useful, depending on the situation.
- This stage needs to be tweaked for each set of images analysed, taking into account soil colour and illumination of the image.

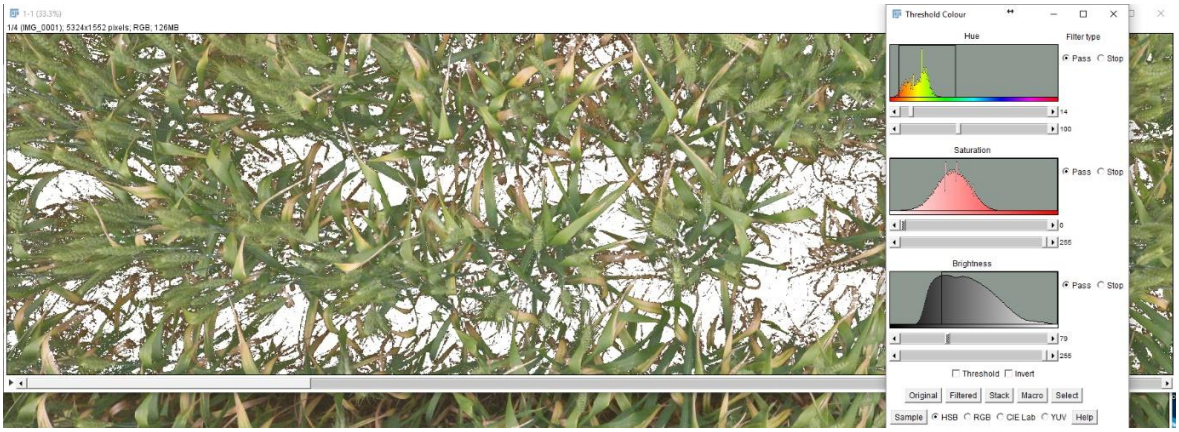

- Press the ‘Stack’ button to apply these selections to all images and check they are suitable
- Once a suitable threshold has been created, check the ‘Threshold’ box and then press the ‘Stack button’ to apply a black and white threshold across all images.

6. Convert to binary image

- Process > Binary > Make Binary
- In the Convert Stack to Binary window, use the settings from the below figure

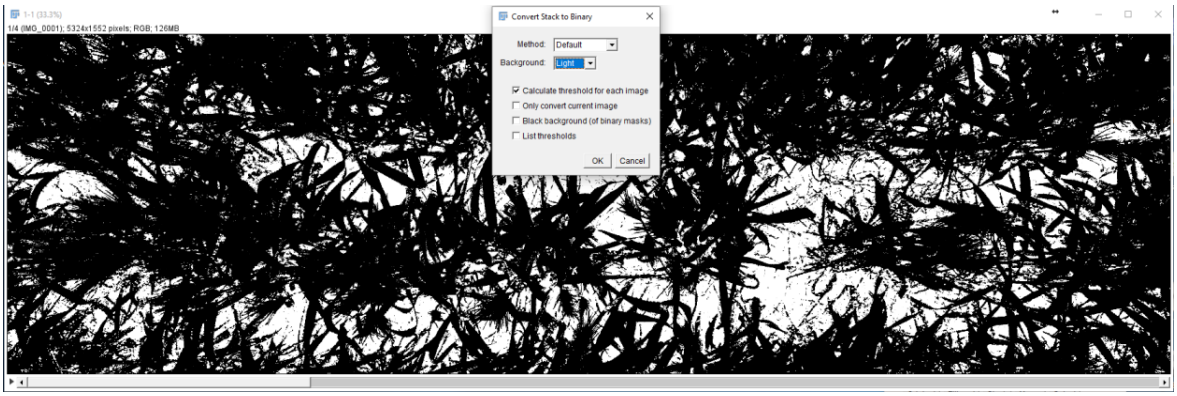

7. Count Total Plant Area Pixels

- Plugins > Voxel Counter
- This will give the number of black pixels per image i.e. the number of plant pixels
- Save data from the results window, or copy to the desired document.

9. Threshold for Yellow Leaf Area

- Select the unprocessed image stack, created in step 4
- Repeat steps 5, 6 and 7. In step 5 instead of thresholding for greens and yellows, threshold for the yellow colour of interest.
- This will likely be in the Hue region of 15-35

10. Calculate percentage of Total Leaf Area and Leaf Area Yellow

- Use (Yellow Leaf Area Pixels/Total Leaf Area Pixels)*100 to get a percentage score of Yellow Leaf Area
- Percentage canopy cover can also be calculated as (Total Leaf Area Pixels/Total Pixels in ROI)*100

A.2 Supplementary Material 2

Image processing examples for Senescence, Septoria Tritici Blotch Severity and Canopy Cover.

Examples of images processed in FiJI, showing different stages of processing for the traits senescence, Septoria Tritici Bloctch and canopy cover.

Also available online:

https://www.frontiersin.org/articles/10.3389/fpls.2019.00449/full#supplementary-material

frontiers

Supplementary Material

Image processing examples for Senescence, Septoria Tritici Blotch Severity and Canopy Cover

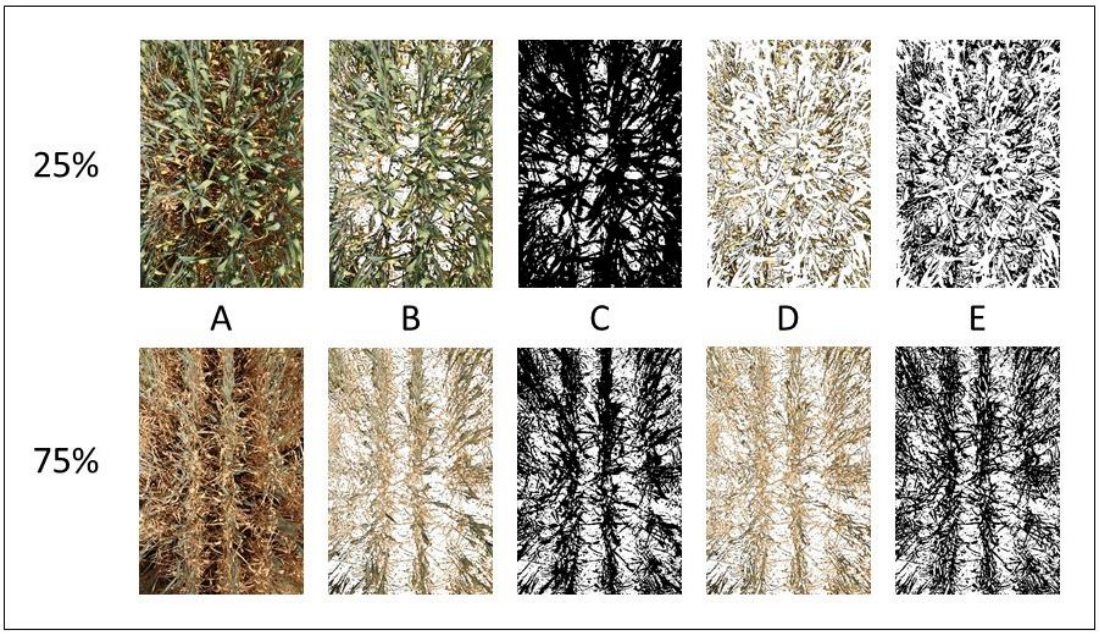

Supplementary Figure 1. Examples of images processed for the assessment of senescence, showing the original image **(A)**, segmented plant material **(B)**, binary plant material threshold **(C)**, segmented senesced material **(D)** and binary senesced material threshold **(E)**, for plots with scored approximately **25%** and **75%** yellow leaf area.

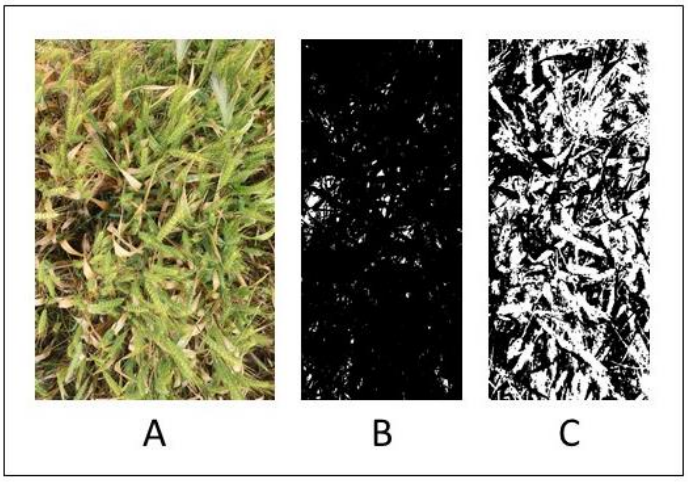

Supplementary Figure 2. Examples of images processed for Septoria tritici blotch assessment, showing **(A)** original image, **(B)** binary plant material threshold and **(C)** binary Septoria tritici blotch material threshold.

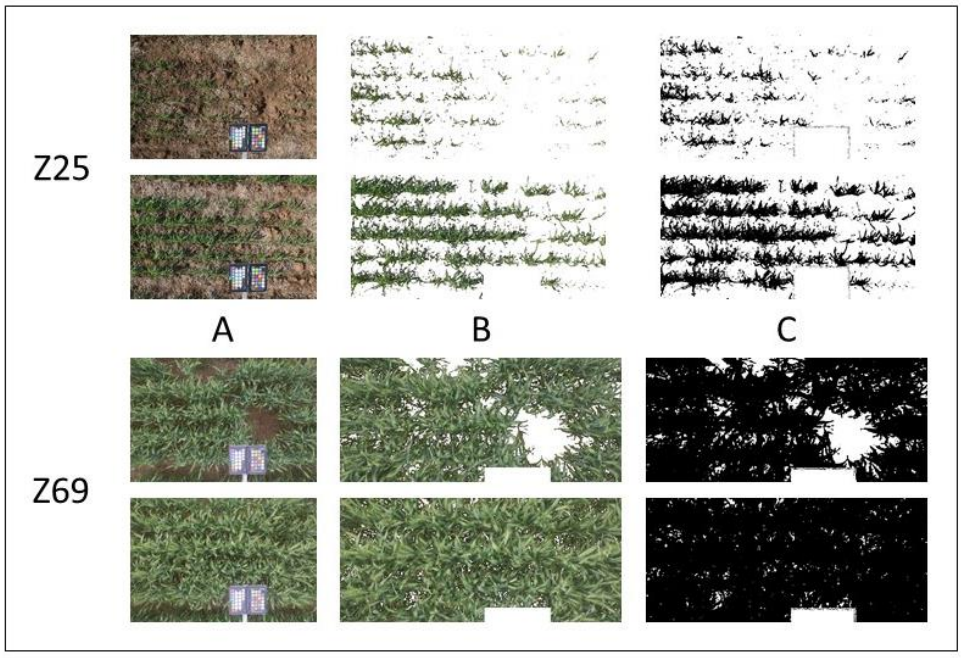

Supplementary Figure 3. Examples of images processed for canopy cover assessment, showing **(A)** original image, **(B)** segmented plant material and **(C)** binary plant material threshold, for plots at **Zadoks growth scale 25 (top)** and **69 (bottom)**.

Appendix B

Chapter 4 Supplementary material

B.1 Supplementary Material 1

Algorithm Selection for LiDAR Canopy Height.

An explanation of the process used for selecting the parameters of the LiDAR Canopy Height algorithm, including figures illustrating the response of the algorithm to different parameters.

Also avialable online:

https://www.frontiersin.org/articles/10.3389/fpls.2019.01145/full#supplementary-material

frontiers

Supplementary Material

Algorithm Selection for LiDAR Canopy Height

Algorithms ranging from the 60th to 99th percentile height across scan lines were compared across all sample times and repeated measures at the Roseworthy site. Each sample time contains 192 observations. Values form each of these algorithms were correlated to their corresponding manual measurement, with the correlation coefficients and the root mean square error (RMSE) of the data, from all time points, being compared in Supplementary Figures 1 and 3 respectively. Due to the reversed relationship between percentile algorithm, correlation coefficients and RMSE for measurements during the first sample time (ZGS 31), these measurements were not included in determining the mean correlation coefficient or RMSE across the data sets. Supplementary Table 1 below indicates which plots relate to which sample time and measurement.

Supplementary Table 1. Labels of scans presented in Supplementary Figures 1 and 3, with the associated Zadoks Growth Scale (ZGS) and scan direction.

ZGS	Scan 1 (Forward)	Scan 2 (Forward)	Scan 3 (Reverse)
31	t11	t12	t13
49	t21	t22	t23
59	t31	t32	t33
65	t41	t42	t44
96	t51	t52	t55

The 89th percentile algorithm produced the greatest mean correlation coefficient, while the 86th percentile algorithm produced the minimum mean RMSE. Looking at Supplementary Figures 2 and 4 it is apparent there is no large peak for either mean statistic, and there is likely very little difference in selecting percentile algorithms within a 5-percentile range. With this is mind the 86th percentile algorithm was selected to broadly represent crop canopy height, and henceforth data referred to as LiDAR Canopy Height (LCH) in the current study was produced with this algorithm.

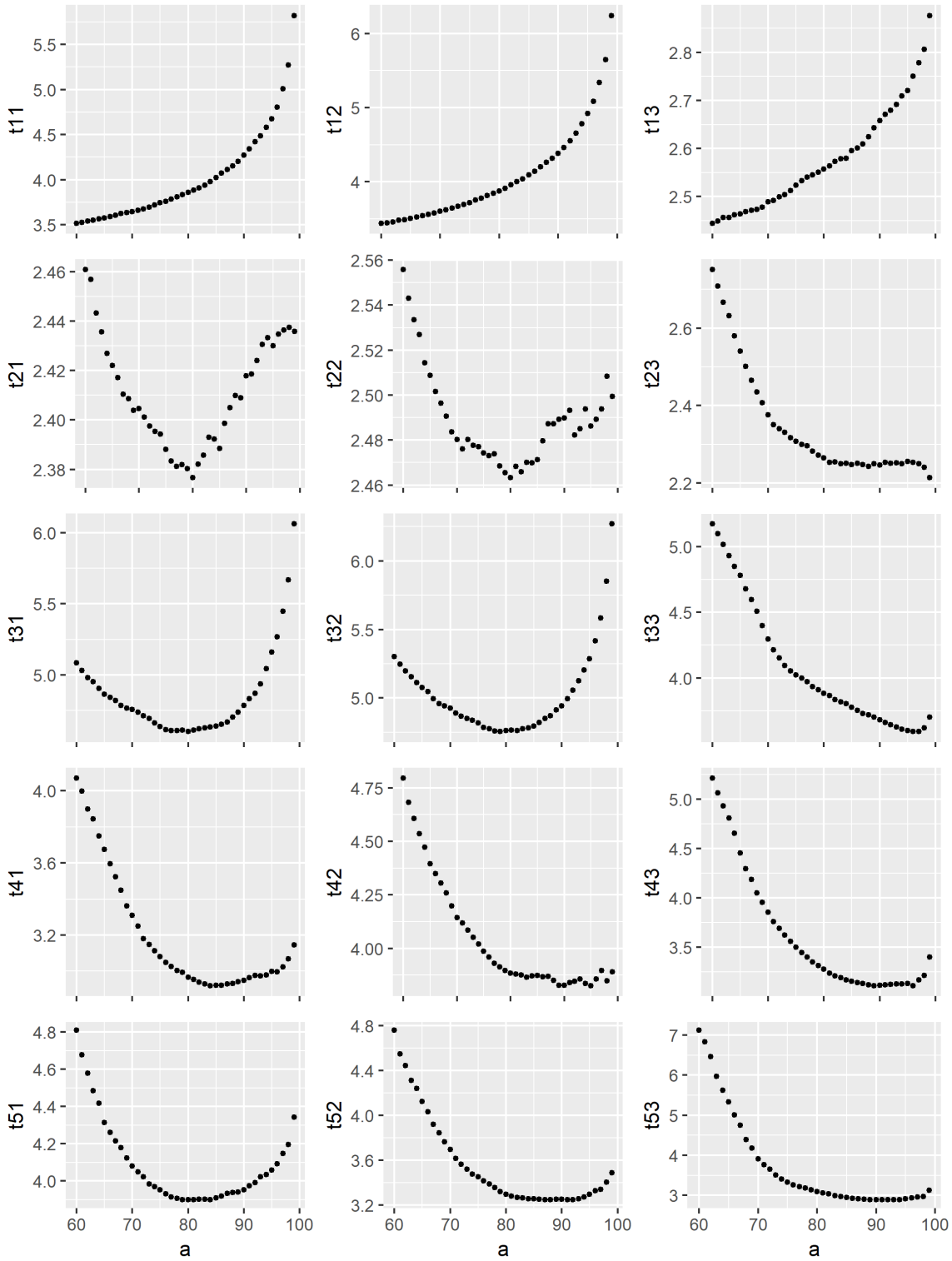

Supplementary Figure 1. RMSE between manually measured canopy height and LiDAR measured canopy height, for percentile algorithms ranging from the 60th to 99th percentile. Where figures are labelled as sample time and LiDAR sample repetition (1: forward, 2: forward, 3: reverse). RMSE is presented on the Y axis, with percentile algorithm on the X axis.

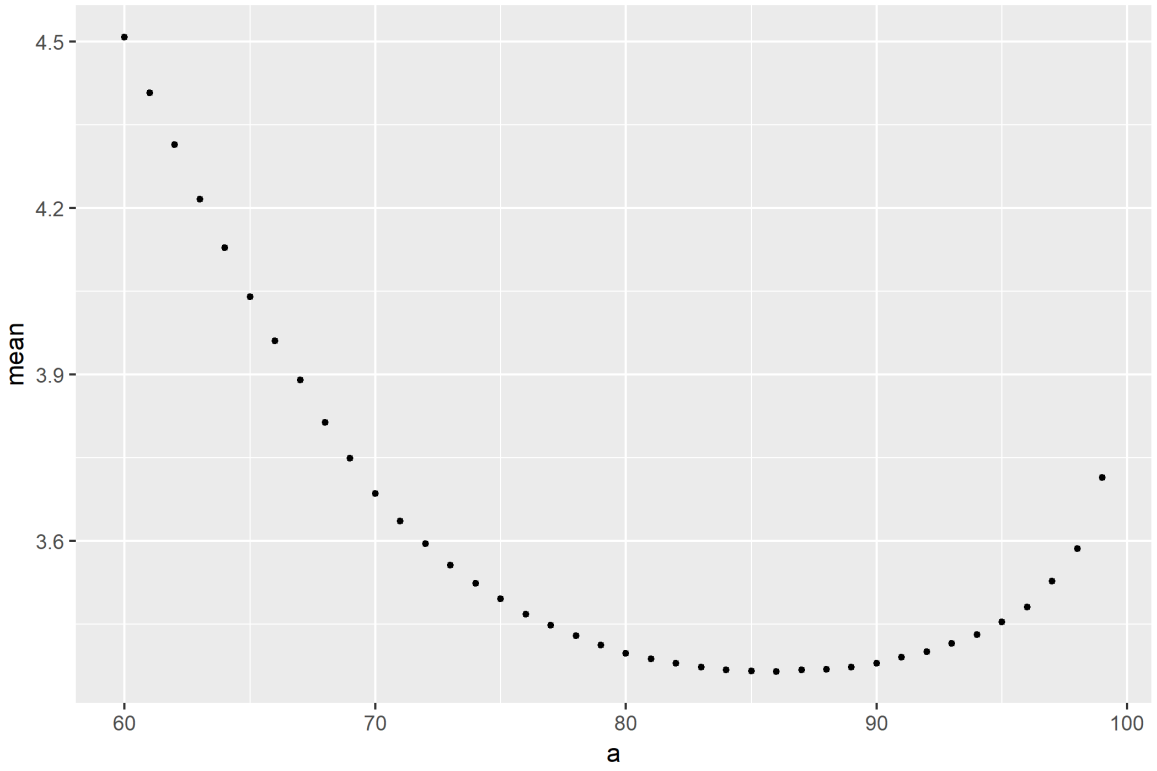

Supplementary Figure 2. Mean RMSE across all sample times, excluding t11, t12 and t13, of manually measured canopy height and LiDAR measured canopy height, for percentile algorithms ranging from the 60th to 99th percentile. RMSE is presented on the Y axis, with percentile algorithm on the X axis.

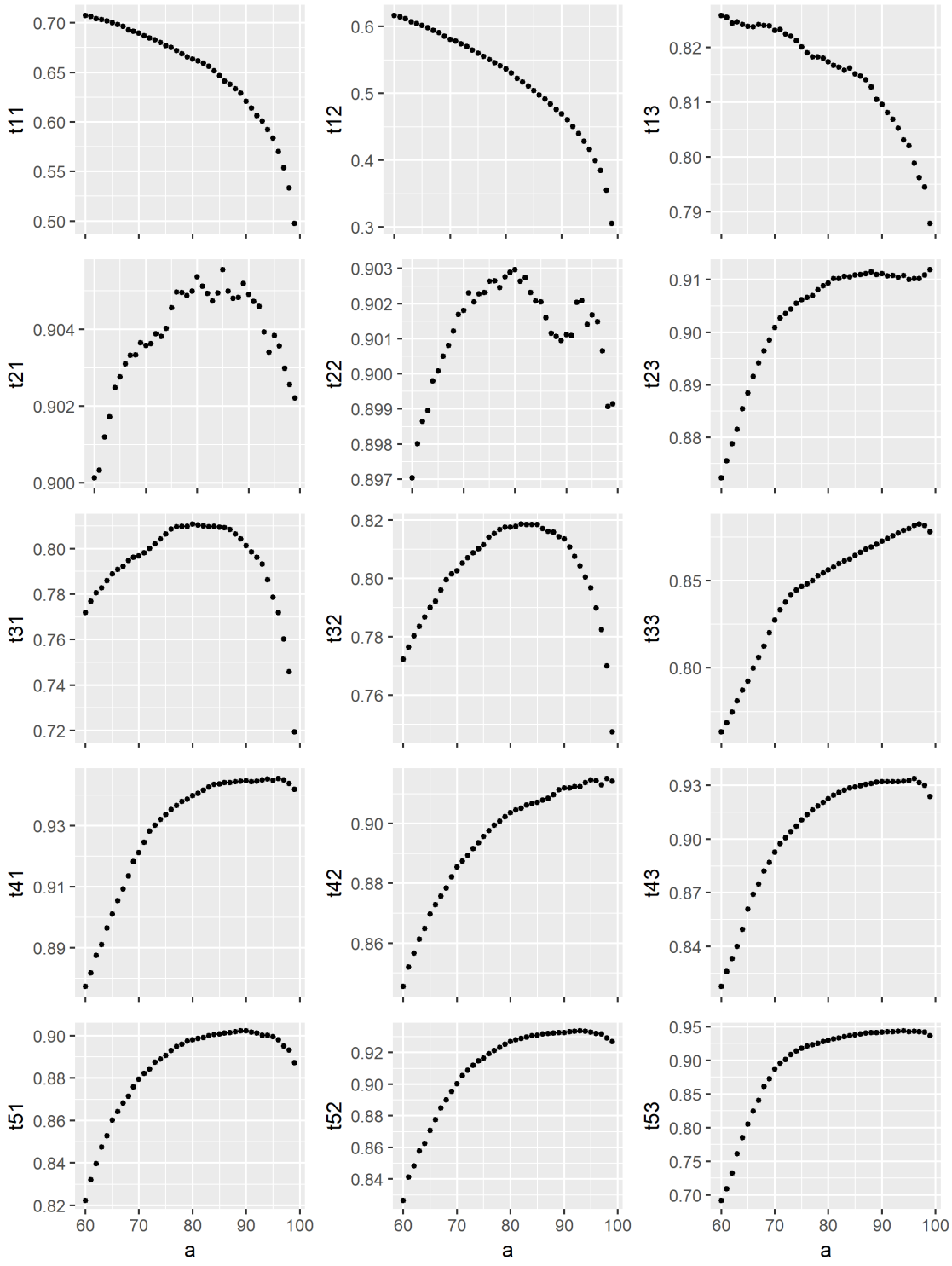

Supplementary Figure 3. Pearson's correlation coefficients between manually measured canopy height and LiDAR measured canopy height, for percentile algorithms ranging from the 60th to 99th percentile. Where figures are labelled as sample time and LiDAR sample repetition (1: forward, 2: forward, 3: reverse). Correlation coefficient is presented on the Y axis, with percentile algorithm on the X axis.

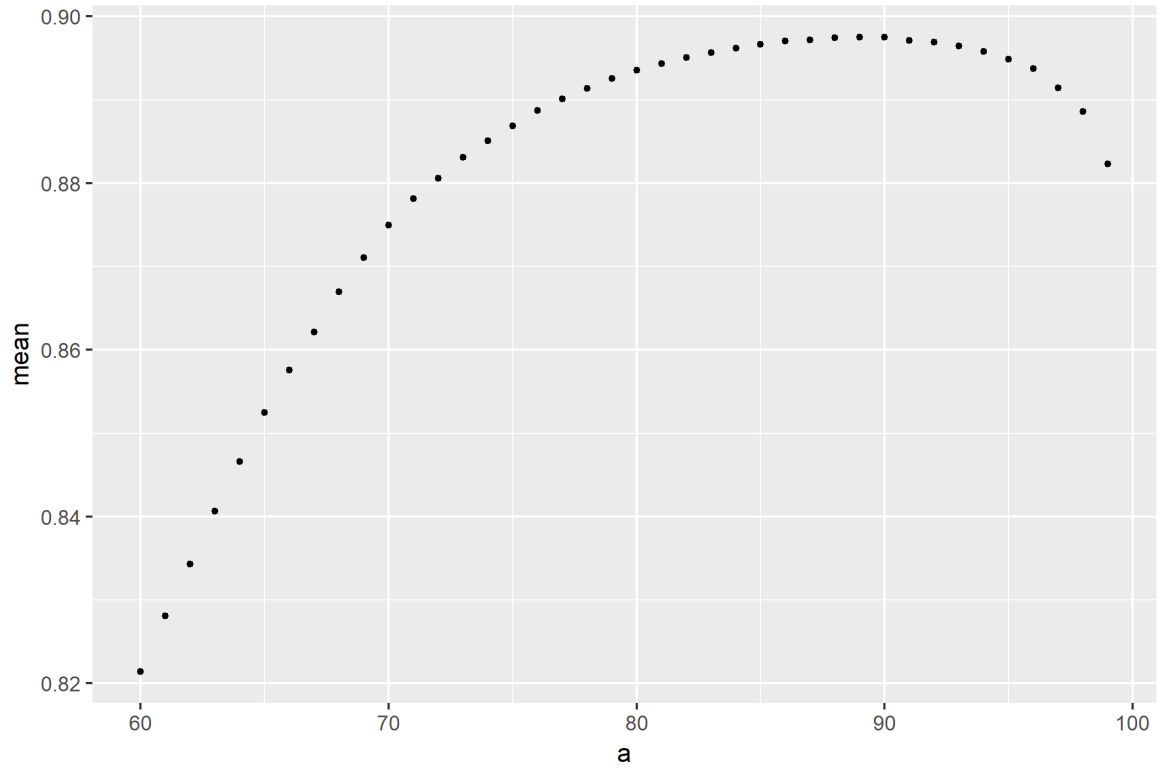

Supplementary Figure 4. Mean Pearson's correlation coefficient across all sample times, excluding t11, t12 and t13, of manually measured canopy height and LiDAR measured canopy height, for percentile algorithms ranging from the 60th to 99th percentile. Correlation coefficient is presented on the Y axis, with percentile algorithm on the X axis.

Bibliography

ADAMSEN, F. G., PINTER, P. J., BARNES, E. M., LAMORTE, R. L., WALL, G. W., LEAVITT, S. W., & KIMBALL, B. A. (1999). Measuring wheat senescence with a digital camera. *Crop Science* **39**, 719–724.

AIROBOTICS (2019). Automated industrial drones [online]. Available at: https://www.airoboticsdrones.com/ [Accessed 10th November 2019].

ALLARD, R. W. (1964). *Principles of Plant Breeding*. John Wiley & Sons, Inc., United States of America, second edition.

AMARAL, L. R., MOLIN, J. P., PORTZ, G., FINAZZI, F. B., & CORTINOVE, L. (2015). Comparison of crop canopy reflectance sensors used to identify sugarcane biomass and nitrogen status. *Precision Agriculture* **16**, 15–28.

ANDRADE-SANCHEZ, P., GORE, M. A., HEUN, J. T., THORP, K. R., CARMO-SILVA, A. E., FRENCH, A. N., SALVUCCI, M. E., & WHITE, J. W. (2014). Development and evaluation of a field-based high-throughput phenotyping platform. *Functional Plant Biology* **41**, 68–79.

ANDUJAR, D., RUEDA-AYALA, V., MORENO, H., ROSELL-POLO, J. R., ESCOLA, A., VALERO, C., GERHARDS, R., FERNANDEZ-QUINTANILLA, C., DORADO, J., & GRIEPENTROG, H. W. (2013). Discriminating crop, weeds and soil surface with a terrestrial lidar sensor. *Sensors* **13**, 14662–14675.

ARAUS, J. L. & CAIRNS, J. E. (2014). Field high-throughput phenotyping: the new crop breeding frontier. *Trends in Plant Science* **19**, 52–61.

ATIENO, J., LI, Y., LANGRIDGE, P., DOWLING, K., BRIEN, C., BERGER, B., VARSHNEY, R. K., & SUTTON, T. (2017). Exploring genetic variation for salinity tolerance in chickpea using image-based phenotyping. *Scientific Reports* **7**, 1300.

AUSTRALAIN GRAIN TECHNOLOGIES (2013). Yellowing in wheat [online]. Available at: https://www.agtbreeding.com.au/assets/docs/general/Yellowing-in-wheat.pdf.

AUSTRALAIN GRAIN TECHNOLOGIES (2016). Our understanding of yellowing in wheat (so far.) [online]. Available at: https://www.agtbreeding.com.au/assets/docs/general/Our-understanding-of-yellowing-in-wheat-so-far.pdf.

AUSTRALIAN PLANT PHENOMICS FACILITY (2015). The plant accelerator (high-throughput phenotyping) [online]. Available at: http://www.plantphenomics.org.au/services/accelerator/ [Accessed 13th September 2015].

BAI, G., GE, Y. F., HUSSAIN, W., BAENZIGER, P. S., & GRAEF, G. (2016). A multi-sensor system for high throughput field phenotyping in soybean and wheat breeding. *Computers and Electronics in Agriculture* **128**, 181–192.

BELASQUE, J., GASPAROTO, M. C. G., & MARCASSA, L. G. (2008). Detection of mechanical and disease stresses in citrus plants by fluorescence spectroscopy. *Applied Optics* **47**, 1922–1926.

BENDIG, J., BOLTEN, A., BENNERTZ, S., BROSCHEIT, J., EICHFUSS, S., & BARETH, G. (2014). Estimating biomass of barley using crop surface models (csms) derived from uav-based rgb imaging. *Remote Sensing* **6**, 10395–10412.

BENDIG, J., YU, K., AASEN, H., BOLTEN, A., BENNERTZ, S., BROSCHEIT, J., GNYP, M. L., & BARETH, G. (2015). Combining uav-based plant height from crop surface models, visible, and near infrared vegetation indices for biomass monitoring in barley. *International Journal of Applied Earth Observation and Geoinformation* **39**, 79–87.

BOCK, C. H., POOLE, G. H., PARKER, P. E., & GOTTWALD, T. R. (2010). Plant disease severity estimated visually, by digital photography and image analysis, and by hyperspectral imaging. *Critical Reviews in Plant Sciences* **29**, 59–107.

BOHONAK, A. (2004). *RMA: Software for Reduced Major Axis regression*. San Diego State University, California, USA.

BOUQUET, A. & JUGA, J. (2013). Integrating genomic selection into dairy cattle breeding programmes: a review. *Animal* **7**, 705–713.

BOYLE, R., CORKE, F., & HOWARTH, C. (2015). Image-based estimation of oat panicle development using local texture patterns. *Functional Plant Biology* **42**, 433–443.

BROWN, J. K. M., CHARTRAIN, L., LASSERRE-ZUBER, P., & SAINTENAC, C. (2015). Genetics of resistance to zymoseptoria tritici and applications to wheat breeding. *Fungal Genetics and Biology* **79**, 33–41.

BUSEMEYER, L., MENTRUP, D., MOLLER, K., WUNDER, E., ALHEIT, K., HAHN, V., MAURER, H. P., REIF, J. C., WURSCHUM, T., MULLER, J., RAHE, F., & RUCKELSHAUSEN, A. (2013). Breedvision - a multi-sensor platform for non-destructive field-based phenotyping in plant breeding. *Sensors* **13**, 2830–2847.

BUTLER, D., C. B. G. A. & GOGEL, B. (2009). *ASReml-R reference manual*. Queensland Department of Primary Industries. Queensland, Australia.

CABRERA-BOSQUET, L., CROSSA, J., VON ZITZEWITZ, J., SERRET, M. D., & ARAUS, J. L. (2012). High-throughput phenotyping and genomic selection: The frontiers of crop breeding converge. *Journal of Integrative Plant Biology* **54**, 312–320.

CASADESÚS, J., KAYA, Y., BORT, J., NACHIT, M. M., ARAUS, J. L., AMOR, S., FERRAZZANO, G., MAALOUF, F., MACCAFERRI, M., MARTOS, V., OUABBOU, H., & VILLEGAS, D. (2007). Using vegetation indices derived from conventional digital cameras as selection criteria for wheat breeding in water-limited environments. *Annals of Applied Biology* **150**, 227–236.

CIVIL AVIATION SAFETY AUTHORITY (2015). Civil aviation safety authority [online]. Available at: https://www.casa.gov.au/ [Accessed 10th September 2015].

COBB, J. N., DECLERCK, G., GREENBERG, A., CLARK, R., & MCCOUCH, S. (2013). Next-generation phenotyping: requirements and strategies for enhancing our understanding of genotype-phenotype relationships and its relevance to crop improvement. *Theoretical and Applied Genetics* **126**, 867–887.

COLEMAN, R. D., GILL, G. S., & REBETZKE, G. J. (2001). Identification of quantitative trait loci for traits conferring weed competitiveness in wheat (triticum aestivum l.). *Australian Journal of Agricultural Research* **52**, 1235–1246.

COLOMINA, I. & MOLINA, P. (2014). Unmanned aerial systems for photogrammetry and remote sensing: A review. *ISPRS Journal of Photogrammetry and Remote Sensing* **92**, 79–97.

COMAR, A., BURGER, P., DE SOLAN, B., BARET, F., DAUMARD, F., & HANOCQ, J. F. (2012). A semi-automatic system for high throughput phenotyping wheat cultivars in-field conditions: description and first results. *Functional Plant Biology* **39**, 914–924.

COOPER, M., MESSINA, C. D., PODLICH, D., TOTIR, L. R., BAUMGARTEN, A., HAUSMANN, N. J., WRIGHT, D., & GRAHAM, G. (2014). Predicting the future of plant breeding: complementing empirical evaluation with genetic prediction. *Crop & Pasture Science* **65**, 311–336.

CRAIN, J., REYNOLDS, M., & POLAND, J. (2016). Utilizing high-throughput phenotypic data for improved phenotypic selection of stress-adaptive traits in wheat. *Crop Science* .

CULLIS, B. R., SMITH, A. B., & COOMBES, N. E. (2006). On the design of early generation variety trials with correlated data. *Journal of agricultural, biological, and environmental statistics* **11**, 381.

DAMISCH, W. & WIBERG, A. (1991). Biomass yield a topical issue in modern wheat breeding programmes. *Plant Breeding* **107**, 11–17.

DEE, H. & FRENCH, A. (2015). From image processing to computer vision: plant imaging grows up foreword. *Functional Plant Biology* **42**, III–V.

DEERY, D., JIMENEZ-BERNI, J., JONES, H., SIRAULT, X., & FURBANK, R. (2014). Proximal remote sensing buggies and potential applications for field-based phenotyping. *Agronomy* **4**, 349.

DEERY, D. M., REBETZKE, G. J., JIMENEZ-BERNI, J. A., JAMES, R. A., CONDON, A. G., BOVILL, W. D., HUTCHINSON, P., SCARROW, J., DAVY, R., & FURBANK, R. T. (2016). Methodology for high-throughput field phenotyping of canopy temperature using airborne thermography. *Frontiers in Plant Science* **7**.

DEKKERS, J. C. M. & HOSPITAL, F. (2002). The use of molecular genetics in the improvement of agricultural populations. *Nature Reviews Genetics* **3**, 22–32.

DEVADAS, R., LAMB, D. W., BACKHOUSE, D., & SIMPFENDORFER, S. (2015). Sequential application of hyperspectral indices for delineation of stripe rust infection and nitrogen deficiency in wheat. *Precision Agriculture* **16**, 477–491.

DISTELFELD, A., AVNI, R., & FISCHER, A. M. (2014). Senescence, nutrient remobilization, and yield in wheat and barley. *Journal of Experimental Botany* **65**, 3783–3798.

DONALD, C. M. & HAMBLIN, J. (1976). Biological yield and harvest index of cereals as agronomic and plant breeding criteria. *Advances in Agronomy* **28**, 361–405.

EHLERT, D., ADAMEK, R., & HORN, H.-J. (2009). Laser rangefinder-based measuring of crop biomass under field conditions. *Precision Agriculture* **10**, 395–408.

EITEL, J. U. H., MAGNEY, T. S., VIERLING, L. A., BROWN, T. T., & HUGGINS, D. R. (2014). Lidar based biomass and crop nitrogen estimates for rapid, non-destructive assessment of wheat nitrogen status. *Field Crops Research* **159**, 21–32.

EITEL, J. U. H., MAGNEY, T. S., VIERLING, L. A., GREAVES, H. E., & ZHENG, G. (2016). An automated method to quantify crop height and calibrate satellite-derived biomass using hypertemporal lidar. *Remote Sensing of Environment* **187**, 414–422.

EUROPEAN PLANT PHENOTYPING NETWORK (2015). European plant phenotyping network [online]. Available at: http://www.plant-phenotyping-network.eu/eppn/home [Accessed 13th September 2015].

FABRE, J., DAUZAT, M., NEGRE, V., WUYTS, N., TIREAU, A., GENNARI, E., NEVEU, P., TISNE, S., MASSONNET, C., HUMMEL, I., & GRANIER, C. (2011). Phenopsis db: an information system for arabidopsis thaliana phenotypic data in an environmental context. *Bmc Plant Biology* **11**, 7.

FALCONER, D. S. (1960). *Introduction to quantitative genetics*. Ronald Press Co, New York.

FISCHER, R. A. & WOOD, J. T. (1979). Drought resistance in spring wheat cultivars. iii.* yield associations with morpho-physiological traits. *Australian Journal of Agricultural Research* **30**, 1001–1020.

FRIEDLI, M., KIRCHGESSNER, N., GRIEDER, C., LIEBISCH, F., MANNALE, M., & WALTER, A. (2016). Terrestrial 3d laser scanning to track the increase in canopy height of both monocot and dicot crop species under field conditions. *Plant Methods* **12**, 15.

GEIPEL, J., LINK, J., & CLAUPEIN, W. (2014). Combined spectral and spatial modeling of corn yield based on aerial images and crop surface models acquired with an unmanned aircraft system. *Remote Sensing* **6**, 10335.

GILMOUR, A. R., GOGEL, B. J., CULLIS, B. R., WELHAM, S. J., & THOMPSON, R. (2015). *ASReml User Guide Release 4.1 Structural Specification*. VSN International Ltd.

GREAVES, H. E., VIERLING, L. A., EITEL, J. U. H., BOELMAN, N. T., MAGNEY, T. S., PRAGER, C. M., & GRIFFIN, K. L. (2015). Estimating aboveground biomass and leaf area of low-stature arctic shrubs with terrestrial lidar. *Remote Sensing of Environment* **164**, 26–35.

GUO, W., ZHENG, B., DUAN, T., FUKATSU, T., CHAPMAN, S., & NINOMIYA, S. (2017). Easypcc: Benchmark datasets and tools for high-throughput measurement of the plant canopy coverage ratio under field conditions. *Sensors* **17**, 798.

HABOUDANE, D., MILLER, J. R., PATTEY, E., ZARCO-TEJADA, P. J., & STRACHAN, I. B. (2004). Hyperspectral vegetation indices and novel algorithms for predicting green lai of crop canopies: Modeling and validation in the context of precision agriculture. *Remote Sensing of Environment* **90**, 337–352.

HAFSI, M., MECHMECHE, W., BOUAMAMA, L., DJEKOUNE, A., ZAHARIEVA, M., & MONNEVEUX, P. (2000). Flag leaf senescence, as evaluated by numerical image analysis, and its relationship with yield under drought in durum wheat. *Journal of Agronomy and Crop Science* **185**, 275–280.

HALLORAN, G. M.; KNIGHT, R. M. K. S. S. D. H. B. (1979). *A Course Manual in Plant Breeding*. Australian Vice Chancellors' Committee, Canberra, Australia.

HAMMER, G., MESSINA, C., WU, A., & COOPER, M. (2019). Biological reality and parsimony in crop modelswhy we need both in crop improvement! *in silico Plants* **1**. diz010.

HASAN, M. M., CHOPIN, J. P., LAGA, H., & MIKLAVCIC, S. J. (2018). Detection and analysis of wheat spikes using convolutional neural networks. *Plant Methods* **14**, 100.

HERRERO-HUERTA, M., FELIPE-GARCIA, B., BELMAR-LIZARAN, S., HERNANDEZ-LOPEZ, D., RODRIGUEZ-GONZALVEZ, P., & GONZALEZ-AGUILERA, D. (2016). Dense canopy height model from a low-cost photogrammetric platform and lidar data. *Trees-Structure and Function* **30**, 1287–1301.

HOLLAMBY, G. M. (1983). *The Staff of Life, The History of Plant Breeding at Roseworthy Agricultural College*. Griffin Press, Roseworthy, Australia.

HOSOI, F. & OMASA, K. (2006). Voxel-based 3-d modeling of individual trees for estimating leaf area density using high-resolution portable scanning lidar. *IEEE Transactions on Geoscience and Remote Sensing* **44**, 3610–3618.

HOSOI, F. & OMASA, K. (2009). Estimating vertical plant area density profile and growth parameters of a wheat canopy at different growth stages using three-dimensional portable lidar imaging. *ISPRS Journal of Photogrammetry and Remote Sensing* **64**, 151–158.

HU, P., GUO, W., CHAPMAN, S. C., GUO, Y., & ZHENG, B. (2019). Pixel size of aerial imagery constrains the applications of unmanned aerial vehicle in crop breeding. *ISPRS Journal of Photogrammetry and Remote Sensing* **154**, 1–9.

JAMES, M. (2009). Differential gps guidance systems for field work in agriculture. *R&D Conference "Precision in arable farming: current practice and future potential", Grantham, Lincolnshire, UK, 28th-29th October 2009* pages 77–88.

JIMENEZ-BERNI, J. A., DEERY, D. M., ROZAS-LARRAONDO, P., CONDON, A. G., REBETZKE, G. J., JAMES, R. A., BOVILL, W. D., FURBANK, R. T., & SIRAULT, X. R. R. (2018). High throughput determination of plant height, ground cover, and above-ground biomass in wheat with lidar. *Frontiers in Plant Science* **9**.

JOHANNSEN, W. (1911). The genotype conception of heredity. *American Naturalist* **45**, 129–159.

JONES, H. G. (2004). Application of thermal imaging and infrared sensing in plant physiology and ecophysiology. In Callow, J. A., editor, *Advances in Botanical Research Incorporating Advances in Plant Pathology, Vol 41*, volume 41 of *Advances in Botanical Research*, pages 107–163. Academic Press Ltd-Elsevier Science Ltd, London.

JULIANA, P., RUTKOSKI, J. E., POLAND, J. A., SINGH, R. P., MURUGASAMY, S., NATESAN, S., BARBIER, H., & SORRELLS, M. E. (2015). Genome-wide association mapping for leaf tip necrosis and pseudo-black chaff in relation to durable rust resistance in wheat. *Plant Genome* **8**, 12.

KESKIN, M., SAY, S. M., & KESKIN, S. G. (2009). Evaluation of a low-cost gps receiver for precision agriculture use in adana province of turkey. *Turkish Journal of Agriculture and Forestry* **33**, 79–88.

KHAN, Z., CHOPIN, J., CAI, J., EICHI, V.-R., HAEFELE, S., & MIKLAVCIC, S. (2018). Quantitative estimation of wheat phenotyping traits using ground and aerial imagery. *Remote Sensing* **10**, 950.

KIPP, S., MISTELE, B., BARESEL, P., & SCHMIDHALTER, U. (2014). High-throughput phenotyping early plant vigour of winter wheat. *European Journal of Agronomy* **52**, 271–278.

KRAUSE, M. R., GONZÁLEZ-PÉREZ, L., CROSSA, J., PÉREZ-RODRÍGUEZ, P., MONTESINOS-LÓPEZ, O., SINGH, R. P., DREISIGACKER, S., POLAND, J., RUTKOSKI, J., SORRELLS, M., ET AL. (2019). Hyperspectral reflectance-derived relationship matrices for genomic prediction of grain yield in wheat. *G3: Genes, Genomes, Genetics* **9**, 1231–1247.

KRONENBERG, L., YU, K., WALTER, A., & HUND, A. (2017). Monitoring the dynamics of wheat stem elongation: genotypes differ at critical stages. *Euphytica* **213**, 157.

KUCHEL, H., FOX, R., REINHEIMER, J., MOSIONEK, L., WILLEY, N., BARIANA, H., & JEFFERIES, S. (2007). The successful application of a marker-assisted wheat breeding strategy. *Molecular Breeding* **20**, 295–308.

KUCHEL, H., YE, G. Y., FOX, R., & JEFFERIES, S. (2005). Genetic and economic analysis of a targeted marker-assisted wheat breeding strategy. *Molecular Breeding* **16**, 67–78.

LEI, L., QIN, Z., & DANFENG, H. (2014). A review of imaging techniques for plant phenotyping. *Sensors* **14**, 20078–20111.

LEINONEN, I. & JONES, H. G. (2004). Combining thermal and visible imagery for estimating canopy temperature and identifying plant stress. *Journal of Experimental Botany* **55**, 1423–1431.

LEMERLE, D., VERBEEK, B., COUSENS, R. D., & COOMBES, N. E. (1996). The potential for selecting wheat varieties strongly competitive against weeds. *Weed Research* **36**, 505–513.

LEMNATEC (2015). Products [online]. Available at: http://www.lemnatec.com/products/ [Accessed 13th September 2015].

LI, Q., JINHAI, C., BERGER, B., & MIKLAVCIC, S. (2014). Study on spike detection of cereal plants. *2014 13th International Conference on Control Automation Robotics & Vision (ICARCV). Proceedings* pages 228–233.

LI, W., NIU, Z., HUANG, N., WANG, C., GAO, S., & WU, C. Y. (2015). Airborne lidar technique for estimating biomass components of maize: A case study in zhangye city, northwest china. *Ecological Indicators* **57**, 486–496.

LI, Y., CHEN, D., WALKER, C. N., & ANGUS, J. F. (2010). Estimating the nitrogen status of crops using a digital camera. *Field Crops Research* **118**, 221–227.

LICHTENTHALER, H. K. & BABANI, F. (2000). Detection of photosynthetic activity and water stress by imaging the red chlorophyll fluorescence. *Plant Physiology and Biochemistry* **38**, 889–895.

LIU, J. & PATTEY, E. (2010). Retrieval of leaf area index from top-of-canopy digital photography over agricultural crops. *Agricultural and Forest Meteorology* **150**, 1485–1490.

LIU, T., WU, W., CHEN, W., SUN, C., ZHU, X., & GUO, W. (2016). Automated image-processing for counting seedlings in a wheat field. *Precision Agriculture* **17**, 392–406.

LOBET, G., DRAYE, X., & PERILLEUX, C. (2013). An online database for plant image analysis software tools. *Plant Methods* **9**, 7.

LONG, D. S. & MCCALLUM, J. D. (2013). Mapping straw yield using on-combine light detection and ranging (lidar). *International Journal of Remote Sensing* **34**, 6121–6134.

LÓPEZ-GRANADOS, F., TORRES-SÁNCHEZ, J., SERRANO-PÉREZ, A., DE CASTRO, A. I., MESAS-CARRASCOSA, F.-J., & PEÑA, J.-M. (2016). Early season weed mapping in sunflower using uav technology: variability of herbicide treatment maps against weed thresholds. *Precision Agriculture* **17**, 183–199.

LUDBROOK, J. (1997). Special article comparing methods of measurement. *Clinical and Experimental Pharmacology and Physiology* **24**, 193–203.

LUDBROOK, J. (2012). A primer for biomedical scientists on how to execute model ii linear regression analysis. *Clinical and Experimental Pharmacology and Physiology* **39**, 329–335.

LUKINA, E. V., STONE, M. L., & RANN, W. R. (1999). Estimating vegetation coverage in wheat using digital images. *Journal of Plant Nutrition* **22**, 341–350.

MAHESH, S., JAYAS, D. S., PALIWAL, J., & WHITE, N. D. G. (2015). Hyperspectral imaging to classify and monitor quality of agricultural materials. *Journal of Stored Products Research* **61**, 17–26.

MESSINA, C., TECHNOW, F., TANG, T., TOTIR, R., GHO, C., & COOPER, M. (2018). Leveraging biological insight and environmental variation to improve phenotypic prediction: Integrating crop growth models (cgm) with whole genome prediction (wgp). *European Journal of Agronomy* **100**, 151 – 162. Recent advances in crop modelling to support sustainable agricultural production and food security under global change.

MESSINA, C. D., PODLICH, D., DONG, Z. S., SAMPLES, M., & COOPER, M. (2011). Yield-trait performance landscapes: from theory to application in breeding maize for drought tolerance. *Journal of Experimental Botany* **62**, 855–868.

MEUWISSEN, T. H. E., HAYES, B. J., & GODDARD, M. E. (2001). Prediction of total genetic value using genome-wide dense marker maps. *Genetics* **157**, 1819–1829.

MONTES, J. M., TECHNOW, F., DHILLON, B. S., MAUCH, F., & MELCHINGER, A. E. (2011). High-throughput non-destructive biomass determination during early plant development in maize under field conditions. *Field Crops Research* **121**, 268–273.

MOORE, G. E. (1965). Cramming more components onto integrated circuits. *Electronics* **38**, 114.

MORGOUNOV, A., GUMMADOV, N., BELEN, S., KAYA, Y., KESER, M., & MURSALOVA, J. (2014). Association of digital photo parameters and ndvi with winter wheat grain yield in variable environments. *Turkish Journal of Agriculture & Forestry* **38**, 624–632.

MOSHOU, D., BRAVO, C., WAHLEN, S., WEST, J., MCCARTNEY, A., DE BAERDEMAEKER, J., & RAMON, H. (2006). Simultaneous identification of plant stresses and diseases in arable crops using proximal optical sensing and self-organising maps. *Precision Agriculture* **7**, 149–164.

MULLA, D. J. (2013). Twenty five years of remote sensing in precision agriculture: Key advances and remaining knowledge gaps. *Biosystems Engineering* **114**, 358–371.

MULLAN, D. J. & REYNOLDS, M. P. (2010). Quantifying genetic effects of ground cover on soil water evaporation using digital imaging. *Functional Plant Biology* **37**, 703–712.

MURAKAMI, T., YUI, M., & AMAHA, K. (2012). Canopy height measurement by photogrammetric analysis of aerial images: Application to buckwheat (fagopyrum esculentum moench) lodging evaluation. *Computers and Electronics in Agriculture* **89**, 70–75.

OKLAHOMA STATE UNIVERSITY DEPARTMENT OF PLANT AND SOIL SCIENCES (2015). *CANOPEO: Rapid and accurate green canopy cover measurement tool*. Oklahoma State University, Oklahoma, USA.

PASK, AJD., P. J. M. D. & REYNOLDS, M. E. (2012). *Physiological Breeding II: A Field Guide to Wheat Phenotyping*. CIMMYT, Mexico, D.F.

PERCEPTO (2019). Solving operational challenges from above [online]. Available at: https://percepto.co/ [Accessed 10th November 2019].

PITTMAN, J. J., ARNALL, D. B., INTERRANTE, S. M., MOFFET, C. A., & BUTLER, T. J. (2015). Estimation of biomass and canopy height in bermudagrass, alfalfa, and wheat using ultrasonic, laser, and spectral sensors. *Sensors* **15**, 2920–2943.

PIX4D (2016). *Pix4Dmapper Pro*. Pix4D, Prilly, Switzerland.

PRECISIONHAWK (2015). Sensors]. Available at: http://www.precisionhawk.com/ [Accessed 17th September 2015].

R CORE TEAM (2017). *R: A Language and Environment for Statistical Computing*. R Foundation for Statistical Computing, Vienna, Austria.

RAMEEH, V. (2014). Multivariate regression analyses of yield associated traits in rapeseed (brassica napus l.) genotypes. *Advances in Agriculture* **2014**, 5.

RASMUSSEN, J., NIELSEN, J., GARCIA-RUIZ, F., CHRISTENSEN, S., & STREIBIG, J. C. (2013). Potential uses of small unmanned aircraft systems (uas) in weed research. *Weed Research* **53**, 242–248.

REBETZKE, G., JIMENEZ-BERNI, J., FISCHER, R., DEERY, D., & SMITH, D. (2019). High-throughput phenotyping to enhance the use of crop genetic resources. *Plant Science* **282**, 40–48.

REBETZKE, G. J., BOTWRIGHT, T. L., MOORE, C. S., RICHARDS, R. A., & CONDON, A. G. (2004). Genotypic variation in specific leaf area for genetic improvement of early vigour in wheat. *Field Crops Research* **88**, 179–189.

REYNOLDS, M., FOULKES, J., FURBANK, R., GRIFFITHS, S., KING, J., MURCHIE, E., PARRY, M., & SLAFER, G. (2012). Achieving yield gains in wheat. *Plant Cell and Environment* **35**, 1799–1823.

RICHARDS, R. A. (2000). Selectable traits to increase crop photosynthesis and yield of grain crops. *Journal of Experimental Botany* **51**, 447–458.

RICHARDS, R. A., REBETZKE, G. J., CONDON, A. G., & VAN HERWAARDEN, A. F. (2002). Breeding opportunities for increasing the efficiency of water use and crop yield in temperate cereals. *Crop Science* **42**, 111–121.

RIEGL (2015). Unmanned laser scanning [online]. Available at: http://www.riegl.com/products/unmanned-scanning/ [Accessed 17th September 2015].

ROSELL POLO, J. R., SANZ, R., LLORENS, J., ARNO, J., ESCOLA, A., RIBES-DASI, P., MASIP, J., CAMP, F., GRACIA, F., SOLANELLES, F., PALLEJA, T., PAL, L., PLANAS, S., GIL, E., & PALACIN, J. (2009). A tractor-mounted scanning lidar for the non-destructive measurement of vegetative volume and surface area of tree-row plantations: A comparison with conventional destructive measurements. *Biosystems Engineering* **102**, 128–134.

RUTKOSKI, J., POLAND, J., MONDAL, S., AUTRIQUE, E., PÉREZ, L. G., CROSSA, J., REYNOLDS, M., & SINGH, R. (2016). Canopy temperature and vegetation indices from high-throughput phenotyping improve accuracy of pedigree and genomic selection for grain yield in wheat. *G3: Genes, Genomes, Genetics* **6**, 2799–2808.

SADEGHI-TEHRAN, P., SABERMANESH, K., VIRLET, N., & HAWKESFORD, M. J. (2017). Automated method to determine two critical growth stages of wheat: Heading and flowering. *Frontiers in Plant Science* **8**, 252.

SADEGHI-TEHRAN, P., VIRLET, N., AMPE, E. M., REYNS, P., & HAWKESFORD, M. J. (2019). Deepcount: In-field automatic quantification of wheat spikes using simple linear iterative clustering and deep convolutional neural networks. *Frontiers in Plant Science* **10**, 1176.

SAEYS, W., LENAERTS, B., CRAESSAERTS, G., & DE BAERDEMAEKER, J. (2009). Estimation of the crop density of small grains using lidar sensors. *Biosystems Engineering* **102**, 22–30.

SANKARAN, S., MISHRA, A., EHSANI, R., & DAVIS, C. (2010). A review of advanced techniques for detecting plant diseases. *Computers and Electronics in Agriculture* **72**, 1–13.

SCHINDELIN, J., ARGANDA-CARRERAS, I., FRISE, E., KAYNIG, V., LONGAIR, M., PIETZSCH, T., PREIBISCH, S., RUEDEN, C., SAALFELD, S., SCHMID, B., TINEVEZ, J.-Y., WHITE, D. J., HARTENSTEIN, V., ELICEIRI, K., TOMANCAK, P., & CARDONA, A. (2012). Fiji: an open-source platform for biological-image analysis. *Nature Methods* **9**, 676.

SCHIRRMANN, M., GIEBEL, A., GLEINIGER, F., PFLANZ, M., LENTSCHKE, J., & DAMMER, K. H. (2016a). Monitoring agronomic parameters of winter wheat crops with low-cost uav imagery. *Remote Sensing* **8**, 19.

SCHIRRMANN, M., HAMDORF, A., GARZ, A., USTYUZHANIN, A., & DAMMER, K. H. (2016b). Estimating wheat biomass by combining image clustering with crop height. *Computers and Electronics in Agriculture* **121**, 374–384.

SCHNEIDER, C. A., RASBAND, W. S., & ELICEIRI, K. W. (2012). Nih image to imagej: 25 years of image analysis. *Nat Meth* **9**, 671–675.

SCHWENKE, G. D., SIMPFENDORFER, S. R., & COLLARD, B. C. Y. (2015). Confirmation of chloride deficiency as the cause of leaf spotting in durum wheat grown in the australian northern grains region. *Crop and Pasture Science* **66**, 122–134.

SHARMA, R. C. (1993). Selection for biomass yield in wheat. *Euphytica* **70**, 35–42.

SHEEN, S. J., EBELTOFT, D. C., & SMITH, G. S. (1968). Association and inheritance of black chaff and stem rust reactions in conley wheat crosses. *Crop Science* **8**, 477–480.

SINGH, R. P. (1992). Association between gene lr34 for leaf rust resistance and leaf tip necrosis in wheat. *Crop Science* **32**, 874–878.

SONG, Y., GLASBEY, C. A., HORGAN, G. W., POLDER, G., DIELEMAN, J. A., & VAN DER HEIJDEN, G. (2014). Automatic fruit recognition and counting from multiple images. *Biosystems Engineering* **118**, 203–215.

STEIN, L. D. (2010). The case for cloud computing in genome informatics. *Genome Biology* **11**, 7.

STEINBERG, G. (2015). Cell biology of zymoseptoria tritici: Pathogen cell organization and wheat infection. *Fungal Genetics and Biology* **79**, 17–23.

STEWART, E. L. & MCDONALD, B. A. (2014). Measuring quantitative virulence in the wheat pathogen zymoseptoria tritici using high-throughput automated image analysis. *Phytopathology* **104**, 985–992.

SUN, J., RUTKOSKI, J. E., POLAND, J. A., CROSSA, J., JANNINK, J.-L., & SORRELLS, M. E. (2017a). Multitrait, random regression, or simple repeatability model in high-throughput phenotyping data improve genomic prediction for wheat grain yield. *The plant genome* **10**.

SUN, S., LI, C., PATERSON, A. H., JIANG, Y., XU, R., ROBERTSON, J. S., SNIDER, J. L., & CHEE, P. W. (2018). In-field high throughput phenotyping and cotton plant growth analysis using lidar. *Frontiers in Plant Science* **9**.

SUN, S. P., LI, C. Y., & PATERSON, A. H. (2017b). In-field high-throughput phenotyping of cotton plant height using lidar. *Remote Sensing* **9**, 21.

TECHNOW, F., MESSINA, C. D., TOTIR, L. R., & COOPER, M. (2015). Integrating crop growth models with whole genome prediction through approximate bayesian computation. *PloS one* **10**, e0130855.

TILLY, N., HOFFMEISTER, D., CAO, Q., HUANG, S., LENZ-WIEDEMANN, V., MIAO, Y., & BARETH, G. (2014). Multitemporal crop surface models: accurate plant height measurement and biomass estimation with terrestrial laser scanning in paddy rice. *Journal of Applied Remote Sensing* **8**, 1–23.

TRIMBLE (2015). Greenseeker crop sensing system [online]. Available at: http://www.trimble.com/Agriculture/greenseeker.aspx [Accessed 4th November 2015].

TRITICEAE COORDINATED AGRICULTURAL PROJECT (2015). The triticeae toolbox [online]. Available at: https://triticeaetoolbox.org/ [Accessed 19th November 2015].

TUCKER, C. J. (1977). Asymptotic nature of grass canopy spectral reflectance. *Applied Optics* **16**, 1151–1156.

UNDERWOOD, J., WENDEL, A., SCHOFIELD, B., MCMURRAY, L., & KIMBER, R. (2017). Efficient in-field plant phenomics for row-crops with an autonomous ground vehicle. *Journal of Field Robotics* **34**, 1061–1083.

VIRLET, N., SABERMANESH, K., SADEGHI-TEHRAN, P., & HAWKESFORD, M. J. (2017). Field scanalyzer: An automated robotic field phenotyping platform for detailed crop monitoring. *Functional Plant Biology* **44**, 143–153.

VISSCHER, P. M., HILL, W. G., & WRAY, N. R. (2008). Heritability in the genomics era concepts and misconceptions. *Nature Reviews Genetics* **9**, 255.

WALTER, A., LIEBISCH, F., & HUND, A. (2015). Plant phenotyping: from bean weighing to image analysis. *Plant Methods* **11**, 11.

WALTER, J., EDWARDS, J., CAI, J., MCDONALD, G., MIKLAVCIC, S. J., & KUCHEL, H. (2019). High-throughput field imaging and basic image analysis in a wheat breeding programme. *Frontiers in Plant Science* **10**.

WALTER, J., EDWARDS, J., MCDONALD, G., & KUCHEL, H. (2018). Photogrammetry for the estimation of wheat biomass and harvest index. *Field Crops Research* **216**, 165–174.

WANG, X., XUAN, H., EVERS, B., SHRESTHA, S., PLESS, R., & POLAND, J. (2019). High-throughput phenotyping with deep learning gives insight into the genetic architecture of flowering time in wheat. *bioRxiv* .

WHITE, J. W., ANDRADE-SANCHEZ, P., GORE, M. A., BRONSON, K. F., COFFELT, T. A., CONLEY, M. M., FELDMANN, K. A., FRENCH, A. N., HEUN, J. T., HUNSAKER, D. J., JENKS, M. A., KIMBALL, B. A., ROTH, R. L., STRAND, R. J., THORP, K. R., WALL, G. W., & WANG, G. Y. (2012). Field-based phenomics for plant genetics research. *Field Crops Research* **133**, 101–112.

WHITE, J. W. & CONLEY, M. M. (2013). A flexible, low-cost cart for proximal sensing. *Crop Science* **53**, 1646–1649.

WINTERHALTER, L., MISTELE, B., JAMPATONG, S., & SCHMIDHALTER, U. (2011). High-throughput sensing of aerial biomass and above-ground nitrogen uptake in the vegetative stage of well-watered and drought stressed tropical maize hybrids. *Crop Science* **51**, 479–489.

WPS (2015). Overview products plant phenotyping [online]. Available at: http://www.wps.eu/en/plant-phenotyping/overview-products-plant-phenotyping [Accessed 13th September 2015].

YOUSEF, G. G. & JUVIK, J. A. (2001). Comparison of phenotypic and marker-assisted selection for quantitative traits in sweet corn. *Crop Science* **41**, 645–655.

ZADOKS, J. C., CHANG, T. T., & KONZAK, C. F. (1974). A decimal code for the growth stages of cereals. *Weed Research* **14**, 415–421.

ZAR, J. H. (1984). *Biostatistical Analysis*. Prentice-Hall, Englewood Cliffs, N.J, 2 edition.

ZERNER, M. C., REBETZKE, G. J., & GILL, G. S. (2016). Genotypic stability of weed competitive ability for bread wheat () genotypes in multiple environments. *Crop and Pasture Science* **67**, 695–702.

ZHANG, C. H. & KOVACS, J. M. (2012). The application of small unmanned aerial systems for precision agriculture: a review. *Precision Agriculture* **13**, 693–712.

ZHANG, J. W., LI, C. S., WU, C. Y., XIONG, L. Z., CHEN, G. X., ZHANG, Q. F., & WANG, S. P. (2006). Rmd: a rice mutant database for functional analysis of the rice genome. *Nucleic Acids Research* **34**, D745–D748.

ZOLKOS, S. G., GOETZ, S. J., & DUBAYAH, R. (2013). A meta-analysis of terrestrial aboveground biomass estimation using lidar remote sensing. *Remote Sensing of Environment* **128**, 289–298.